Identification of a glass-feeder process

van Vucht, Geert

Award date:
1987

IDENTIFICATION OF A GLASS-FEEDER PROCESS

Geert van Vucht

DEPARTMENT OF ELECTRICAL ENGINEERING
EINDHOVEN UNIVERSITY OF TECHNOLOGY
Group measurement and Control

IDENTIFICATION OF A GLASS-FEEDER PROCESS

by G.N.M. van Vucht

This report is submitted in fulfilment of the requirements of the degree of electrical engineer (M.Sc.) at the Eindhoven University of Technology.
The work was carried out from december 1986 until oktober 1987
in charge of:

Prof. Dr. Ir. P. Eykhoff

under supervision of:

Ir. A.C.P.M. Backx (Philips Glass)
Dr. Ir. A.J.W. van den Boom

IDENTIFICATION OF A GLASS-FEEDER PROCESS

SUMMARY

This report describes the modelling of the dynamic behaviour of a glass-feeder process. An identification method on the basis of impulse response models has been used.

The feeder process has been studied and attention has been paid on the difficulties that arise when the process is controlled with feedback. For the identification, a transportable measuring system has been developed on a Micro-VAX. A host computer running a software package for 'on-line' analysis of the measured signals has been connected to the measuring computer. The measurements have been performed on the BH-F feeder of the Universal furnace in Eindhoven.

The identification of the input/output behaviour of the feeder in one of its working points has been done in several steps. After preparation of the measured data, these have been used to estimate impulse response models. In a final step, from a minimal polynomial impulse response model, a 4-th order state space model is derived. The model describes the output temperature of the feeder with an accuracy of 10%. Also more insight in the underlying mechanisms of the feeder process has been gained.

The state space model is suitable for the design of a process controller with state feedback. Simulations have shown that with this controller the output temperature can be set to another value within a time period of two hours. With the common feedback control it took up to one day to switch the feeder to another set point.

Although the feeder is a non-linear, non-stationary process with distributed parameters, the method described in this report apparently was valid for the identification of this industrial process.

IDENTIFICATION OF A GLASS-FEEDER PROCESS

TABLE OF CONTENTS

1 INTRODUCTION

1.1 GENERAL INTRODUCTION

This report deals with a project carried out at the PICOS group (Process Identification and Control Systems) of the Philips Glass Division.

The PICOS group works on modern system control theory and applies this theory to industrial processes. The research is focused on identification (or modelling) of processes. The models found by identification are mainly used for the design of multi-input multi-output process-controllers.

The group participates in projects to improve the quality of glass production processes. Recently, increasing demands are made upon the control of glass production processes. To stay in competition with other glass-industries, the production-tolerances must be kept small and the production must become independent of disturbances occuring. Flexibility must be increased, i.e. changeover times must be shortened.

The subject described in this report is part of the work done in the 'feeder-project'. 'Feeder' here refers to the last part of a glass-melting furnace in which the glass-temperature is controlled to be able to shape the glass at the outlet as good as possible. The objective of this feeder-project was to gain knowledge about the principles and properties of the feeder-process. This is done to obtain better control, to increase the flexibility of glass-feeders and to improve the quality and shaping of the glass.

To be able to improve the control of the feeder, it is important to get insight in the dynamic behaviour of the feeder process, because the dynamics tell how -in time- the responses will be to changeovers, disturbances, load changes etc.. It was this part of the research of the feeder project that PICOS took care of. The control objective, formulated in the feeder project, determines what must be known of the behaviour of the process. Analysis of the dynamics of the process finally has to lead to a model in which the behaviour of the process is stored. This is called identification. The model must be suitable for controller design. This puts constraints on the identification. Once the proper identification result is obtained, a control system can be designed to control the feeder within the limits of its capabilities.

Several steps are distinguished when identification is done.
First of all preliminary investigation has to be done on the process. In this case, the 'BH-F feeder' of the Universal furnace in Eindhoven is studied. In section 1.2 the feeder-process is described and some important properties are stipulated.

From this knowledge we can define what model can be used best (which inputs, outputs), what measuring system will be needed, what will be the duration of the experiments etc. Then, the measuring system can be provided. A great part of the work was to prepare a universally applicable measuring system for the feeder experiments. In chapter 2 this system is explained.

After the measuring system is tested, the experiments can be performed (chapter 3). In chapter 4 the identification on the feeder data is presented.

In the previous projects, PICOS has gained experience in the analysis of the dynamic behaviour of specific glass-production (sub)processes. This experience, and the tools developed until now, formed the basis of the analyses done at the feeder. The method applied was kind of a 'protocol' for identification developed within PICOS. This method is abstracted in chapter 1.3.

On theoretical aspects of identification a lot of research has been done. Less time has been spent on the application of identification to industrial processes. The challenge here was to investigate whether the newly developed methods would still be valuable in application on such a difficult to model process as a feeder.

1.2 FEEDER PROCESS

First it has to be determined what is already known about the process. This knowledge is also used to formulate the objectives of the identification.

In section 1.2.1 the glass-melting installation of the pilot plant in Eindhoven is described 'from the outside'. It is shown how the glass is manufactured and what equipment is used.

In section 1.2.2 a refinement is given. Main properties of glass and the feeder process are surveyed here, together with the control principles that are used until now. It is not a scientific description and it only presents in words the main mechanisms of the feeder process.

1.2.1 Furnace installation

Before we consider properties of the feeder process, it is useful to take a view at the entire glass-furnace installation.

A pilot glass-melting furnace has been installed at the plant in Eindhoven. As it is only used for various experiments in behalf of other commercial plants which produce products like T.V.-screens, lamps, tubes etc., it is called the 'Universal furnace'. The dimensions of that furnace have been kept small to reduce costs. It produces 130-160 kg glass per hour. The produced glass is partly recycled as glass-fragments for input, partly it is thrown away.

Figure 1-1 shows the universal furnace. It consists of two major parts; the melting tank and, behind it, the forehearth (we will call it 'feeder'). In the melting tank the glass-silicat is molten to glass. The feeder is used to cool the molten glass to manufacturing temperature in a controlled manner. It takes care of the 'thermic conditioning' of the glass.

Melting tank

In the melting tank the glass-blend is heated to about 1400 ^{0}C. The heating is done mostly by radiation, so the air is heated first. The atmosphere at the middle of the roof, the hottest point in the furnace,

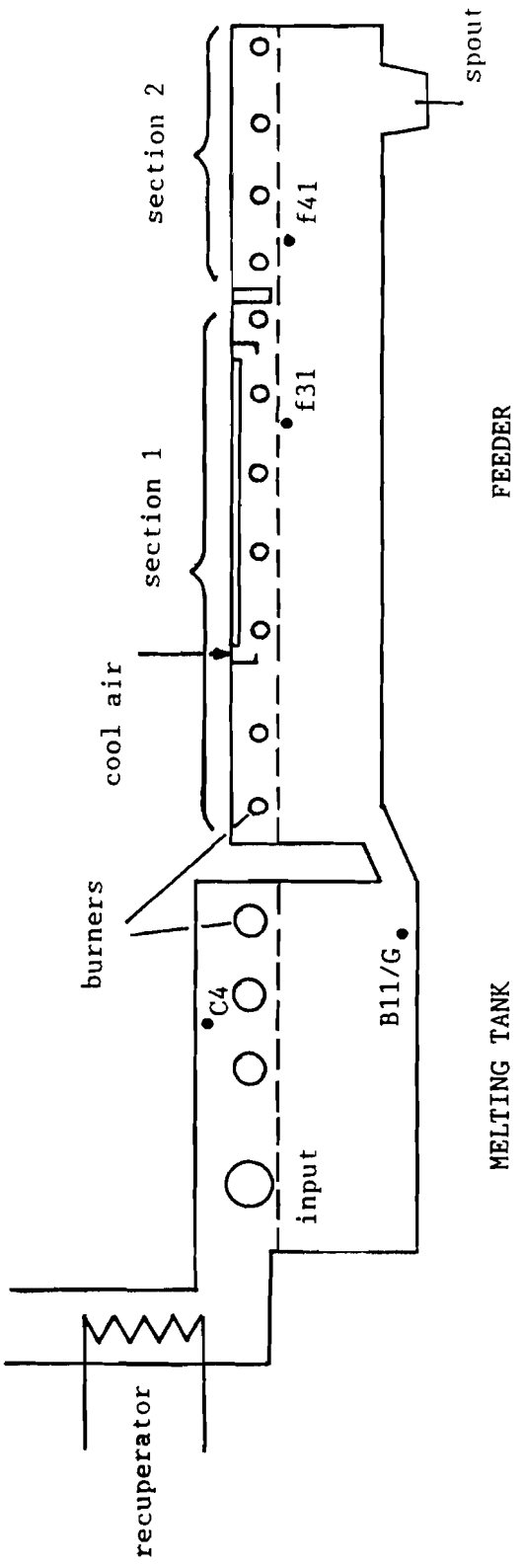

Fig. 1-1 Schematic side view of the Universal furnace installation

is about 1550 ^{0}C. The effective pressure inside the furnace is always kept positive to avoid air coming in. The gas mixture has an air/gas ratio of 10, so slighty above the stochiometric point (the ratio at which all the gas is just oxidized, which is 8.7). The inflated air is pre-heated at 500^{0}C by a recuperator which is fed by the combustion air of the furnace.

The furnace temperature is kept constant by manual control. The controlled temperature may be either the hottest point of the furnace (C4 in fig 1-1) or the glass-temperature just before the feeder (B11/G). For very big furnaces control at C4 is preferred. Control of glass-temperature may cause rather large temperature changes of the furnace roof, which causes little stone-pieces to chip off and pollute the glass. In case the roof is not very much affected by these changes, control of the glass-temperature is preferred, letting the temperature of the incoming glass of the feeder constant.

The melting tank is fed at the sides, as opposed to the more common front-inlet. Because the inlet determines the depth of the glass-bath it is controlled. Every half minute the glass-level is measured and on the basis of the level measured, the speed of the wormwheel of the inlet is adjusted.

To provide circulation and mixture in the melting tank, bubbling with pure oxygen is applied.

Finally the glass is passed to the feeder through a short channel at the bottom*.

Feeder

The feeder is a 40 cm wide channel, 4m long and with 15 cm of glass in it. It has some equipment to influence the temperature of the glass coming through. The glass entering the feeder contains bubbles from the chemical reaction of the melting. Due to the bad heat-conduction of the silicat in the melting tank, the glass still contains layers with different temperatures. In the feeder the glass must become homogeneous. The main purpose of the feeder is to cool the glass and let its temperature-distribution at the exit be homogeneous.

---

*Notice that before a separate section between the melting tank and the feeder was used. Its purpose is taken over by the feeder nowadays, and the section is skipped completely.

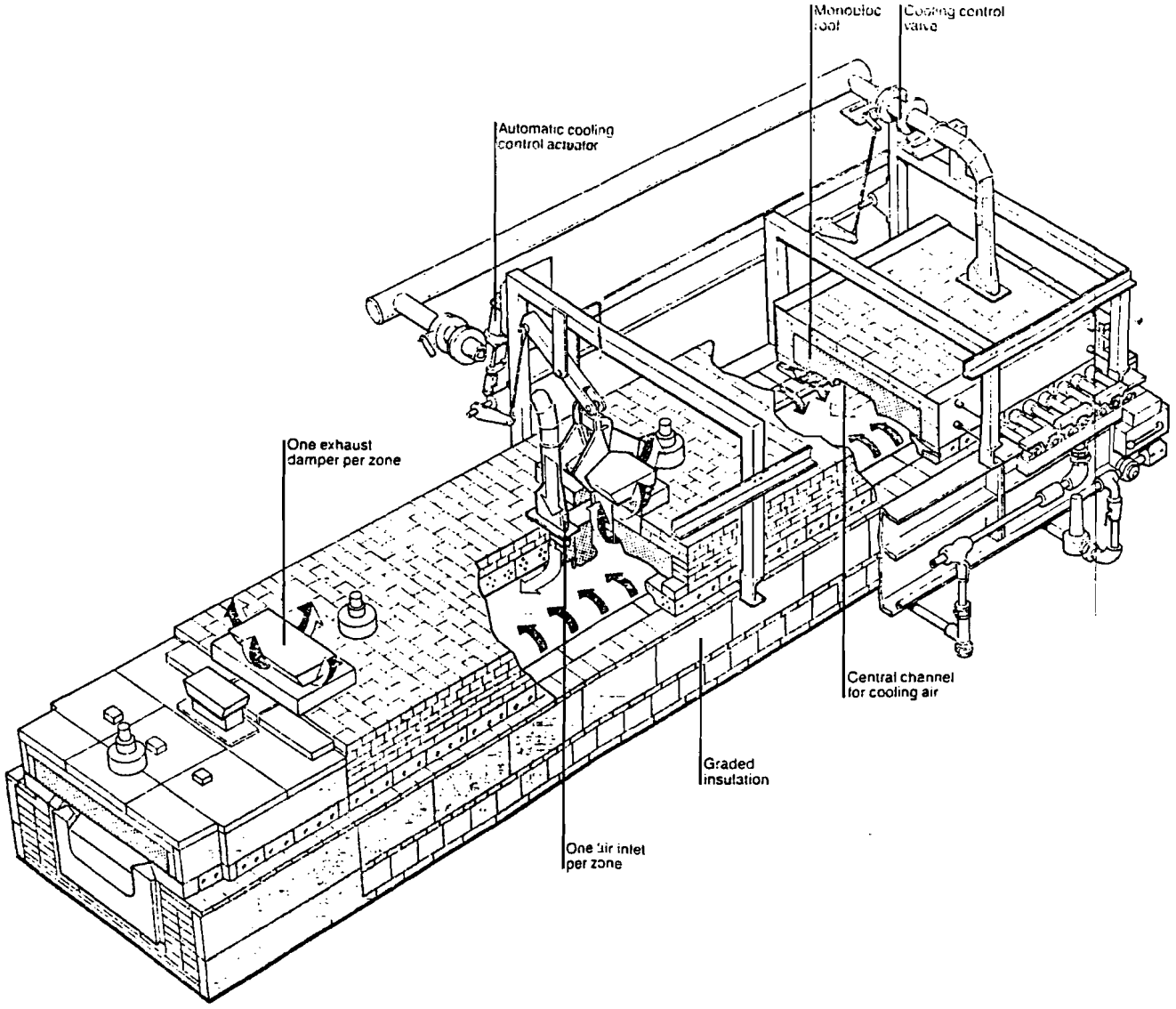

Fig. 1-2 BH-F feeder

At different sections of the feeder the glass can be heated by burners. Cooling of the glass is controlled by damper blocks at its roof.

Just before the experiments started, a new feeder was installed at the pilot plant. It has been a 400-series forehearth of BH-F limited England (cf fig. 1-2). It has been bought with the intention of possible installation at commercial plants within Philips, of course depending on its functioning at the pilot plant.

An important feature of the BH-F feeder is that it has an active cooling system beside the conventional damper blocks. Cooling air is fed through a channel along the long axis of the feeder just above the

center of the stream of glass. Burners are, as usual, located at the sides of the feeder. Control of the temperature distribution of the cross-section of the feeder is done as follows; cooling air mainly influences the center of the glass and burners predominately control the side of the glass.

In order to control temperature along the long axis of the feeder, it is divided into two sections. The atmosphere of the sections is separated by a little wall above the glass. The first section contains burners and a cooling channel. The second section, in which the spout is located, only contains burners. The burners of the sections (17 at each side in section 1, 8 in section 2) are fed with premixed gas/air, each section through a single conduit-pipe.

With help of these three inputs the operator controls the feeder to obtain the right temperature and temperature distribution at the spout. He is supported by 2 separate PID-controllers. At section 1 the temperature of section 1 is used as control valuable and either the gas or the cool-air is used for control. The non-controlled input is manually controlled. The temperature of section 2 is determined by the second PID-controller that controls the gas inflation of section 2.

Shaping of the glass coming through the spout is done by the 'vello' process (cf fig. 1-3). The glass flows along a hollow pipe (mandril) which is positioned in the outlet and through which air is fed. The tube is pulled out partly by gravitation, partly by means of a drawing machine. Around the outlet an electrical heated ring controls the outflow. We will call it the 'cup-heating'. The amount of extra energy applied is determined by the glass temperature. If the temperature raises, the heating is decreased. This temperature is measured with a radiation sensor.

Summarizing, 5 shaping parameters can be distinguished:

- Glass-temperature in the spout
- Air flow through the mandril
- Position of the mandril
- Cup-heating
- Drawing-speed

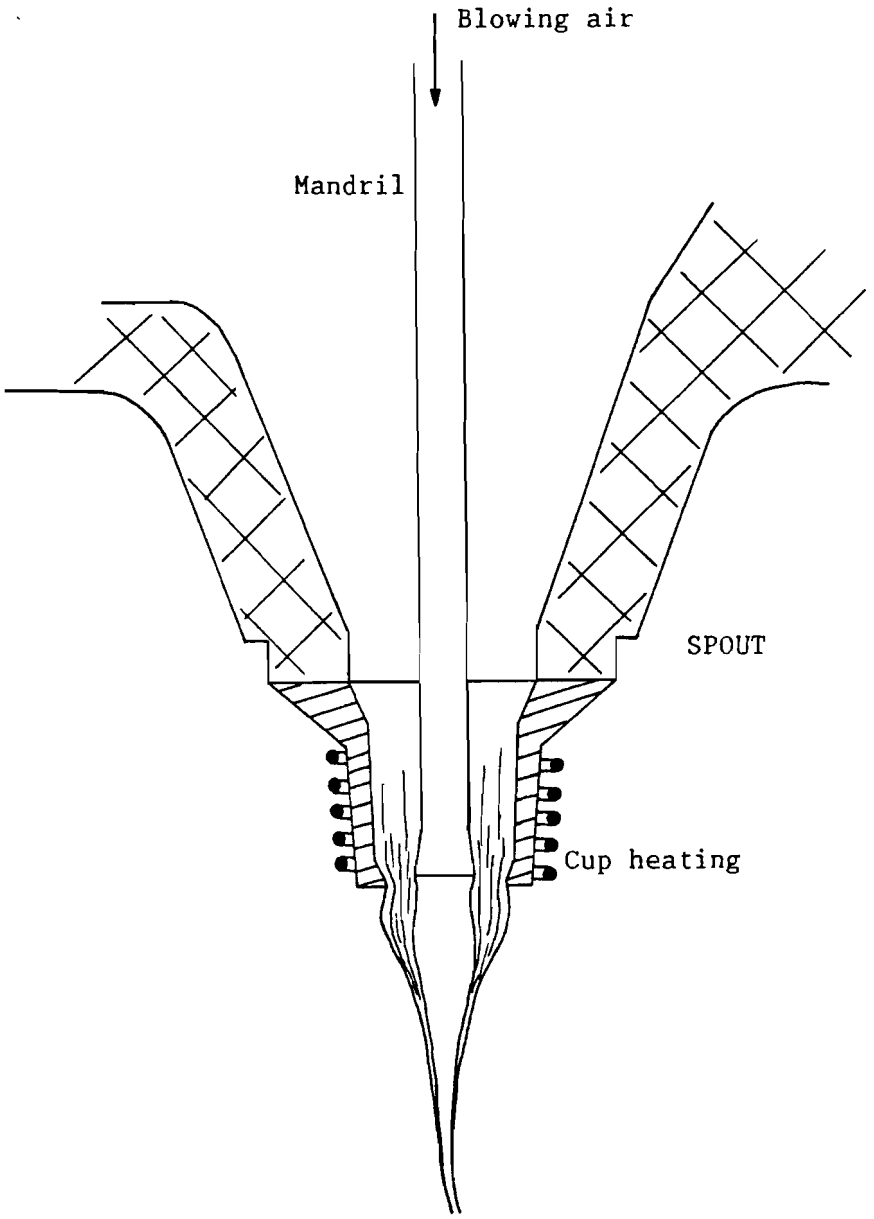

Fig. 1-3 Outline of the vello-principle

Behind the drawing machine the tube is cut and some samples are taken at random to measure properties like wall-thickness and tube-diameter. Next, the tubes are put in packing cases.

To keep the universal furnace going, 8 to 10 people are working in the plant on an 8 hour shift system.

1.2.2 Properties

In the previous section we considered the furnace installation and the the control variables that are available to affect the temperature distribution in the feeder, and hereby the final glass product. Next, we will further investigate how these variables are used, and what production properties the feeder possesses. We will also have a short view at the thermic properties of the feeder-system.

The dimensions of a feeder are determined by the temperature fall (i.e. energy loss) that is needed between the inlet and outlet of the feeder. This energy loss depends on several items:

- Exit temperature of the glass.
  The feeder must be capable of reaching the lowest temperature ever intended to be used at the specific plant. Once a feeder is built it is easier to put extra energy in it than to extract extra energy from it.
- Type of glass used.
  Different glass-types have different heat-capacities. Also the optical density of the glass is important, e.g. darker glass takes less time to lose its heat.
- Pull rate used.
  At higher pull rate (more glass consumption) more heat per time unit must be lost to reach the same exit temperature.

As explained above, the feeder is brought to its operation temperatures by heating. In this situation, one is able to control the feeder around its operation point by increasing as well as decreasing the heat.

To attain a homogeneous temperature distribution, control on the following principle is used (cf. fig. 1-4).
The glass can only be heated from above. The temperature of the atmosphere above the glass is very good controllable, but the temperature of the lower layers of the glass and the refractory material beneath the glass are not. They can only be influenced indirectly. Therefore, the atmosphere temperature of the first section is taken lower than the glass coming in, in order to cool it down. Doing so, the upper layers get cooler than the lower layers. Next, the atmosphere temperature of the second section is taken higher. As a result the upper

glass temperature is increased and top and bottom temperature are equalized.

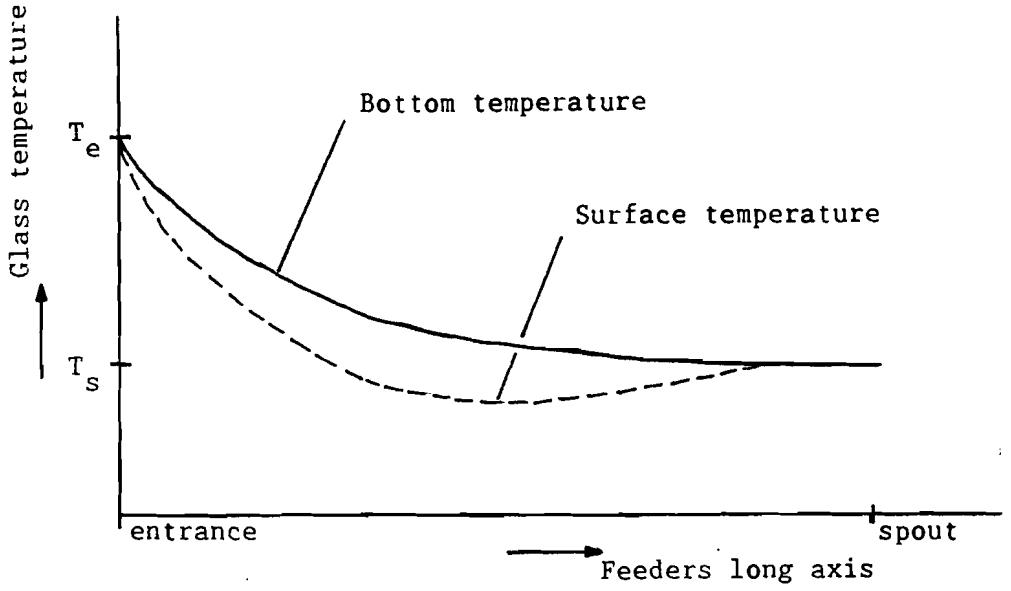

Fig. 1-4 Principle used to provide a constant temperature profile at the exit of the feeder.

The importance of the small temperature gradients in the feeders cross-section is based on the need for small temperature fluctuations (in time) of the glass at the outlet, together with homogenous temperatures around the tube in the outlet. Shaping of the glass requires a very exact temperature because the viscosity of the glass strongly depends on this temperature. Inhomogeneity of the temperature causes tension in the glass-tube.

For this reason the settings of the feeder are very critical. Besides this, the feeder reacts very slowly to adjustments. We have already seen that the bottom temperature is not very much affected by the heating. Only after a few hours the transients of adjustments in the first section are died out.

The controllers which are used to control the temperatures are mentioned in section 1.2.1. Regarding the effects described above, it is easy to understand why difficulties arise with the two PID-controllers.

Let us reconsider figure 1-4. At the present feeder installation the setpoints used for the PID-controllers are the surface-temperatures f31

and f41. Because the bottom temperatures react too slowly, they cannot be used for control. When temperature f31 is kept constant by certain adjustments, this will cause slow fluctuations of the bottom temperature. These fluctuations will affect the spout temperatures in section 2. Here the PID-controller reacts to these fluctuations, but only on the basis of surface temperature. This means that finally the most important temperature, the spout temperature at the outlet, is not very well under control! Even instabilities can occur, depending on the settings of the PID-controllers.

In practice, gas-heating and air-cooling are set so that the exit temperature is fairly constant and finally fine adjustments to this outflow temperature are done with the 'cup-heating'. Because the outflow-temperature cannot be corrected to a lower temperature, it is very important to keep the cup-heating within control-range. Once the exit-temperature is so high that the cup-heating is zero, the outflow of glass increases. If the outflow increases, the 'throughput time' of the glass in the feeder decreases, the energy loss decreases, and the outflow keeps increasing!

Not only it is difficult to keep the temperature stationary, also the changing to another set point is troublesome. E.g. after changing to another set-point it may take up to one day before all temperatures are stabilized!

Of course the phenomena shown here have their physical background. Globally, a combination of the following effects may explain the behaviour of the feeder; all dealing with energy and impulse transport:

- radiation — e.g. burner-heating
- convection — e.g. glass-flow through the feeder
- conduction — e.g. heat conduction through the refractory material
- friction — e.g. forces due to viscosity
- other forces — e.g. gravity

The following will illustrate that it is very difficult indeed to obtain a useful mathematical model of the feeder based on physical laws.

The differential equations describing energy and impulse transport in the feeder are (cf. H. Wilming, 1979):

(a) Law of conservation of mass

$$\frac{\partial \rho}{\partial t} = -\mathrm{div}(\rho.\underline{v}) \qquad (1.1)$$

where ρ = mass-density

$\underline{v}$ = velocity vector,

(b) Law of conservation of energy

$$\frac{\partial}{\partial t}(c\rho T) = -\mathrm{div}(c\rho T.\underline{v}) - \mathrm{div}\ \dot{q} \qquad (1.2)$$

where c = heating capacity

T = temperature (dependent on place; $T(\underline{x})$)

$\dot{q}$= heat flow density,

(c) Law of conservation of impulse (impulse due to gravity neglected)

$$\frac{\partial}{\partial t}(p) = -\mathrm{div}(\underline{p}) - \mathrm{div}\ \underline{\phi} \qquad (1.3)$$

where $\underline{\phi}$ = impulse changes due to viscosity forces.

Further

$$\dot{q} = \lambda_{eff}\ \mathrm{grad}(\underline{T}) \qquad (1.4)$$

where λ_{eff} represents an approximated coefficient for the heat-conduction and radiation together,

and

$$\underline{\phi} = \eta\ \mathrm{grad}(\underline{v}) \qquad (1.5)$$

where η is the viscosity coefficient (dependent on place; $\eta(\underline{x})$).

Equation (1.2) and (1.3) now become

$$\frac{\partial}{\partial t}(c\rho T) = -\mathrm{div}(c\rho T.\underline{v}) + \lambda_{eff}\left(\frac{\partial^2}{\partial x^2}T_x + \frac{\partial^2}{\partial y^2}T_y + \frac{\partial^2}{\partial z^2}T_z\right) \qquad (1.6)$$

and

$$\frac{\partial}{\partial t}(p) = -\mathrm{div}(\underline{p}) + \eta\left(\frac{\partial^2}{\partial x^2}v_x + \frac{\partial^2}{\partial y^2}v_y + \frac{\partial^2}{\partial z^2}v_z\right) + \frac{\partial \eta}{\partial x}\frac{\partial v_x}{\partial x} + \frac{\partial \eta}{\partial y}\frac{\partial v_y}{\partial y} + \frac{\partial \eta}{\partial z}\frac{\partial v_z}{\partial z} \qquad (1.7)$$

We see that we are dealing with a system of coupled partial differential equations. Because the viscosity changes with the temperature according to

$$\eta \simeq K_1 \, e^{-\frac{K_2}{T}}, \qquad (1.8)$$

the temperature depends on the velocity vector, and finally the viscosity again depends on the velocity. Moreover we see that we have a distributed parameter system, the coefficients being dependent on place. This means that in each location of the feeder a system of differential equations with different coefficients is valid which, of course, is expected from the type of process of the feeder.

For these reasons obtaining valid mathematical models is very difficult. The computational effort using final element methods becomes very high. That is why severe assumptions must be made with unavoidable model errors. For instance often the assumption is made of no convection except in direction of the feeders long axis. However, a model with this assumption cannot describe the feeder's behaviour appropriately (cf. fig. 1-5). Because of cooler side walls, always circular convection will occur.

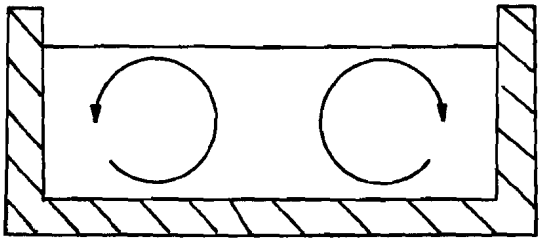

Fig. 1-5 Circular convection because of cool side-walls.

It can be stated that until now no mathematical models are obtained, that can fulfil the conditions posed by automatic control.

1.2.3 Concluding remarks

Despite of the fact that the feeder process needs an accurate control, and control is difficult because of the slow responses and other difficult properties, there is a lack of knowledge from mathematical modelling.

This implies that the control of the feeder still is based above all on experience. During the last decades the glass-trade mastered the problems of producing glass predominantly by trial and error. Only little has been known about the exact effects of the underlying mechanisms.

Notice that essentially this will not be changed by identification, as identification often deals with black box models and does not consider physical phenomena. But, having knowledge of the input-output behaviour, one might be able to deduce what mechanism is of major influence to the output.

1.3 IDENTIFICATION METHOD

1.3.1 Introduction

Modelling of a process by means of identification techniques intends to provide a dynamical model of the process in one of its specific working areas. In an industrial environment, when identification is done for the purpose of automatic control, the identification is followed by controller design and realization.

In general all methods used for identification have the same set-up (cf. A. van den Boom e.a.,1986). Still we present an overview of the identification protocol used in this project for two reasons:

- Summing up the phases of identification will clarify the rest of this report to those who are not very familiar with the subject of identification.
- Now we are able to emphasize certain aspects in the identification protocol and describe the method more specifically for this industrial application.

Identification itself is only a small part of the activities needed for automatic control. The following phases are discerned:

A. Preparation
B. Measuring
C. Identification
D. Control

We will split up each phase and discuss there major aspects.

1.3.2 PREPARATION (A)

Before starting identification first it has to be determined what has to be identified and what knowledge is already available.

A.1 Intended use of the model

On application to industrial processes the idea of 'automatic control' first has to be specified. Mostly these specifications are formulated within the project in which the identification takes place. In this stage of the project specification of quantities

and/or variables that are to be controlled within certain tolerances are hypothetical because dynamic properties are not yet entirely known.

In the feeder project the objectives have been formulated fairly general: The temperatures have to be controlled 'better'; a global specification is made on what temperature gradients would be desirable. It should be possible to set the temperatures to another value with an accuracy of $1^{0}C$ and it should be possible to stabilize the temperatures, over a long period, in between $0.1^{0}C$.

Because the result of the Universal furnace will be used for other plants, it is more important to get insight in what improvements can be made than the exact figures of tolerances and changeover times of this particular feeder.

The intended use also determines the kind of model that is to be used. Because of the control purpose, an output-error model is needed. The aim is to prescribe the feeder's temperatures to a strict behaviour over a long period. Hence, we let the model outputs fit on the process outputs in least square sense.

A.2 A-priori knowledge

To identify a model, preliminary investigations have to be done on the process. It is important to dig up all the knowledge available in order to find the major characteristics of the process like

a Physical understanding.
  What physical phenomena are underlying the process?
b What are the most relevant inputs and outputs of the process?
c Sensitivities (gain) of the inputs to the outputs
d Insight into dynamics
  What are the main time constants of the process?
e Process limitations
  To what extent the experimentator is allowed to change the process?
f Other properties like disturbances, time-delays, linearity etc.

From this a-priori knowledge choices for constructing the model are made ('global modelling'). From section 1.2 we can derive the 'global model' of the feeder:

ad a see 1.2.

ad b inputs: cool air, gas of section 1 and 2
outputs: glass-temperatures.

ad c Operators adjust inputs not more than 5 to 10%. This causes already significant temperature changings.

ad d Transfer functions to lower layers in the glass of section 2 have time constants of up to several hours!

ad e Excitation of inputs cannot be to large otherwise the feeders outflow will get out of control. Either no tube can be made (too low a temperature) or an ever increasing outflow occurs (too high a temperature).

ad f We do expect non linearities (e.g. heating depends non-linearly on the gas flow). Time-delays will surely occur because of flow of glass from section 1 to section 2.

This information is also necessary for the experiment design of phase B.

To gather a-priori information, the following sources can be used:

- Experience of technical specialists, operators, etc.
- Earlier experiments
- Literature

1.3.3 MEASURING (B)

B.1 Measuring system

In most cases the measuring equipment already available at the plant will not satisfy identification purposes. Usually more variables are to be measured at a higher sampling rate than required for control only. Also injection of excitation-signals has to be taken care of.

In an industrial environment high demands are made upon the measuring system. Moreover, there is always lack of time when measuring on industrial processes and it is difficult to repeat measurements when later on they appear worthless.

Therefore a reliable measuring system must be designed, in which malfunctioning of sensors and other errors can be discerned quickly. 'On-line' measuring will be of great help. In section 2 the measuring system that is used at the feeder will be described.

B.2 Experiment design

To be able to identify the process, application of special excitation signals will almost always be required.
Here we summarize in short what experiments should, or can, be done. A more detailed discussion of the experiments particularly done at the feeder is given in chapter 3.

Before starting the experiments first those working points are to be determined in which the measurements have to be done, and around which the excitation signals will be injected. Normally these will be the working points that are used in the common production situation. The feeder's working points are determined at 130 and 160 kg/hour pull rate.

I Sensitivity and dynamical speed analysis

For each input-output relation the sensitivity (gain) has to be investigated. Even more important is with what speed the outputs follow the inputs (main time-constant of the transfer function). This is done by injection of a step function at each input, and measuring until all instationarities are died out. The amplitude is taken within the common adjustments done at the process.
The smallest time-constant of all transfer-functions determines the sample rate to be used in the experiments. The ratio of input-amplitudes of these experiments is chosen so that, at the outputs, the influence of all inputs is about the same.

II Linearity and hysteresis analysis

To recognize non-linearities and hysteresis of the process around its working point, a staircase input is applied.

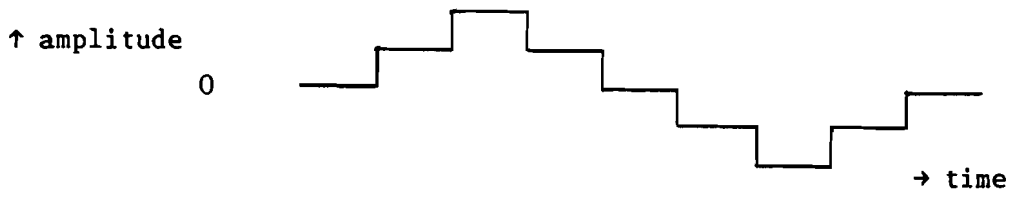

Each staircase has to be long enough for the process transients to be died out.

Non-linearities are noticed when the measured staircases are not of equal level , hysteresis when they do not return to zero.

III Bandwidth analysis

Semi-white noise is applied for input by means of a Pseudo-Binary-Random-Noise-Sequence (PRBNS). The clock frequency of the generating shift register of the PRBNS determines the bandwidth of the input signal. The clock period is taken small to be sure the excitation signal is wide-band compared to the process. The bandwidth of the process can be deduced from the frequencies of the output signals.

IV Disturbance analysis

To investigate the disturbance-behaviour of the process a measurement of the uncontrolled process is done. In case the stationarity of the disturbances are doubtful, this experiment should be repeated between several experiments.

V Estimation experiment

Experiment to collect data to be used for modelling.
In order to gather all information about the dynamic behaviour a PRBN-sequences are applied at all inputs. The clock frequency is chosen such that the noise can be considered white compared to the process dynamics, in order to assure convergence and numerical stability of the estimation algorithms. The amplitude has to be large enough to influence the outputs significantly but small enough to keep the process within its linear area.

VI Validation experiment

Experiment to be used for validation of the estimated model.
Same experiment as V but the frequency is not restricted here.
Of course it is necessary that all frequencies that will be used when the model will be applied, are available.

B.3 Measuring experiments

Not always all desired experiments can be done within the time constraints of a project. Conscientious planning is required and

with help of the 'on-line' analysis during the measurements, adjustments of the planning can be done.

1.3.4 IDENTIFICATION (C)

Identification itself, the modelling of the process dynamics, consists of three phases, each of them equally important:

1. Signal preparation
2. Estimation
3. Validation

C.1 Signal preparation

Even if phase B has been successful and all the required data are available, the estimation of the model cannot be started yet. In chapter 4 the preparation work on the feeder data is explained in detail, here we will survey the signal processing activities in short.

Estimation algorithms try to find (dynamic) relations between the input- and output data offered to them. Each part of the data that not belongs to (or is yielded by) the dynamic behaviour of the process can influence or deteriorate the estimation, or even make estimation impossible. Therefore , all the data that is known to be irrelevant for estimation has to be extracted. What is supposed to be irrelevant is often not easy to determine. These, sometimes crucial, decisions are made on the basis of

- a priori information or intended use (from phase A)
- signal analysis
- demands of the estimation algorithms used

The following preparation activities have to be done:

- **Visual inspection of the data**
  The human eye is a valuable tool for inspection of the measured data. If the source of possible irregularities is known, or if they are known certainly not to be part of process information, they can be removed. In section 4.1 it will be shown how.

- **Peak-shaving**
  All measuring errors (e.g. if the sensor gets stuck) that cause excessive amplitudes, can be removed. Boundary determination and interpolation to remove the peaks, are done by the peak-shaving algorithm.

- **Spectral analysis**
  Frequency information will provide insight in the disturbance behaviour and noise components of the signals. Bandwidth analysis must be done and checking whether constraints for estimation are fulfilled.

- **Correlation analysis**
  Cross-correlation of inputs and outputs can be done in order to estimate time-delays. Hereby the estimation algorithm can be saved from estimating time-delays.

- **Trend- correction**
  All measured data contains offset (dc-component) and frequencies that are low compared to the process dynamics. These are called trends. The estimation algorithm cannot deduce dynamics out of trends because the duration of the experiments will be too short for this. Still the trends contain relatively much energy. Trends must be removed by high-pass filtering. Here, choice of the cut-off frequency needs great attention.

- **Data-reduction and scaling**
  The measuring is always done with a higher sampling rate than needed for estimation. These data are used for the signal preparation described above. Now this information can be thrown away by reduction, taking one sample out of more at a constant interval.

  The last step is scaling. In order to estimate all variables with equal weight, each input-output relation must be represented with the same importance. This means that the power of the signals must be equal. The amplitude of all signals is multiplied by factors such that their variances become equal (the signals had already zero mean).

C.2 Estimation

Out of the wide offer of estimation procedures, PICOS developed one approach that should provide adequate estimation results on industrial processes. It is an output-error method that finally leads to a state space model that is particularly suitable for control use. This approach will be outlined here (cf. fig. 1-1). In chapter 4 more details are presented on this subject.

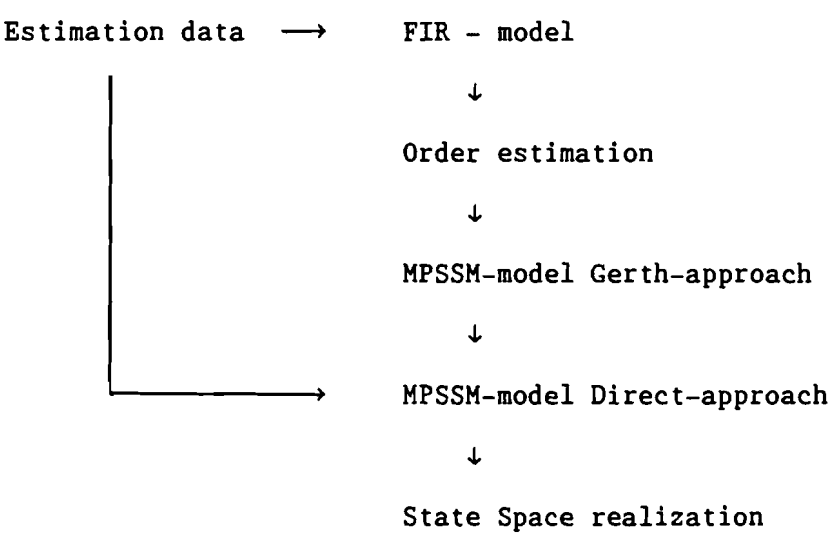

Fig. 1-6 Outline of estimation procedure.

Industrial processes, as we can see from the feeder example, always have difficult properties like non-linearities, non-stationarities, etc. Moreover they are often distributed parameter systems. The dynamical models available cannot cope with these aspects; they represent the process as linear, stationary and with a lumped parameter system (i.e. it is supposed that the properties can be described by a partial differential equation of which the coefficients are independent on place). In other words the process observed is always outside the modelset; we try to describe a process with a model that principally cannot describe it completely.

Nevertheless it is possible to use a large modelset and reduce the model-errors to a minimum. Therefore, a Finite Impulse Response (FIR)-model is used (cf. J. Vaessen, 1983). The impulse response of each transfer function (p inputs to q outputs) is represented by a finite number of parameters $M(k)_{ij}$ (i=1..p, j=1..q, k=1..n with n finite). The

matrices M(k) with elements M_{ij} are called Markov-parameters. A disadvantage of the FIR-model is that it needs a huge number of parameters (nxpxq).

In the next step a polynomial fit is made on the impulse responses of the FIR-model (cf. H van der Weijden, 1984, ch.2). It can be shown that from a model with order r, at least r Markov-parameters are mutually independent and the others can be related to these by a recurrent relation. After determination of the order r the Minimal Polynomial Start Sequence Model (MPSSM-model) is yielded. To this end the minimal polynomials are fitted on the FIR-impulse responses in a least square sense. This is called the Gerth-approach. The polynomials are described by the following parameters:

r polynomial coefficients a_i (i=1..r)

start sequence consisting of r Markov parameters M(i) (i=1..r),
dim[M]: pxq,

with p the number of inputs,
q the number of outputs.

The number of parameters is now reduced to rx(pq+1).

Because the Gerth-model used only the FIR-model as input, and the FIR-model did not describe the process in the most adequate way (it was a finite approximation), it is advantageous to use the estimation data again.
With the Direct-approach (cf. H. van der Weijden, 1984, ch.3) the parameters a_i and M(i) are estimated directly from the data. The Gerth-model is used as start value for the algorithm.

Finally we deduce (cf. R. Oudbier, 1986) from the MPSSM-model a state space model (state space realization). At this stage, the dynamic behaviour of the process is available in a representation with a limited number of parameters. The states of the process that are available now, are used profitable for control-design.

C.3 Validation

As it is known that the model is not in the modelset, it is not guaranteed that the model is a valid one, i.e. that the model describes the dynamic behaviour appropriately.

This is checked by:

- comparing the model with the a-priori knowledge available
- simulation with the model on a different dataset as the one used for the estimation and comparison of the simulated outputs with the measured outputs (model-error). In this validation experiment also the performance of the model can be judged.

1.3.5 CONTROL (D)

Because this phase is outside the scope of this report it is only illustrated what is done after the identification phase has produced a useful model.

D.1 Controller design

On the basis of the model a controller is designed, that is able to control the process in its working area. The use of the model is twofold;
the dynamical properties stored in the model are used indirectly for design and simulation,
and/or the model is used directly for control when a model-reference controller is used.

D.2 Controller testing

With the help of the measuring system used for identification the controller is tested at the process in practice.

D.3 Realization

New hardware is installed at the process and automatic control is applied for production.

2 MEASURING SYSTEM

2.1 INTRODUCTION

Higher demands are made upon a measuring system used for identification purposes than upon the standard measuring and control system available at a plant. PICOS has developed such a special measuring system in a former project. However, it had not been developed until completion, and new demands were formulated. For the feeder project a new transportable measuring system is developed on the basis of the former one. The system will be used in general for various identification purposes, but its first full application was taking measurements at the Universal furnace.

Before the system is described in this chapter, the main demands that were formulated, together with some underlying considerations, are surveyed.

- **Measuring from up to 40 signals.**
  40 Input channels are required with the possibility of extension to more.

- **Output of testsignals.**
  Up to 8 output channels that can be applied with various kinds of testsignals.

- **Data-storage.**
  All measured data are used 'off-line'. Flexible data-storage of measuring- and excitation-signals, together with the corresponding experimental set-up and signal-description is therefore needed.

- **Transportability.**
  The system is used at different processes in different plants. Its size must be restricted.

- **Flexibility.**
  As few constraints as possible are to be made beforehand. Although measuring of glass-(sub)processes is the prospect, no assumptions are made in advance on the process, signals or environment.

- **Reliability.**
  The main task, registration of the process-data, must always be continued, whatever malfunctioning of peripheral equipment and/or the user may occur.

- **'On-line' facilities.**
  To avoid wasting of time by doing useless experiments, one must be able to get insight in the validity of the measurements during the experiment. Wrong experiment design, malfunctioning of sensors and any other errors, should be noticeable at an early stage. Specially if the duration of each experiment may be several days, as is the case in the feeder-experiment.

  For this reason the interactive package PRIMAL is connected to the front-end. With help of PRIMAL, graphic display and early analyses can be done.

- **User-interaction.**
  The measuring system must be an independent system that is controlled directly. Hence, the user must be able to operate all functions at the system terminal. With the help of data display, signal descriptions, experiment status etc., the user controls the progress of the experiment he wants.

The description of the system is divided in a hardware and a software part. At the end some experiences are presented on the development activities.

The user of the PICOS measuring system is referred to 'PICOS Measuring System User Manual', G. van Vucht (1987).

2.2 HARDWARE

In fig. 2-1 the hardware configuration of the PICOS measuring system is shown. The central part of the system is the VAXELN front-end, a Micro-VAX computer with realtime programming software. The measured data are collected here and testsignals are sent out. Input is provided by the PICOS UNiversal INput Cards (PUNIC) and analog/digital converters. Output is provided by digital to analog converters. The front-end

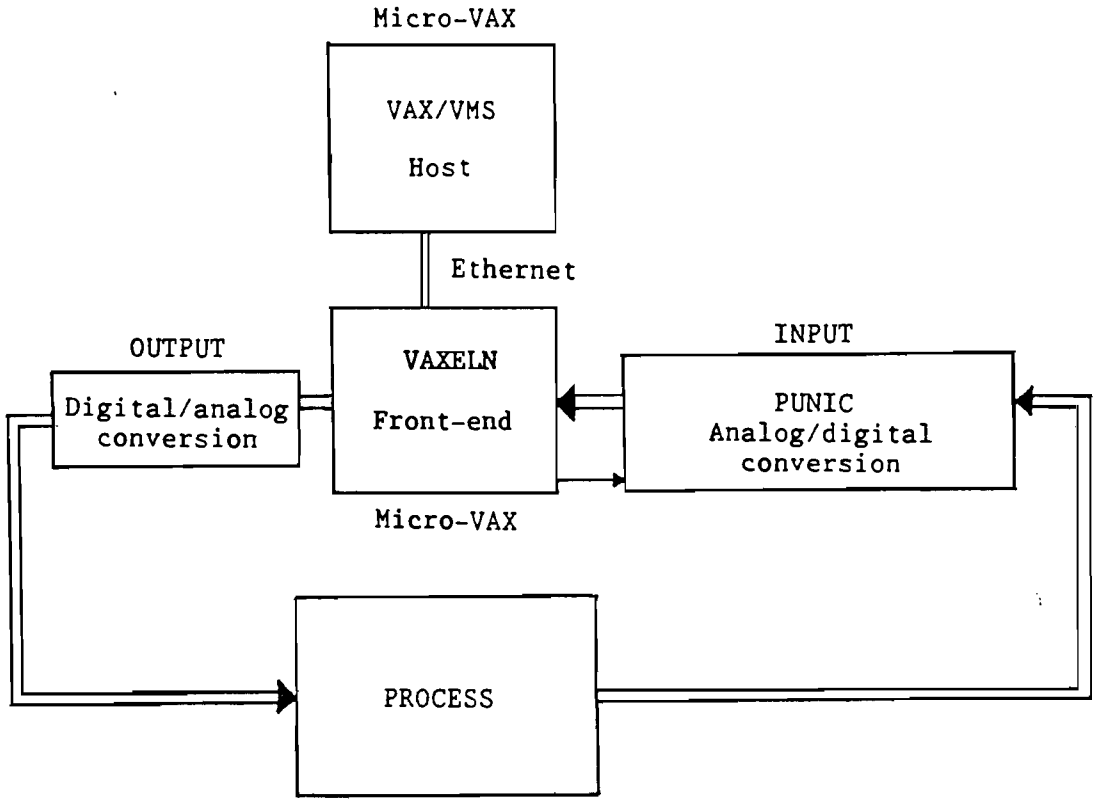

Fig. 2-1 Configuration of the PICOS measuring system.

computer is connected via a DEC-Ethernet link to the host computer, a Micro-VAX with VAX/VMS operating system. The host is used to build the VAXELN software, and to run the software package PRIMAL.

The two Micro-VAX's together with their peripheral equipment, power supply and cooling are put in a transportable 4-wheel-cart of 1.8m long x 0.85 wide x 1,5 m high.

2.2.1 VAXELN front-end

The heart of the measuring system is the VAXELN realtime programming software, running on the front-end Micro-VAX. VAXELN is a software product for the development of dedicated, realtime systems on VAX-processors. VAXELN applications run on Micro-VAX microcomputers (targets), with no general purpose operating system present. The development and building of the software is done under a common VAX/VMS operating system (host processor). Once the application is developed

with the 'Toolkit System Builder', it can be loaded downline into the target computer. With the system builder one combines all programs together with system software, drivers and services to a functioning system. Thus, the target is not bothered by operating system 'overhead'.

The main features of VAXELN are:

- **Concurrent executing programs.**
  Multi-tasking and multi-programming is provided. Because the same CPU is used, this concurrency is only virtual.

- **Transparant network support.**
  Transparant communication between jobs across a network with more computers is provided. The VAXELN-network service supports 'high level' virtual communication via DEC-net links. This means the user does not 'see' lower communication levels and is not bothered by hand-shaking protocols or whatsoever.

- **File service.**
  The VAXELN file service supports I/O operations from programs to local and/or remote file storage devices.

- **Program debugging with VAX/VMS.**
  The target system can be debugged remotely from the host if target and host are connected with Ethernet.

Chapter 2.3 deals with the software that is made with VAXELN on the front-end.

2.2.2 Input

To provide flexible and reliable measuring, PICOS developed a 'signal conditioning card' called 'PUNIC': PICOS UNiversal Input Card. Analog signals are measured and conditioned so that they get optimal amplitude, level and bandwidth.

The conditioning that the card applies is optional to the user. The various settings of the card are software-controlled from the front-end.

The amplification, offset correction and filtering is specified in a 14-bits 'signal conditioning word' that the card reads in from a digital output card at the front-end.

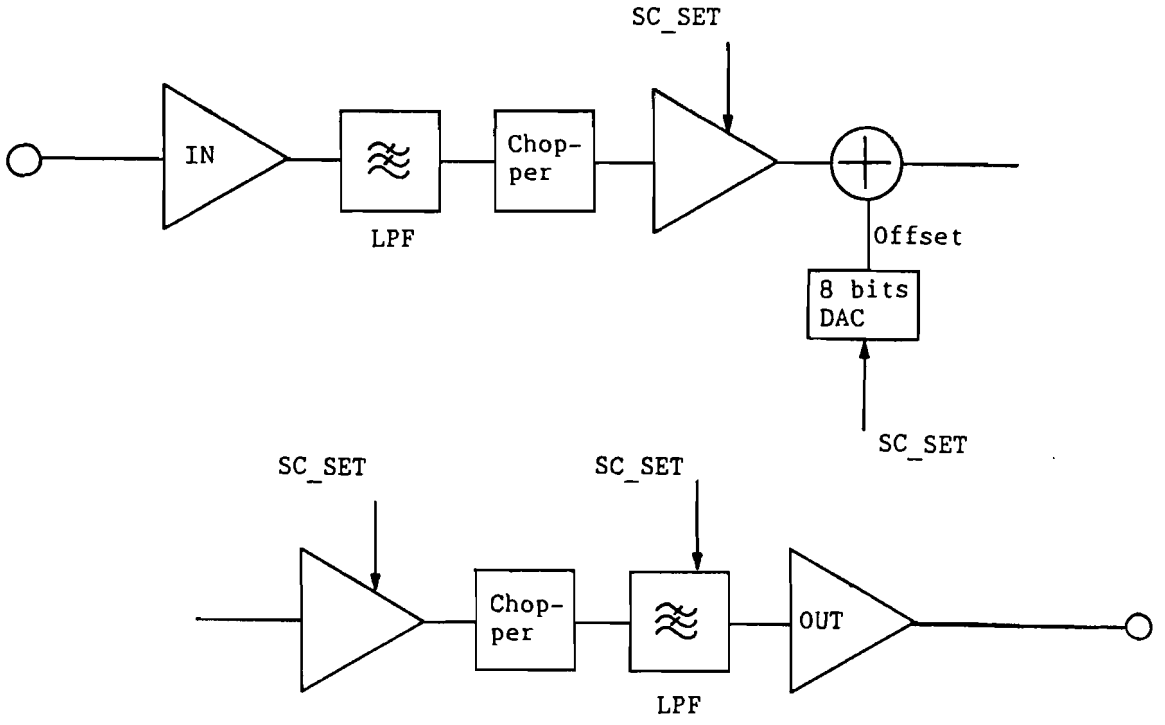

Fig. 2-2 Block diagram of PICOS UNiversal Input Card.
Sc_set = 'signal conditioning word'

The block-diagram of the PUNIC is depicted in fig 2-2. We see:

- Input amplification for high input impedance. To avoid temperature drifts, it is embedded in a small furnace keeping the temperature at 50^{0}C.
- Low-pass filtering with 250 Hz to remove high frequent noise.
- Chopper-circuit to avoid drifts in the electronic circuit of the PUNIC.
- Amplification at choice. The amplification level (one out of 8 possible choices) is specified by three bits of the signal conditioning word (sc_set).
- Offset correction. Offset levels at choice can be added to the signal. Specified by 8 bits of the signal conditioning word.
- Amplification after offset correction. Choice out of 4, specified by 2 bits of the signal conditioning word.

- Low-pass filtering. Frequency at choice specified by 3 bits of the signal conditioning word.
- Output amplifier.

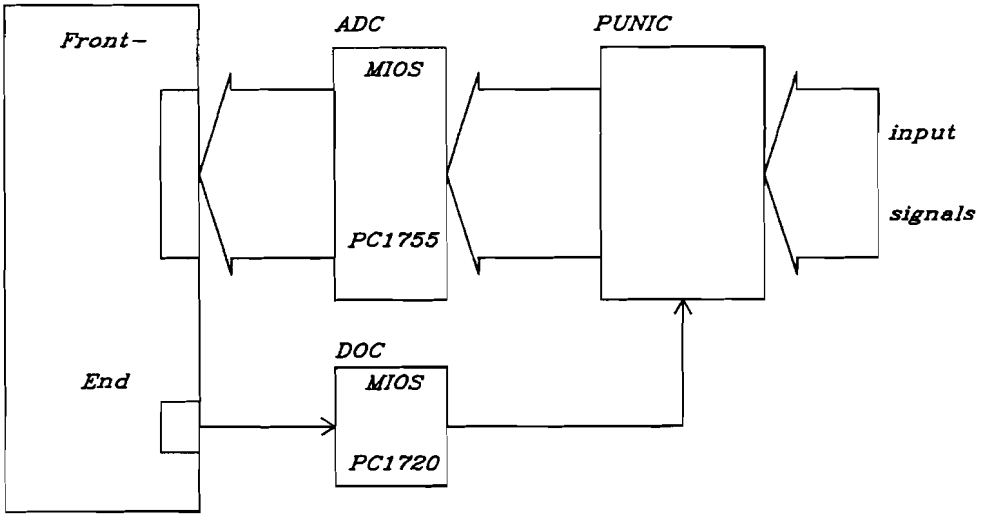

Fig. 2-3 Scheme of 'INPUT BLOCK'.
AIC = Analog Input Card
DOC = Digital Output Card

The analog output of the PUNIC has a voltage range between -10 and 10 volt. The analog values are converted to 12-bit words by an Analog Input Card (of the 'MIOS' system), which is connected to the Micro-VAX. In the front-end software the signals can be converted to physical units again.

The channels to which the signals are connected can be chosen such that 'arranging' becomes possible: which signal is measured via which PUNIC-channel, via which ADC-channel (cf fig. 2-3). In the front-end each channel of the ADC is assigned to a data-element in an array.

2.2.3 Output

Identification requires injection of testsignals to the process. This will always be variations around the nominal settings of the inputs of the process. In the front-end the necessary values of testsignals are calculated. Each sample moment the calculated values are sent to an 8 bits D/A converter (MIOS). The converter has a current output of 0 to 20 mA. This current is converted to a voltage (C/V circuit, cf. fig. 2-4). Finally this voltage is put in an adding-circuit that adds it to the voltage control of the input-actuator of the process.

By limiting the voltage range of the output of the C/V converter we are able to limit the changes of the actuator input signal. This means that safety is guaranteed, because in the worst case, when the front-end program is ordered to send out 100% amplitude, the actuator input is only changed with the maximum of the C/V converter output.

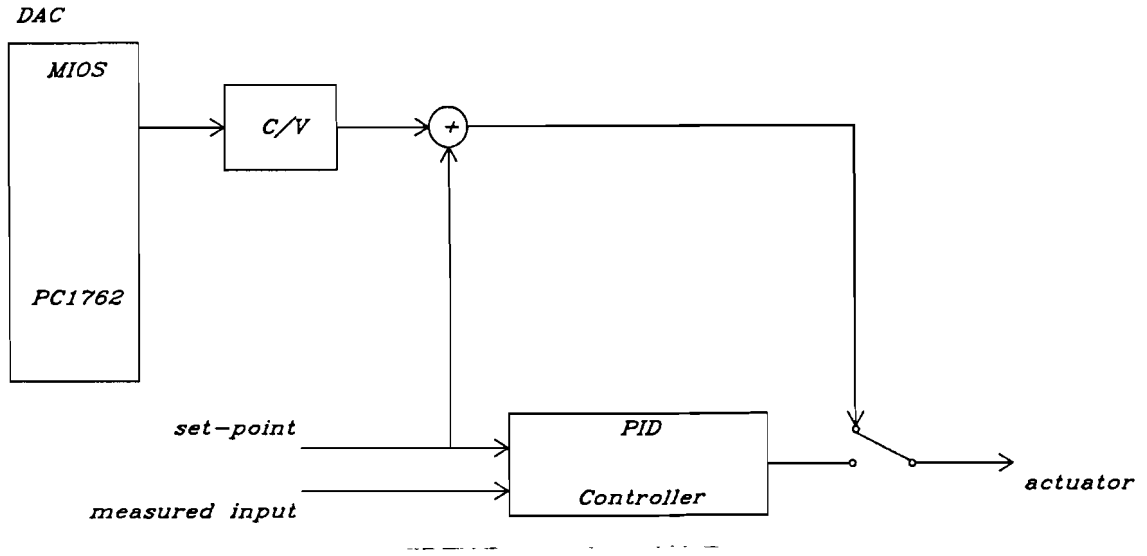

Fig. 2-4 Scheme of 'OUTPUT BLOCK'.
DAC = Digital to Analog converter
C/V = current to voltage converter

2.3 SOFTWARE

As can be seen from the hardware structure, the software can be divided into two parts. First, the front-end task that runs on the target VAX. Second, we have the software package PRIMAL (Package for Real-time Interactive Modelling, Analyses and Learning) running on the host VAX. In section 2.3.1 PRIMAL and the interface environment with the front-end will be described. Section 2.3.2 deals with the software of the front-end as an independent system.

2.3.1 Interface with PRIMAL

PRIMAL was developed at the group System and Control, Department of Applied Physics of the Eindhoven University of Technology. The package is made for dynamical process-analysis. For real-time modelling interactive collection, processing, and presentation of signals is

provided. When PRIMAL is connected to the front-end measuring system, it is a sophisticated tool for 'on-line' graphical display and analyses of the signals. However, because PRIMAL is a complete package to do identification experiments, it has also the facilities for interaction between user and measuring experiment (like experiment definition, start/stop, etc.).

The development of the transportable PICOS-measuring system intended to yield a system with control facilities at the target itself. To avoid confusion, operation of the front-end just by using PRIMAL is made possible too. An independent front-end system is realized with communication facilities with PRIMAL. A communication task is made on both sides together with a suitable communication protocol. The messages are sent over a DEC-Ethernet link between the two VAXs.

Viewed from PRIMAL, the user operates the front-end system by

- Defining an experiment within PRIMAL with
  - .experiment name
  - .sample time
  - .start time
  - .end time

- Defining measuring signals with optional
  - .name
  - .physical unit
  - .conversion factors to physical units
  - .software filter Y/N
  - .local storage Y/N
  - .ADC-channel number
  - .PUNIC-channel number
  - .etc.

- Defining testsignals (process-inputs) with same options as above but this time with a DAC-channel number.

- Connecting the front-end and downloading the experiment definition to it.

- Experiment control like

.start experiment
.stop experiment
.put test signal on channel
.etc.

Once the experiment is started, PRIMAL reads in the data-messages from the front-end which are sent every sample moment. To control the flow of these data-messages the front-end contains a data-buffer. For the command-messages to the front-end, the buffering of the Ethernet-circuit only suffices.

2.3.2 Front-end task

In section 2.2 we have seen that the PICOS transportable measuring system should be an independent system. This implies that the front-end task must provide more than a front-end system in the literally sense of the word. It appeared that with the demand of a sample rate of about 10 Hz, more than enough time was left to realize user environment facilities. Indeed the present front-end contains these facilities. We summarize here the functions of the front-end task:

- Measuring signals, i.e. reading of signals prepared and digitalized by the 'input block'.
- Filtering, i.e. software-filtering of the signals.
- Data-storage, i.e. local file storage of data and experiment description.
- Generation and output of excitation-signals, i.e. calculation of various testfunctions and sending the values to the 'output block'.
- Communication with PRIMAL.
- User-interaction, i.e. operation commands and display.

In this chapter it will be explained how the front-end software is structured. For reasons of clarity, less relevant parts of the program, such as lower level procedures, are not mentioned. Those who want to work with the software are referred to the user's manual (G. van Vucht, 1987).

In fig. 2-5 the software structure is schematically outlined. It is neither a complete flow-chart, nor a complete data-flow diagram. It is only a visual help to the following concise program explanation.

Startup

After the front-end program is booted from the host the program starts to run automatically ('start' label in fig. 2-5). The front-end program is a multitask application. This means a single job is running with several subprocesses.

The main program does the necessary preparations:
All needed variables that are shared by the subprocesses are initialized. They form the global structure of the program. Part of this global structure are the variables that contain the experiment description; those parameters that completely determine a measuring experiment. To understand the functions of the subprocesses, knowledge of the experiment description variables is helpful. We have:

- System parameters
  - .experiment name
  - .sample time
  - .filter coefficients (set of 2 filters, each containing 5 filtercoefficients)
  - .measuring-signal set (set of signal numbers to be measured)
  - .test-signal set (set of signal numbers used for output
  - .display set (set of display screens each containing signal numbers to display)
  - .display select (number of currently selected display set)

- System status
  - .Store (boolean indicating that an experiment with local file storage is running)
  - .Primal (boolean indicating that a PRIMAL experiment is running)
  - .end time (number of samples after which the experiment* expires)

---

* In the front-end program an experiment is defined as running if either 'store ' or 'primal' or both are true.

- Signal-description
  - .signal name
  - .physical unit
  - .conversion factors to physical units (multiplication and offset)
  - .measuring signal (boolean, indicating whether the signal is a measuring signal to read from the AIC)
  - .excitation-signal (boolean, indicating whether the signal is an excitation-signal used for output)
  - .filter (boolean, indicating whether the signal is to be filtered
  - .filter type (which filter to use)
  - .display (boolean indicating whether the signal is to be displayed on the screen)
  - .store (boolean indicating whether the signal is to be stored)
  - .PUNIC address (channel number of PUNIC card, not in use for testsignals)
  - .MIOS address (channel number of ADC or DAC-card)

  Up to 256 signal descriptions can be specified. Input as well as output signals are specified with these variables. In case of output signals the calculated function-value is treated as the signal value

- Excitation-signal description.
  - .signal type (step, sine, stair, prbns, pulse)
  - .signal parameters (amplitude, period, level, duration)

The main program also takes care of the declaration of procedures and processes. After initialization, files are opened and communication ports are created.

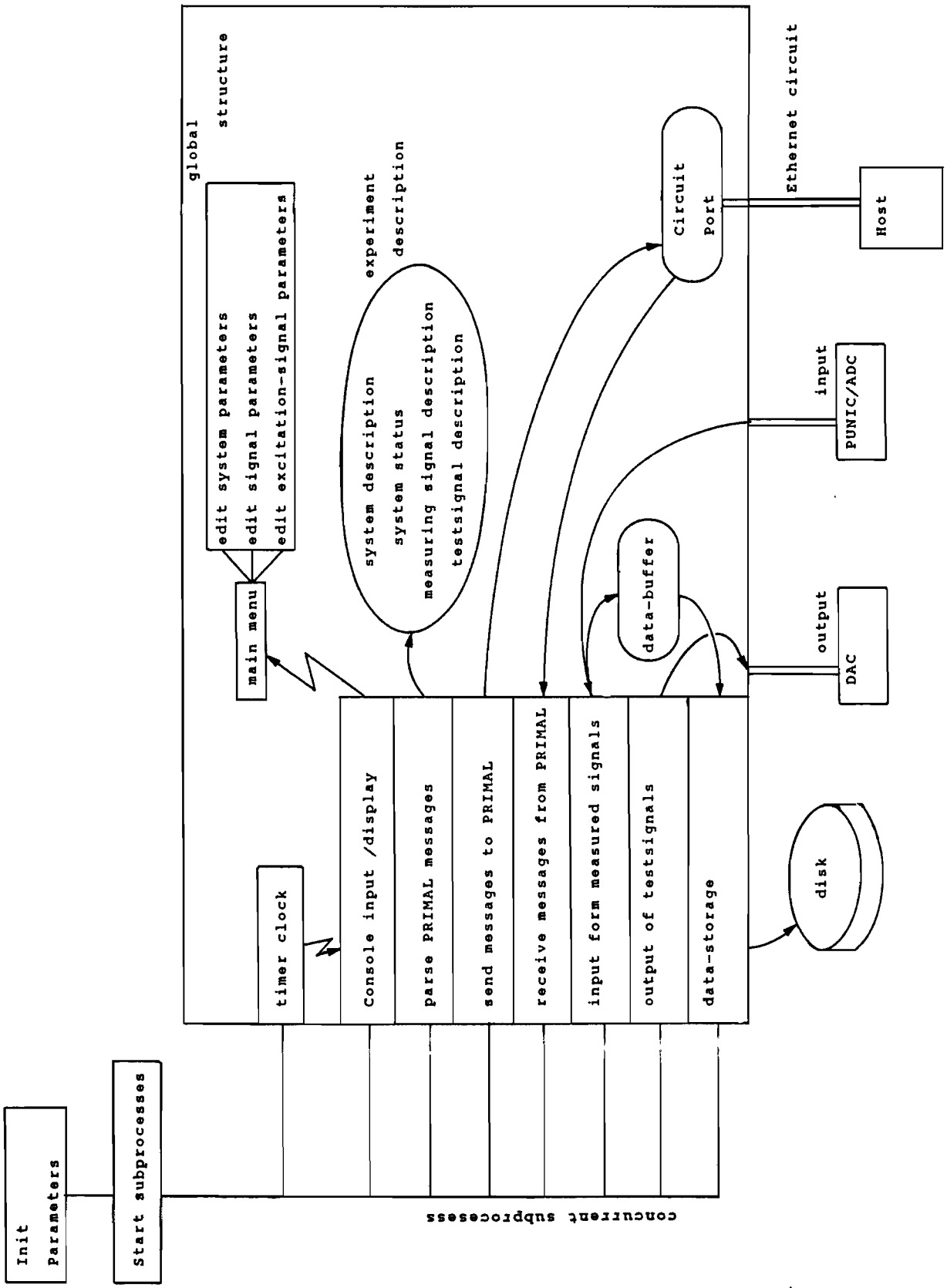

Fig. 2-5 Simplified scheme of front-end software structure.
The arrows show only a part of the data-flows!

Now the subprocesses can start. First the timer clock is initialized. The absolute time of the host-computer is read in and hereafter the clock of the target synchronizes all subprocesses. They all run 'in parallel' and are mutually dependent by synchronization mechanisms as mutexes, semaphores and events. The synchronization structure is not discussed here; the function of each subprocess is described below:

Input from measured signals

Each sample moment this process reads in all (40) channels from the AIC. Dependent on the specification in the experiment description the values are converted to physical units, filtered, put in a data-array, and sent to a circular data-buffer.

Console input and display

This process serves the communication with the user. The signals specified for display are displayed in optionally 5 different display screens (20 signals each). The user can interrupt the display to edit experiment parameters by means of several menu-screens. When the front-end is used without PRIMAL the front-end is operated via these menu screens. After a new experiment is defined the PUNIC-card can be reset by the 'set signal conditioning function'.

The screens can also be used for displaying experiment parameters without changing them. When PRIMAL is used for operation, connection has first to be established by selecting the 'connect PRIMAL' option at the system menu. Then the Ethernet circuit between target and host is established.

Receive messages from PRIMAL

This process is only occupied with waiting for messages at the receiver port of the Ethernet circuit. After the message is received an event is signaled to indicate this to the parser process. The next message is not received until the parser process 'liberated' the former message.

Parse PRIMAL messages

The messages from PRIMAL are parsed by a separate process. The actions taken on the PRIMAL commands have the same effect as the user who operates the front-end via the menu-screens. In both cases the experiment description is changed first, and all processes react on those changes that deal with their particular task.

Send messages to PRIMAL

Because the Ethernet circuit assures a communication without errors, no affirmation messages are needed. The only messages that have to be send to the host are data-messages. The send-data process gets the data from the data-buffer, constructs a message string from it (ASCII-string) and puts it on the circuit port.

Output of excitation-signals

In a global variable structure the values of the output-signals are administrated. In a chain of pointer variables a superposition of testfunctions is stored. Out of 5 different functions the user constructs an excitation signal for up to 8 channels. The 'process output' keeps up the calculation of the proper output values and sends these to the DAC-card each sample moment.

Data storage

To store all information gathered during an experiment, first a 'configuration file' is made. In this file all variables that determine an experiment are stored. To avoid non unique filenames they consist of a standard name (like 'feeder') and are extended with a number. Each time a new file is created this number is incremented. For example we get a name like: 'feeder002.cnf'. The data corresponding with with this experiment is stored in 'feeder002.dat'. Each time data is put in the data-buffer the process data-store writes the data in this file. The buffer that is used is the same as the one used for sending the data to PRIMAL, but with a different semaphore.

After an experiment is stopped the files are closed. Experiment parameters cannot be changed during an experiment. If the user still changes parameters by the menu screens, a new configuration- and data-file are opened.

Once closed, the files can be copied to a tape on the Micro-VAX or to another disk, using the VAX/VMS operating system at the host. Before closing it is impossible to look into the files because 'shared opening' of files under VAXELN appeared not to function.

2.4 CONCLUDING REMARKS

Remember that a part of the components of the measuring system were already present before the development activities as described in this report, were done. Our development was particularly focussed at the front-end program in which the data-storage, excitation of signal output, and menu screen operating facilities are new. The interface with PRIMAL is also realized. Finally the integral system is built in in the 4-wheel cart*. Here some aspects about the system that may be of interest are remarked:

- Performance of the system

  A test of an experiment at a sample rate of 10 Hz showed that this was easily reached. Operation with the menu-screens worked very well. The disadvantage of less flexibility -compared to a command language- is compensated by the fast and reliable operation via the menu's. Sometimes affirmation questions are built in to avoid mistakes.

  The operation with PRIMAL also fulfilled the expectations. Only some difficulties arised from tuning the mutual experiment descriptions completely.
- The communication with PRIMAL via the Ethernet-link is established with two separate circuits. Although the Ethernet-circuit should support full-duplex communication it turned out to be malfunctioning under some circumstances. Finally two circuits are used, each for one direction.
- The terminal of the target is at the same time console of the Micro-VAX, that always must be 'on(-line)'. By blocking the keyboard key 'break' unexpected breaking is avoided. Input of ctrl Z at the keyboard can also 'hang up' the program. This is cleared by implementing an exception handler especially for ctrl Z-input at all console- and edit-functions.
- Synchronization of the processes is done without using special design methods that support real time programming. With the powerful debugging facility proper functioning can be assured. A lot of the synchronization problems are solved by the following 'release' construction:

---

*Several persons have been involved. Kindly read the acknowledgements.

```
wait for event  ('EVENT1' or 'LIBERATOR')
begin
  if (not 'LIBERATOR') then do
    'In case of EVENT1.....'
  else
    'released from waiting for EVENT1'
end;
```

- Before, the experiment-definition loading was done by reading in a file from the host. At present loading is done from PRIMAL. It is recommended to recover this file loading option again, to provide easier loading than with the menu's can be done. Other, more detailed recommendation for future improvements are given in the PICOS Measuring System User Manual (G. van Vucht, 1987).

3 MEASURING EXPERIMENTS

3.1 MEASURING SITUATION

For the experiments for the feeder-process identification, the PICOS measuring equipment is used as described in chapter 2 (cf. fig. 3-1). In this section it is described which signals have been measured. Next, something is said about the characteristics of these signals. The last section deals with the disturbances that appeared during the measurements.

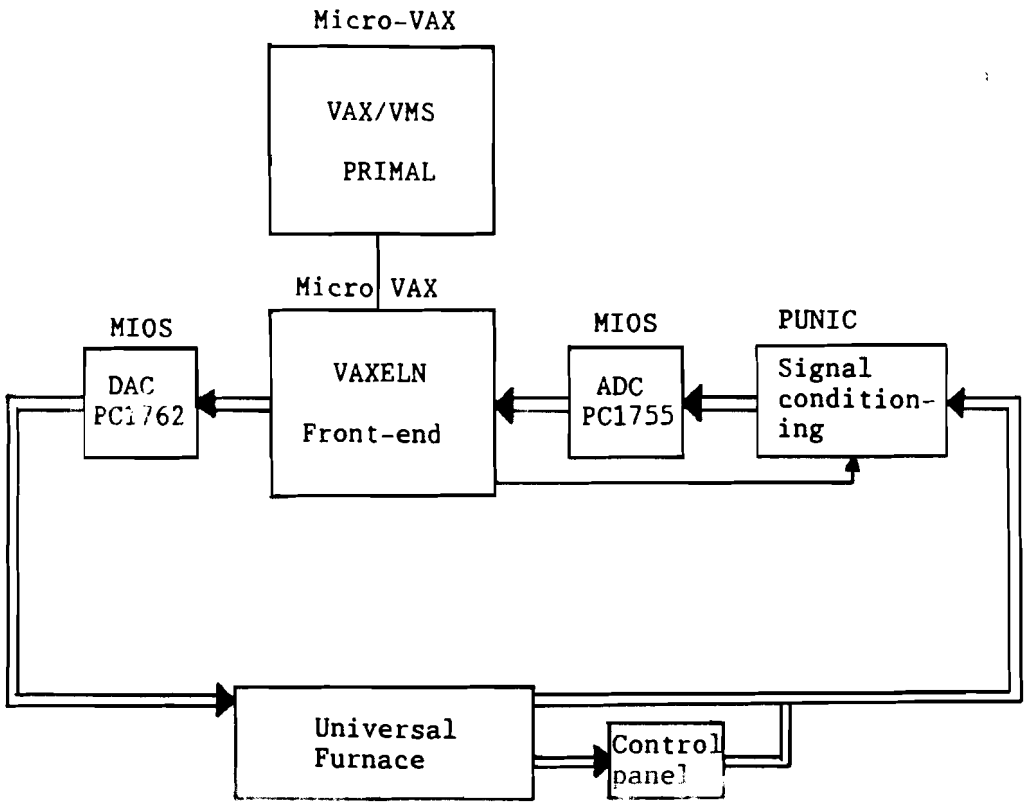

Fig. 3-1 PICOS measuring system connected to the Universal furnace.

3.1.1 Measuring points

From the description of the feeder process in section 1.2 we know what quantities of the process are relevant for identification. All inputs and as many outputs (glass-temperatures) as possible are measured. To obtain more information about the temperature distribution in the

feeder, thermocouples have been installed in the spout section. In fig. 3-2 the positions of all thermocouples in the feeder are shown. A code is assigned to each measuring point.

The feeder is divided into four parts. The front-part of section one with code 'Fdfr_' (from feeder-front), the middle part of section one with code 'Fdmi_', the back part with 'Fdba_' and finally the spout section (section 2) with code 'Fdsp_'. In total we have 25 thermocouples, 5 threefold, one sixfold and 4 single couples. In section one, 3 threefold couples are positioned in the center of the glass. Their height is indicated in figure 3-3. The upper couple is always positioned in the atmosphere above the glass level. It has code fai, with i the number of the feeder part. The lower two couples in the glass have code fi1 and fi2. At the beginning of the spout section a temperature profile is measured at the cross-section of the feeder with the sixfold couple in the center, and 2 threefold couples at the left and right of it (cf. fig. 3-4). The codes are based on their left-, middle-, and right-position. The couple Fdsp_fm2 of the six-fold couple was broken from the beginning and therefore is omitted. The temperatures fa4, fa6 and fa7 are atmosphere couples positioned at the edge of the refractory material. Temperature f51 (Fdsp_f51) is positioned centrally in the spout.

There are 3 inputs of the feeder's process:

- F1_gas gas flow of the burners of section 1
- Cool_air Cool air flow through the cooling channel of section 1
- F2_gas gas flow of section 2

Besides the gas flows, the air flows are measured too:

- F1_air air flow of the burners of section 1
- F2_air air flow of the burners of section 2

During the identification phase, it might be necessary to check the origin of certain disturbances, or other unexpected phenomena. It is important to know whether other variables than the process in- and outputs have been changed during the experiments. Therefore it is useful to measure the environmental conditions of the experiment.

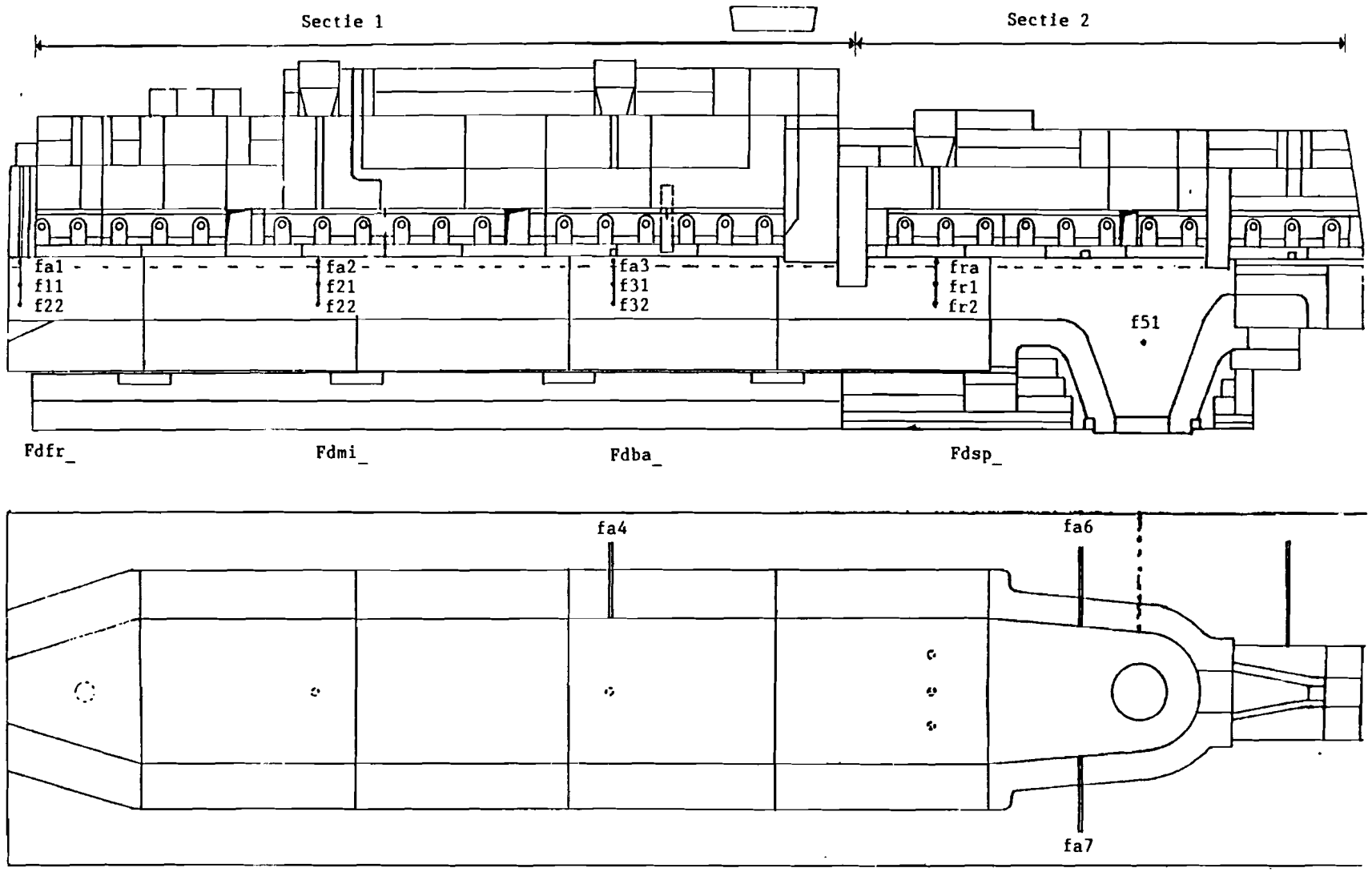

Fig. 3-2 Position of thermocouples in the feeder.

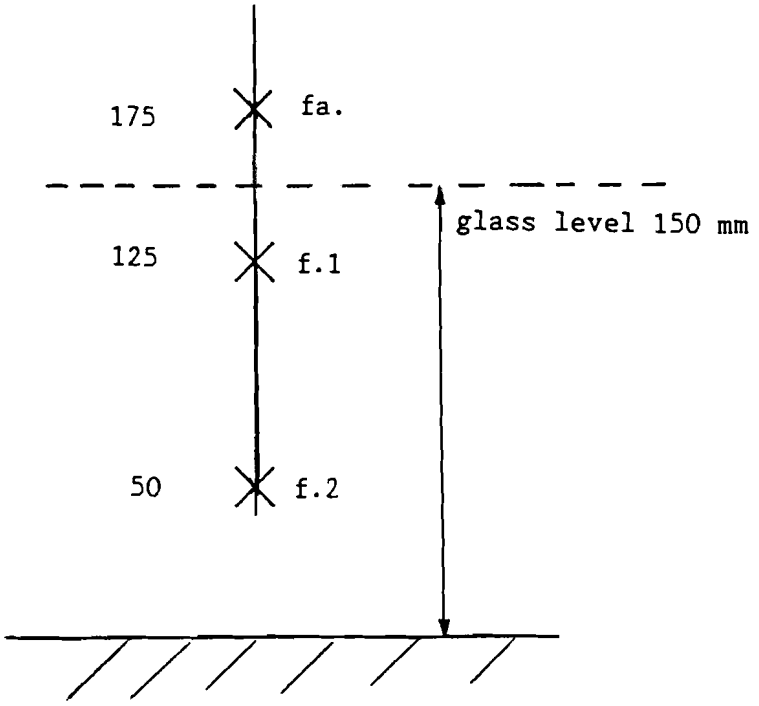

Fig. 3-3 Height (in mm above the channel bottom) of the threefold thermocouples.

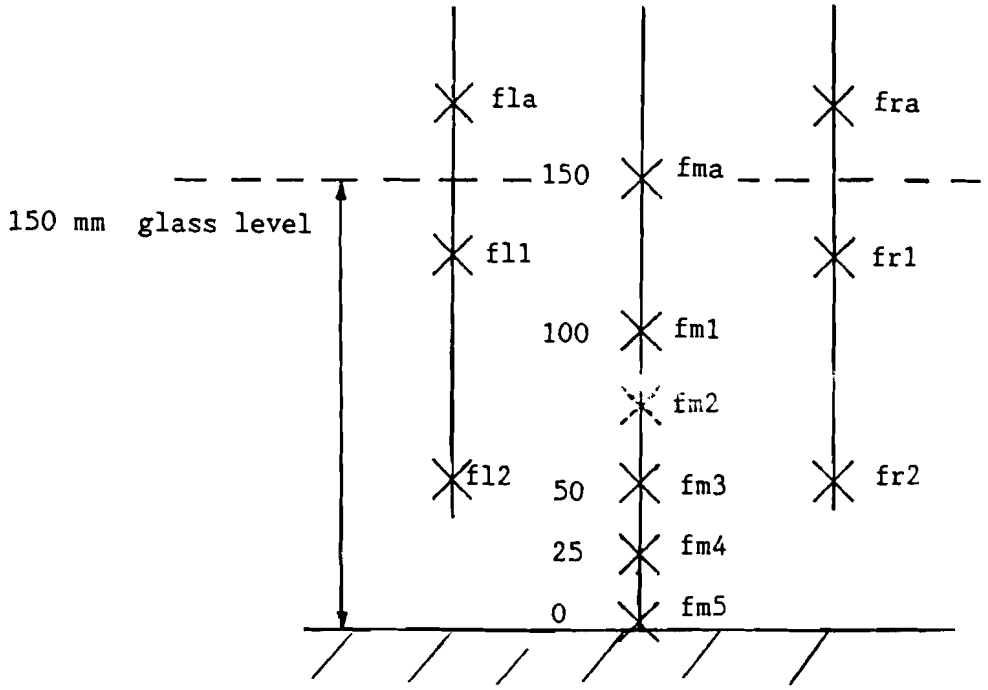

Fig. 3-4 Height (in mm above the channel bottom) of the profile thermocouples at the cross section of the spout section.

The following environmental quantities are measured:

Melting furnace (cf fig. 3-5)

- Input actuator signal of the speed of the wormwheel of the input (proportional to mass of silicat per second)
- Gastot_t total gas flow of the 6 burners together
- Gastot_m same as gastot_t but measured with a different sensor
- Airtotal total air flow of the burners
- Furnpres furnace pressure
- Smel_B11 glass temperature B11/G, the entrance temperature of the glass to the feeder
- Smel_hot atmosphere temperature C4, the hottest point just under the roof of the melting furnace

'Shaping' parameters:

- Velocity control signal (tacho-voltage) of the speed of the pulling machine, representing the speed of the glass on the track
- Diameter diameter of the glass-tube on the track
- Thicknes wall-thickness of the tube

In table 3-6 an overview is given of all measuring points. In the column 'CODE' the codes that are used throughout this report are mentioned. The column 'UO-CODE' contains the codes that are used at the plant of the Universal furnace. In the last column, dimensions of the signals are given.

3.1.2 Signal measuring

Next we will discuss by what type of signals the measuring points are represented.

0-10 Volt signals

View figure 3-1. The universal furnace is controlled from a control panel. Part of the signals are displayed here and plotted on paper. From most of these signals a linear 0 - 10 Volt signal is available.

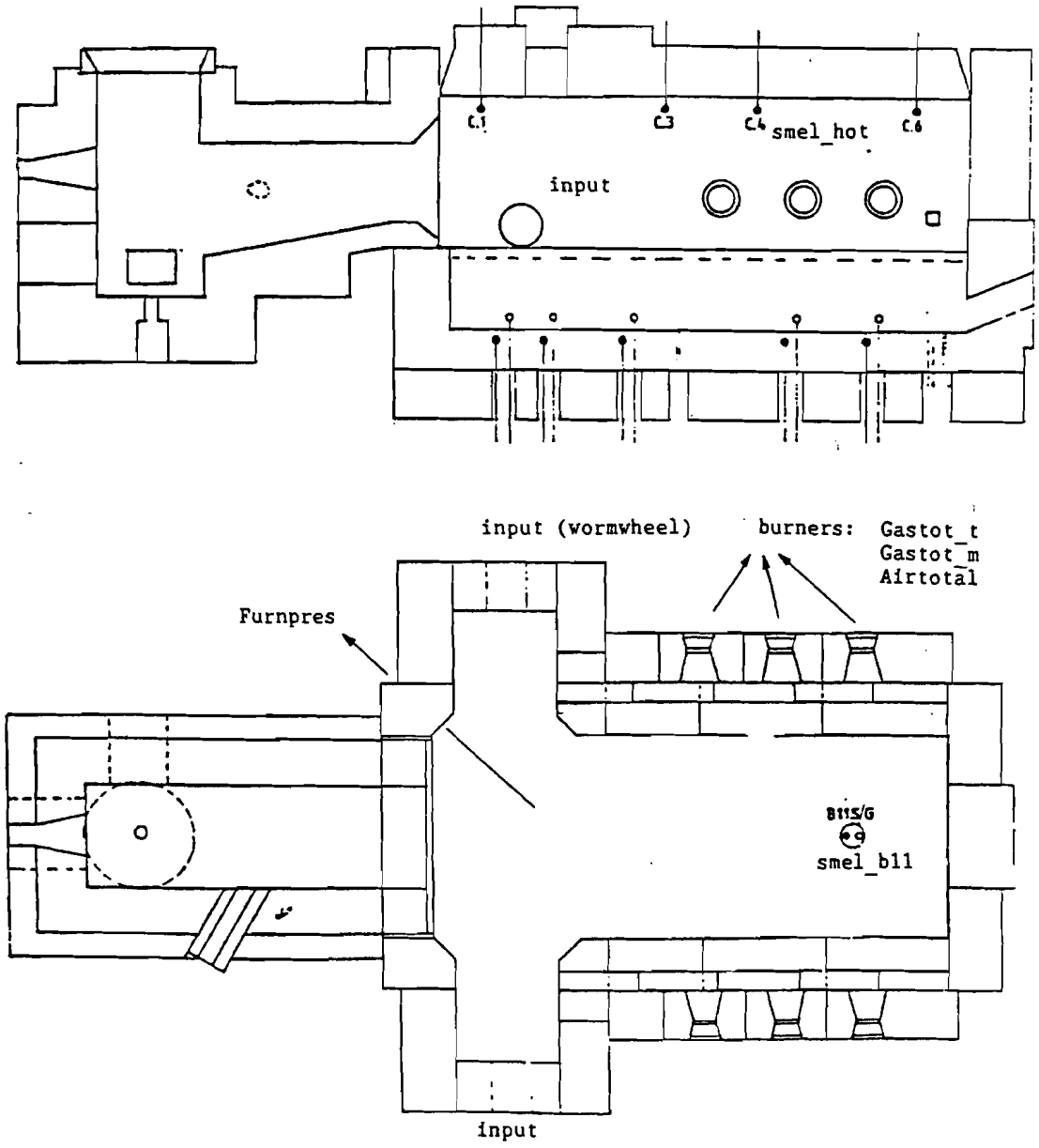

Fig. 3-5 Measuring points of the melting tank.

The corresponding physical units can be derived from the functions given in the column with '[units]=F(V)' in table 3-6, where V is the voltage signal.

Before a measurement is started, from each signal the range is determined (in what range it could vary). When the feeder was in a

stable situation, the corresponding measured values were taken as working points. The variations around these working points are determined from operator knowledge and previous experiments. If later on it appeared that these ranges were too small or that improper working points were chosen, these values were adapted. By means of a small computer program the PUNIC-card settings are calculated such that the output becomes as large as possible (between -10 and 10 Volt) to obtain maximum accuracy. For example:

> Smel_B11 was expected to vary between 1410 and 1470 ^{0}C. The corresponding voltage signal from the control panel is 6.8 to 7.8 Volt (1000+60*V). The PUNIC settings provide an outputsignal of -5 to 5 Volt. The next amplification setting would let the output exceed 10 Volt.

The signals representing the shaping parameters have a different, but also linear voltage range. Their fitting functions are also given in table 3-6.

S-couple signals

In addition a group of signals is measured directly, not via the control panel. These signals are indicated in table 3-6 with 'S-couple'. Here, directly the thermo-voltage of the S-type (Platinum- 10% Rhodium) thermocouples (cf. NBS, 1974) is measured. The PUNIC amplification factor is determined by linearizing a third order polynomial fitting function. Linearization is done around the working points of the temperature. It is done just by taking the derivative of the polynomial in the working point. The errors due to linearization when a temperature range of 100 degrees is assumed, are smaller than 0.1%.

Because the voltages of the thermocouples are very small (11 $\mu V/^{0}C$), those signals are amplified maximally by the PUNIC-cards. In general the S-couple signals have a signal to noise ratio that is worse than that of the signals from the control panel.

Moreover these signals are relatively more sensitive to offset-errors. At the input-circuit of the PUNIC an offset voltage is used such that 0 volt input causes no output. Small errors of this offset already may cause a large change of the output signal. Consequently the absolute temperature is not always reliable. However, the signal changes, which for identification are of interest only, are measured properly.

SIGNAL	PUNIC	MIOS	CODE	UO-CODE	[UNIT]=F(V)	[unit]
1	-1	0	GAS_1_IN	GAS-I	0-20	[%]
2	-1	2	GAS_2_IN	GAS-II	0-20	[%]
3	-1	1	AIR_IN	KOELLUCHT	0-20	[%]
4	0	0	SMEL_B11	B11G	1000+60*V	[DEGR C]
5	1	1	SMEL_HOT	C4	1000+60*V	[DEGR C]
6	2	2	FDFR_FA1	FA1	900+50*V	[DEGR C]
7	3	3	FDFR_F11	F11	1000+60*V	[DEGR C]
8	4	4	FDFR_F12	F12	1000+60*V	[DEGR C]
9	5	5	FDMI_FA2	FA2	S-COUPLE	[DEGR C]
10	6	6	FDMI_F21	F21	S-COUPLE	[DEGR C]
11	7	7	FDMI_F22	F22	S-COUPLE	[DEGR C]
12	8	8	FDBA_FA3	FA3	1000+60*V	[DEGR C]
13	9	9	FDBA_F31	F31	900+50*V	[DEGR C]
14	10	10	FDBA_F32	F32	S-COUPLE	[DEGR C]
15	11	11	FDSP_FLA	FA5	S-COUPLE	[DEGR C]
16	12	16	FDSP_FL1	F41	900+50*V	[DEGR C]
17	13	17	FDSP_FL2	F42	900+20*V	[DEGR C]
18	14	18	FDSP_FM5	(1)	S-COUPLE	[DEGR C]
19	15	19	FDSP_FM4	(2)	S-COUPLE	[DEGR C]
20	16	20	FDSP_FM3	(3)	S-COUPLE	[DEGR C]
21	17	21	FDSP_FM2	(4)	S-COUPLE	[DEGR C]
22	18	22	FDSP_FM1	(5)	S-COUPLE	[DEGR C]
23	19	23	FDSP_FMA	(6)	S-COUPLE	[DEGR C]
24	20	24	FDSP_FR2	(7)	S-COUPLE	[DEGR C]
25	21	25	FDSP_FR1	(8)	S-COUPLE	[DEGR C]
26	22	26	FDSP_FRA	(9)	S-COUPLE	[DEGR C]
27	23	27	FDBA_FA4	FA4	S-COUPLE	[DEGR C]
28	24	32	FDSP_FA6	FA6	900+20*V	[DEGR C]
29	25	33	FDSP_F51	F51	900+20*V	[DEGR C]
30	26	34	FDSP_FA7	FA7	900+20*V	[DEGR C]
31	27	35	F22_TCT	F22	700+70*V	[DEGR C]
34	30	38	INPUT	INLEG	10*V	[%]
35	31	39	GASTOT_T	GASTOT_T	12*V	[Nm3/h]
36	32	40	GASTOT_M	GASTOT_M	12*V	[Nm3/h]
37	33	41	AIRTOTAL	LUCHTTOT	120*V	[Nm3/h]
38	34	42	FURNPRES	OVENDRUK	-2.5+2*V	[mmH2O]
39	35	43	F1_GAS	F1_GAS	10*V	[%]
40	36	48	F1_AIR	F1_LUCHT	10*V	[%]
41	37	49	COOL_AIR	KOELLUCHT	28*V	[Nm3/h]
42	38	50	F2_GAS	F2_GAS	10*V	[%]
43	39	51	F2_AIR	F2_LUCHT	10*V	[%]
44	40	52	VELOCITY	SNELHEID	0.17+2.40979*V	[m/min]
45	41	53	DIAMETER	DIAMETER	0.1+5*V	[mm]
46	42	54	THICKNES	WNDDIKTE	0.25*V	[mm]

Table 3-6 Signal overview. SIGNAL= signal number, PUNIC= channel number of PUNIC used, MIOS= channel number of MIOS-card used, CODE= code, UO-Code= codes used at the plant, '[units]=F(V)'= fitting functions (process inputs have no fitting functions), [unit]= unit of the signal.

3.1.3 Disturbances

During the experiments already some insight has been obtained about the disturbances of the process and measuring equipment. Some aspects are reviewed here.

- The environment at the plant was very 'polluted' in electrical sense. This hindered the installation of the measuring system and proper measuring.
- The PUNIC cards were sensitive for capacitive loads. Long wires at the input caused an input oscillation of 3 MHz. This caused at the output of the PUNIC a disturbance with a frequency of 3 KHz. Installation of separate coax-cables sometimes prevented the oscillation. A few signals still are disturbed so severely that they could not be used later on. When a signal is omitted because of these oscillations this will be noted further in the report.
- The glass level sensor measures the depth of the glass bath. A sensor stick at a small voltage is let down slowly to the surface of the glass. At the moment it contacts the glass a small current is conducted through the glass. This moment determines the glass level and the stick is raised quickly. Because the sixfold thermocouple was not enveloped with a platinum grounding pipe (all other couples were), this current caused little peaks on the thermo-voltage of the sixfold couple. These peaks are oversampled and caused disturbances on the measured temperatures of the sixfold couple.
- Just by observing the temperature plots it was clear that low frequency disturbances of the process would be of greater nuisance than the high frequency (measuring) noise. The temperatures of the feeder were always changing slowly, even when over a long period no excitations were done. The origins of these 'drifts' were never completely clear, but some possible causes are given:
  . day and night temperature fluctuations
  . fluctuations of gas mixture or gas (and air) pressure
  . changes of the feeder environment, such as draught
  . fluctuations of the glass silicat composition
  . fluctuations of inlet temperature (B11/G)
  . glass-level fluctuations

- No variances or probability density functions of the noise were known. The only known was that high frequency signals did not contain process information.

  'On-line' a few actions were taken to improve the disturbance behaviour:

  . a platinum grounding pipe has been installed close to the glass level sensor
  . the temperature inside the measuring cart has been kept constant (by air-conditioning), to avoid fast temperature drifts of the PUNIC-cards.
  . low pass-filtering with PUNIC has been provided, with the cut-off frequency at 0.25 Hz.

  How the disturbances are treated 'off line' is explained in chapter 4.

3.2 EXPERIMENT DESCRIPTION

In section 1.3.3 part B.2 is summarized what experiments should, or can, be done. Because of time shortage not all these experiments are carried out. According to the primary planning the experiments would take 90 days! The actual available time was 5 weeks in total.

It is clear that only the experiments with the highest priority could be done. The aim of doing experiments at two working points (130 kg/hour and 160 kg/hour pull rate) was dropped very soon. Separate experiments for bandwidth analyses are not done. In this chapter the experiments that actually were done (table 3-10 experiment overview) are discussed sequentially. A comprehensive description with plots and detailed remarks is found in O. Burg and G. van Vucht (1987) 'Registration feeder experiments Universal furnace spring 1987'. Here more attention is paid to the 'why' of the experiment design.

Experimental conditions

The gas flow of section 1 and 2 and the cool air is input of the process that is to be modelled. All other variables must be kept constant. The control circuits that make in- and outputs dependent must be switched off. The others must be kept 'on', for these controls will also be in use when later on control according to the model will be applied.

- Feeder control is put on hand (the two PID-controllers 'off'). Input excitation is done only according to the experiment design.
- Glass level control (inlet and 'cup-heating) 'on' to provide constant outflow at the working point.
- Inlet temperature B11/G constant. Control of the melting tank on this temperature (manual control!).
- Shaping of the glass (drawing speed etc.) 'controlled'.

Preceding experiment

Because it took a few days to install the measuring system properly, sensitivity and dynamics analyses are done with the measuring system of the plant (3 samples/hour). Step functions are set on the single inputs at a constant pull rate of 130 kg/hour.

It was known that an amplitude of 10% extra on f1 gas caused the outflow to increase with 24% (if not controlled with the 'cup-heating'). Because this outflow change was still easy to control with the cup-heating, input amplitudes of + and - 10% of the nominal value are used.

The time in between each step is 8 hours, because the transients were expected to be over after that period.

Results:

Sensitivity of the transfer of f1 gas to the spout temperature f51 is 1.5 à 2 time less than of cool air and of f2 gas. One step from -10% to +10% of cool air or f2 gas caused f51 to vary 10 ^{0}C.

When the transfer functions are considered as first order, a main time constant can be derived from the step responses

$$y \approx K(1-e^{-t/\tau_m})$$

as in figure 3-7. Hereby we do not take the very large time constant into account, of which the response is not even died out after 8 hours. We find a τ_m which represents the dominant 'fast' behaviour of the particular transfer. The τ_m of the fastest transfer function is an indication of the bandwidth of the feeder with the considered in- and outputs. It determines the highest frequency that must be used later on during the estimation experiment.

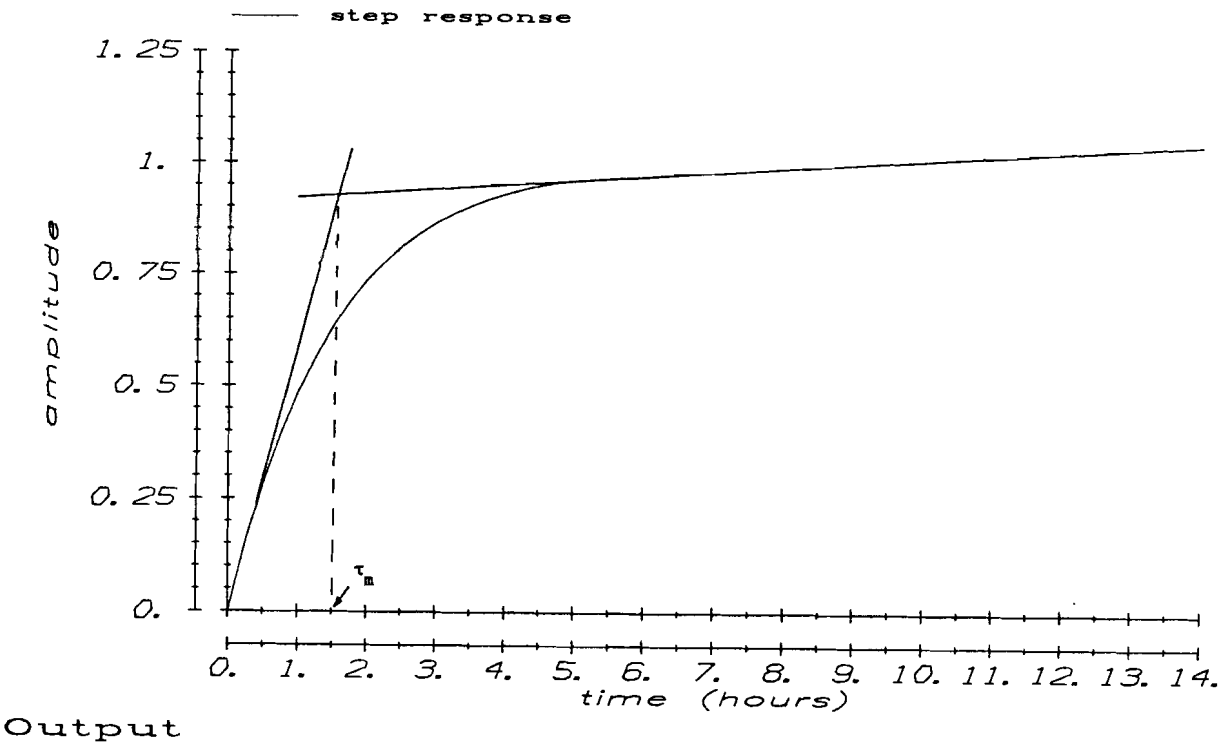

Fig. 3-7 First order approximation of the step response. Outline of the derivation of the 'fast' time constant τ_m.

A smallest τ_m is found of 1.5 to 2 hours, corresponding to the transfer of f2 gas to fdsp_f11. The other transfer functions to the surface temperatures were of the same order. The transfers to the atmosphere couples were of course much faster, but (for this reason) the feeder model considers only glass-temperatures.

PRE130

This experiment concerns the last part of the preceding experiment. The sampling time is chosen at 30 seconds. With this sampling rate the fast reaction of the atmosphere couples could still be observed. A few installation problems and a very large 'drift' of the entrance temperature B11/G made the experiment not very valuable. The quantities mentioned above were derived from a period before the experiment PRE130.

PRE160

Experiment with step functions but at a pull rate of 160 kg/hour.

During this experiment the outflow went two times out of control. The glass poured out at a rate of 200 kg/hour! When this occurs the feeder is reset to its working point and the glass-track is installed again. It takes about 10 hours to stabilize the feeder again.

After this experiment, it is decided to continue with experiments at a working point of 130 kg/hour only, because the chance of an excessive outflow is smaller at 130 kg/hour.

KANT130

Linearity analysis. Only for the input f2 gas because it was expected that the other transfers would not have a different behaviour in essence. Because of a lack of time no full staircase is injected. Steps of 2 and 4% are applied:

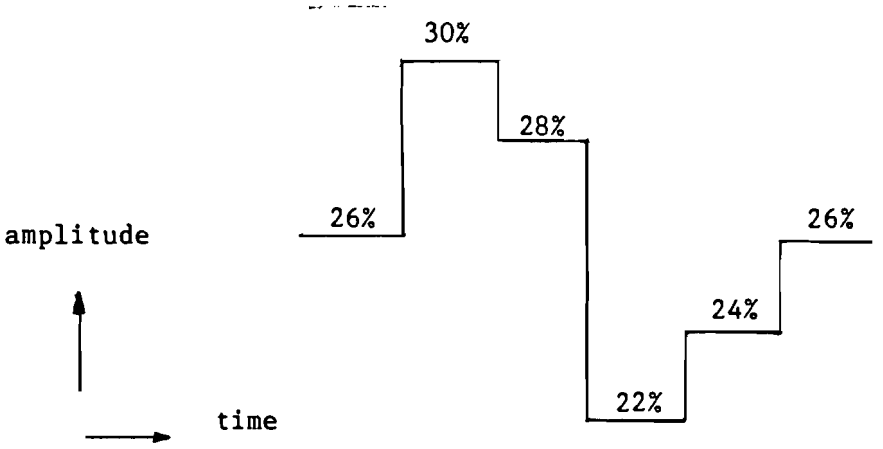

The amplitude is given in absolute units. As in the former experiments, the excitations of the inputs are done by hand.

Results:

The entrance temperature varied 5 ^{0}C during the experiments. When drifts are 'subtracted' from the response as well as possible in order to measure the temperature difference caused by the step excitations only, the process seemed quite linear: the corresponding temperature steps on f51 are estimated on +7.5, -4, -10, +3.8, +3.8 ^{0}C. However no reliable judgement can be done because the accuracy is not within 3 to 4 ^{0}C. This means no real conclusion about linearity can be drawn from this experiment.

PRBNS1

First estimation experiment.

The inputs are now excited by the PICOS measuring system. The clock period of the generating shift register of the PRBN-sequence is taken such that the input can be considered white compared with the process transfer. For no bandwidth analysis experiments are done, the process bandwidth is derived from the smallest time constant τ_m found in the sensitivity experiment.

Assume the transfer of the process to be of first order, figure 3-8. If f_c is the clock frequency of the PRBN-sequence we see that its 3 dB point lies at $0.4f_c$ (fig. 3-9). If we chose such an f_c that this 3 dB point lies at the -20 dB point of the approximation of the spectrum of the process, the high frequency signals with 1% power of the DC-component are still excited properly. With this T_c we are sure that all frequencies of the process will be excited equally by the PRBN-sequence:

$$0.4 \frac{1}{T_c} = \frac{10}{2\pi} \tau_m \quad , \; T_c = \frac{1}{25} 2\pi.\tau_m \approx 0.25 \; \tau_m .$$

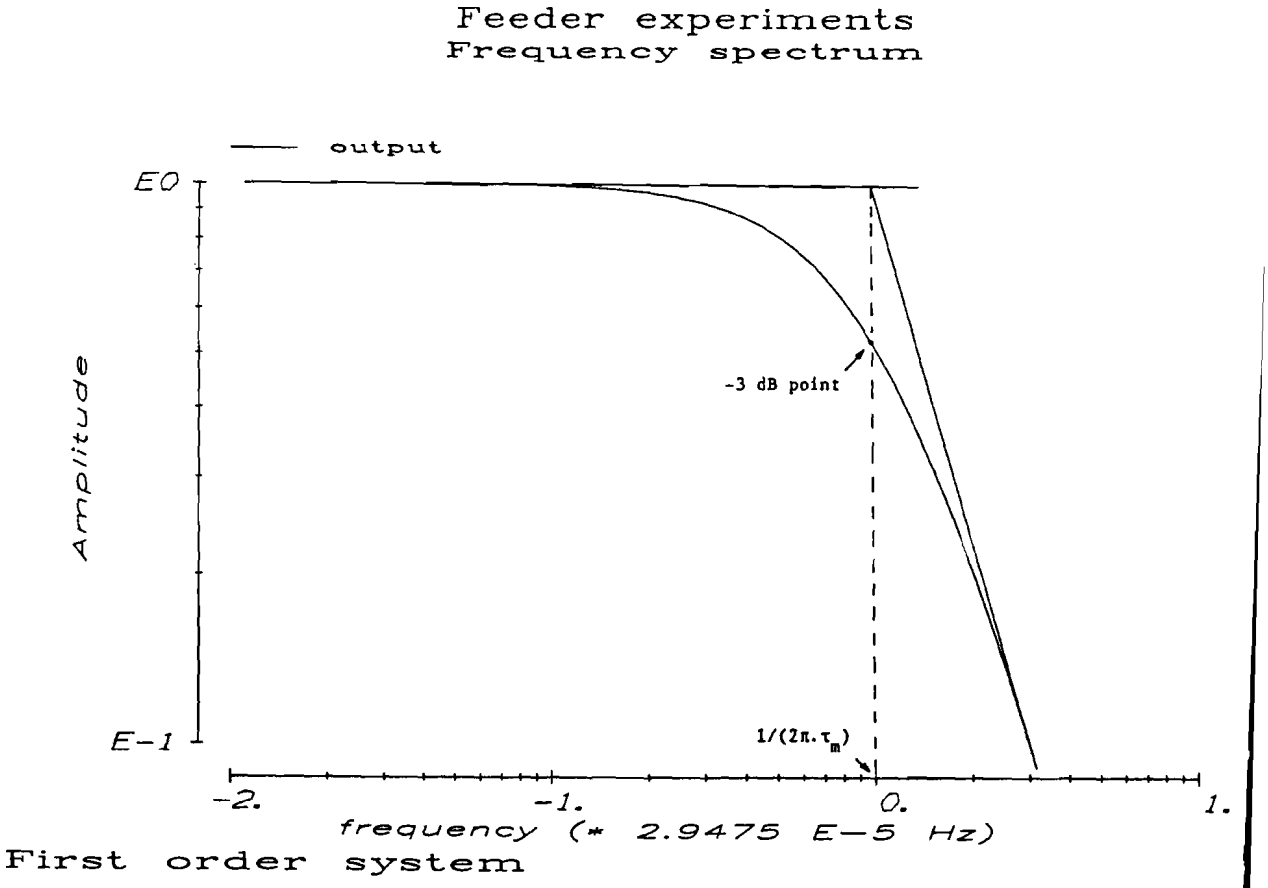

Fig. 3-8 Frequency spectrum and bandwidth of first order process approximation.

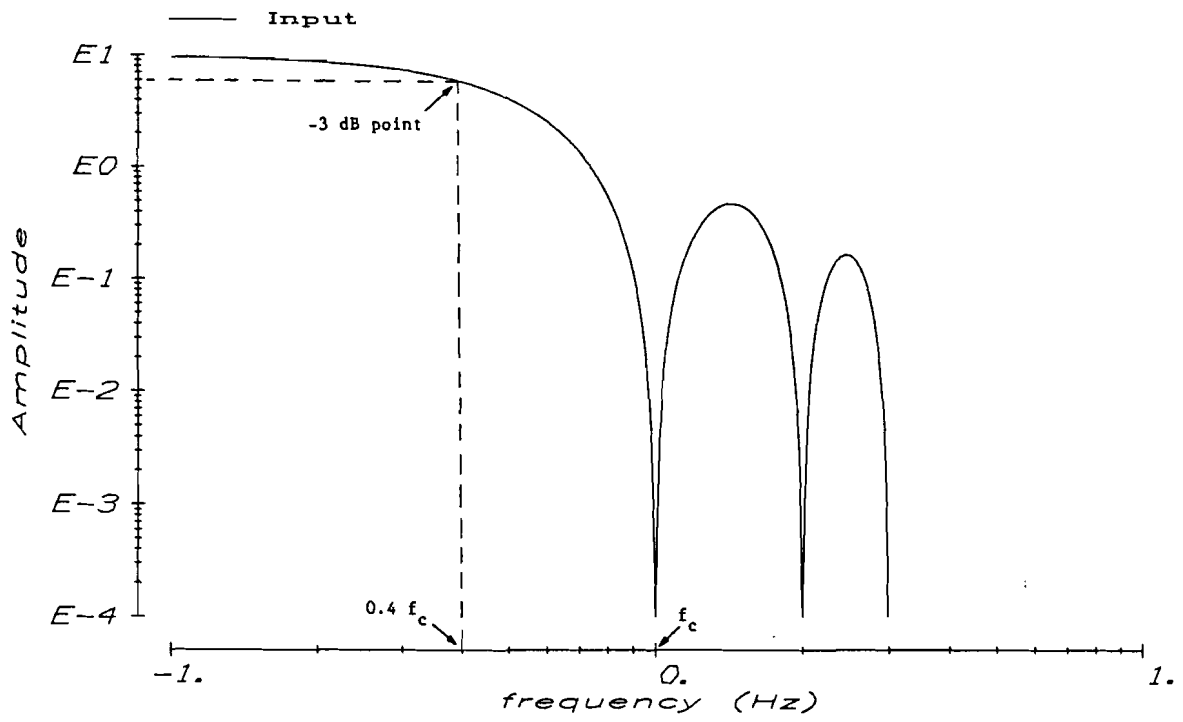

Fig. 3-9 Frequency spectrum and bandwidth of PRBN-sequence with clock frequency f_c.

If we take τ_m 1.5 hour we find a T_c of 22 min.

The information contents we will get in the data of the estimation experiment, only depends on the number of switches we excite. From previous PICOS experience we know that to be able to do reliable estimations, the experiment must contain 1250 switches. With T_c=20 min we than get an experiment duration of more than 16 days! Because that much time was not available, a clock period of only 5 minutes is used in this experiment. We know, however, that this can cause difficulties too because, using the same amplitude, the lowest frequencies are now excited with approximate 1/16th of the power of the sequence with T_c=20 min. To compensate this loss of excitation power an amplitude of + and - 20% on the nominal input is used.

Different start values (seeds) are chosen for the generating shift registers of the sequences. To be sure that all 3 PRBN-sequences are independent, independence is checked using the regarded seeds.

To acquire a redundancy of information, each clock period of the PRBNS is sampled 10 times: sampling time of 300/10 s. The experiment duration is 1250 X 10 X 0.5min = 4.3 days.

T_c= 5 min, sampling time is 30 seconds

	-	+	nominal [absolute %]
f1 gas	44%	64%	54%
cool air	11%	16%	13.5%
f2 gas	21%	31%	26%

PRBNS2

At PRBNS1 it appeared from the output plots that the excitations caused far to little changes of the spout temperature f51. Therefore, the clock period of the PRBN-sequence is increased with 5/3, such that the experiment duration becomes 7 days. In addition the excitation amplitude is doubled, in spite of the fact that we have little idea of the non-linearities that this may cause. The same seed is used as in PRBNS1.

T_c= 8 1/3 min, sampling time is 50 seconds

	-	+	nominal [absolute %]
f1 gas	33%	72%	51%
cool air	10%	20%	16%
f2 gas	15%	32%	23%

Indeed now the glass-temperatures, including f51, showed satisfactory amplitude changes.

PRBNS4

Validation experiment. A different seed from experiment PRBNS2 is used. Because the 1250 switches of the PRBN-sequence are not needed for validation and 7 days experiment time was not available anymore, the clock periods of the PRBNS is chosen at 15 min. The experiment of 450 switches takes 4.7 days. In order to avoid excessive excitation of the feeder, and thus too large changes of f51, the amplitude is taken 20% of the nominal input values (as in experiment PRBNS1):

T_c= 15 min, sampling time is 30 seconds, (30 per clock period)

	-	+	nominal [absolute %]
f1 gas	44%	64%	54%
cool air	12%	16%	14%
f2 gas	18%	27%	23%

It must be noticed that the excitation of f1 gas went wrong, while it functioned properly in all previous experiments. The negative values of the sequence were not always excited. Instead of 44%, 54% is excited, so the mean value of f1 gas became in fact 59%. The origin of this effect is not yet recovered, but it must be caused by a failure somewhere in the MIOS DAC-card.

The amplitude of the changes of outputs were again satisfying.

SIM130

Experiment without excitation. Sampling time of 30 seconds is chosen to provide easy comparison with the experiments PRBNS2, which had the same sampling time.

PRBNS5

Validation experiment with a clock period of the PRBNS of 15 minutes. Same amplitude as PRBNS4 but with a sampling time of 50 s to make validation of PRBNS2 easier. Duration of 450 switches. Same seed is used as in PRBNS4.

T_c= 15 min, sampling time is 50 seconds, (18 per clock period)

	-	+	nominal [absolute %]
f1 gas	44%	64%	54%
cool air	11%	16%	13.5%
f2 gas	19%	29%	24%

Again the negative excitation of f1 gas got stuck as in PRBNS4.

Overview experiments Universal Furnace. 1 may - 9 june 1987.

NAME	PERIOD	SMPLTIME	NUMBER	INPUT/DESCRIPTION.
PRE130	1/5 18.49 - 4/5 9.00	30 s	7543	Step functions on gas_1 and cool air
PRE160_0	4/5 22.06 - 6/5 9.35	30 s	1377	Changeover to 160 kg/hour Back to -10,-10,-10%
PRE160_1	6/5 14.53 -	30 s	2911	Step functions. PRIMAL files lost
PRE160_2	7/5 10.17 - 11/5 9.15	30 s	11443	Step functions
KANT130	13/5 18.45 - 15/5 11.05	30 s	4841	130 kg/hour Staircase function First step not measured
PRBNS1	15/5 18.15 - 20/5 2.29	30 s	12500	PRBN-sequence 5 min clock period 10 samples/switch
PRBNS2	20/5 11.53 - 27/5 16.46	50 s	12472	PRBN-sequence 8 1/3 min clock period 10 samples/switch
PRBNS4	27/5 18.20 - 1/6 11.05	30 s	13531	PRBN-sequence 15 min clock period 30 samples/switch
SIM130	1/6 12.35 - 4/6 16.16	50 s	5451	Process without excitation, during transmission experiments
PRBNS5	4/6 16.28 - 9/6 10.08	50 s	8176	PRBN-sequence 15 min clock period 18 samples/switch

Table 3-10 Experiment overview.

3.3 CONCLUDING REMARKS

- The experiments were clearly dominated by one issue:
  The very slow responses of the feeder and consequently the long duration of the experiments. Because of the slow feeder behaviour it was always difficult to discern process-responses from 'drifts'. Fortunately the estimation procedure used in chapter 4 is not too sensitive to slow frequency disturbances, because the information that is looked at is injected in the process by the PRBN-sequences itself.

- Time was a very important factor in the experiment design. A lot of experiments have been sacrificed to be able to do the crucial estimation experiments. Even these experiments could not be done completely the way it was desired.
  The validity of the experiments can best be judged from chapter 4.

- A lot of experience has been obtained about the use of the new measuring system. In fact three new subjects were applied for the first time:
  . PICOS measuring cart. The cart-installation was new.
  . PRIMAL. PRIMAL was never used before in a 'real' industrial environment.
  . Coupling of PRIMAL to the PICOS system. The developments for the use of the PICOS measuring system as front-end of PRIMAL were just finished.
  The proper functioning is tested only partly before the experiments. Another small test is performed by comparing the measured values of the PICOS system by that of the control panel, although accuracy of the control panel values was too small to do reliable comparison.

- The utilization of PRIMAL was easy and clear.
  Of the available 'on-line' analyses, above all the plot utilities are used. It can be stated that without these plots, proper measuring and experiment validation were impossible.
  Because detrending (high pass filtering) without phase distortion was not possible, other 'on-line' analyses (beyond bandwidth analysis), are hardly done. Checking if the PRBN-sequence parameters were chosen correctly is done primarily by viewing the plots.

- The communication between the PICOS system and PRIMAL worked very well. However, because the experiment description of both systems did not fit completely, a lot of time was needed to adjust the experiment description at the front-end. Therefore in chapter 2 is recommanded to provide a separate experiment definition-loading for the front-end, also when PRIMAL is used as host.

4 IDENTIFICATION

4.1 INTRODUCTION

In chapter 3 we have seen what experiments have been done with the feeder. The required data have been copied on tape and transfered to another computer. Here the software is available that is needed to do the (off-line) identification activities described in this chapter. Signal preparation, estimation, and validation are discussed. No profound mathematical backgrounds will be presented, but at each step some of the conditions, properties, constraints etc., are explained. Of course interim results are discussed.

From all measured feeder temperatures only a few are chosen for the modelling. To obtain insight about the behaviour of the feeder towards the temperature in the spout, a model is derived with the two gas flows and cool air flow as inputs and the spout temperature fdsp_f51 as output (cf. fig. 4-1a). We will call this the 'spout model'. In order to get also information about the temperature distribution in the spout, a second model is derived with the same inputs but with the temperature profile in the spout as output. From the these temperatures we take 6 temperatures to describe the temperature distribution: fm1, fm4, fm5, fl1, fl2 and fr2. We will call the model with the profile temperatures of the cross-section of the spout as output, the 'profile model' (cf. fig. 4-1b).

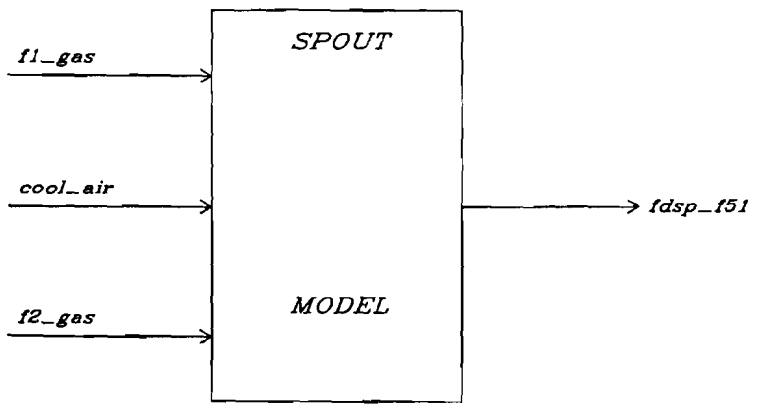

Fig. 4-1 a Inputs and outputs of the spout model.

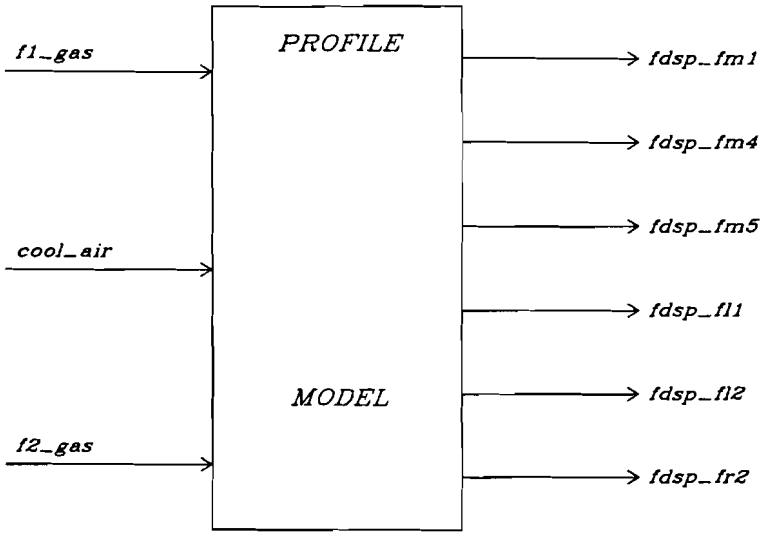

Fig. 4-1 b Inputs and outputs of the profile model.

The successive identification steps will be explained with the spout model as an example. Only some results of the profile model will be presented.

4.2 SIGNAL PREPARATION

The data that will be used for estimation must contain as much relevant information as possible about the process dynamics. To obtain a good signal/noise ratio, the irrelevant information that can be removed, must be removed. This is what signal preparation deals with.

The examples given in this section all concern the experiment 'PRBNS2', for this experiment will be used for estimation in section 4.3.

4.2.1 Visual inspection of the data

Many disturbances can be observed by the human eye. From the log-book of an experiment, the source of these disturbances may be known. It is also possible to detect disturbances of the measured signals from the knowledge that the observed disturbance cannot possibly be a representation of a process disturbance.

After detection of the disturbance, the signal have to be repaired. Note that we consider here only measuring noise, for errors due to process disturbances cannot be repaired without unjustified speculation about the process behaviour. The disturbances may be of such different character and occur for such a short time that it is not worthwhile to

develop software that automatically corrects the disturbances of the whole dataset of the considered experiment. An example of such an 'automatic' repairing is the peak-shaving algorithm. To repair less regular measuring disturbances, it is more efficient to do repairing on a short part of the dataset 'by hand'. Therefore a 'PICOS repair kit' was developed. In the standard package CTRL-C, functions are written that together form the PICOS repair kit. The principle is that a part of the dataset is read in a SIGFILE in CTRL-C. Next, one signal can be selected and several operations can be executed upon it. After repairing, the signal is put back in the SIGFILE. When all signals have been repaired, the SIGFILE is written back to the dataset (cf. fig. 4-2).

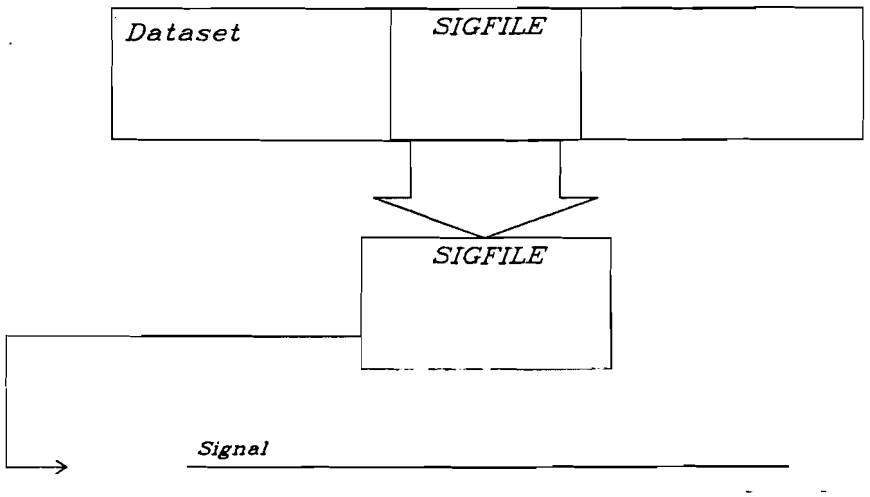

Fig. 4-2 Selection of a signal-piece with the 'PICOS repair kit'

The following functions are available:

a. Load SIGFILE with signals
b. Select signal
c. Add a constant value
d. Interpolate
e. Assign absolute value
f. Plot signal
g. Plot SIGFILE
h. Put signal back
i. Save SIGFILE
j. Keyboard control
h. Exit

A. and b. are described above. With c. a constant value can be added to a specific range of samples. With d. interpolation can be done between two points. The boundary values, between which the signal is interpolated, are either real boundaries or boundaries extrapolated with a line piece (cf. fig. 4-3). To this end a straight line-piece if fitted in least square sense on a few data points. The number of these data points is optional.

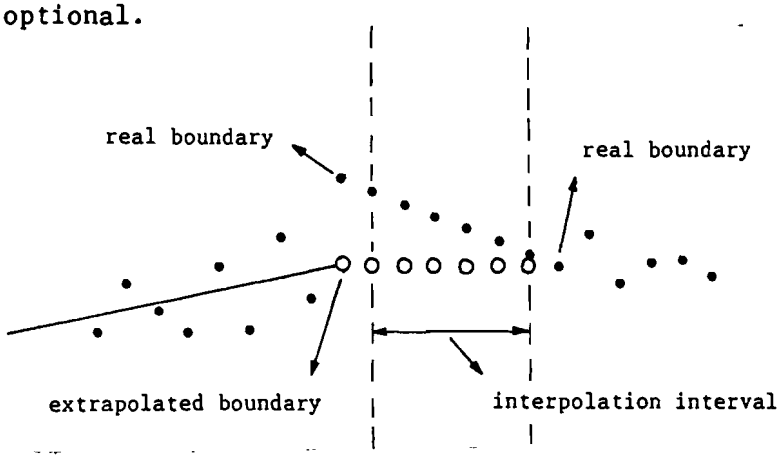

Fig. 4-3 Interpolation (with 6 samples) with real or extrapolated boundary.

When the boundary cannot be determined properly (e.g. when the boundary is the first sample of a PRBNS switch), e. allows to assign a value or range of values to the signal. To view the repairing results f. and g. are used. With h. and i. the repaired signal is stored back in the dataset. 'j.' Allows to return in between to CTRLC and provide whatever the user wants with the signal. For example, a function written by the user can be applied, sample values can be displayed, etc..

The following example illustrates the use of the 'PICOS repair kit'. View the measured signals in the figures 4-4a to d. At f2 gas we see a strange disturbance of the first 1935 samples of the PRBN-sequence. During this period the offset of the analog signal conditioning card was wrong, so that the measured negative values were clipped by the power supply of the card. After sample 1935 the PUNIC-setting was corrected. With help of a simple program the mean amplitude of the PRBN-sequence is calculated and this value is used to assign the right negative amplitudes to the signal before the sample 1936.

At sample 8663 two store files are concatenated with one sample lost in between. With 'interpolate' this sample is recovered. Also the few peaks at the cool air signal are repaired with d. and e.. Because of the

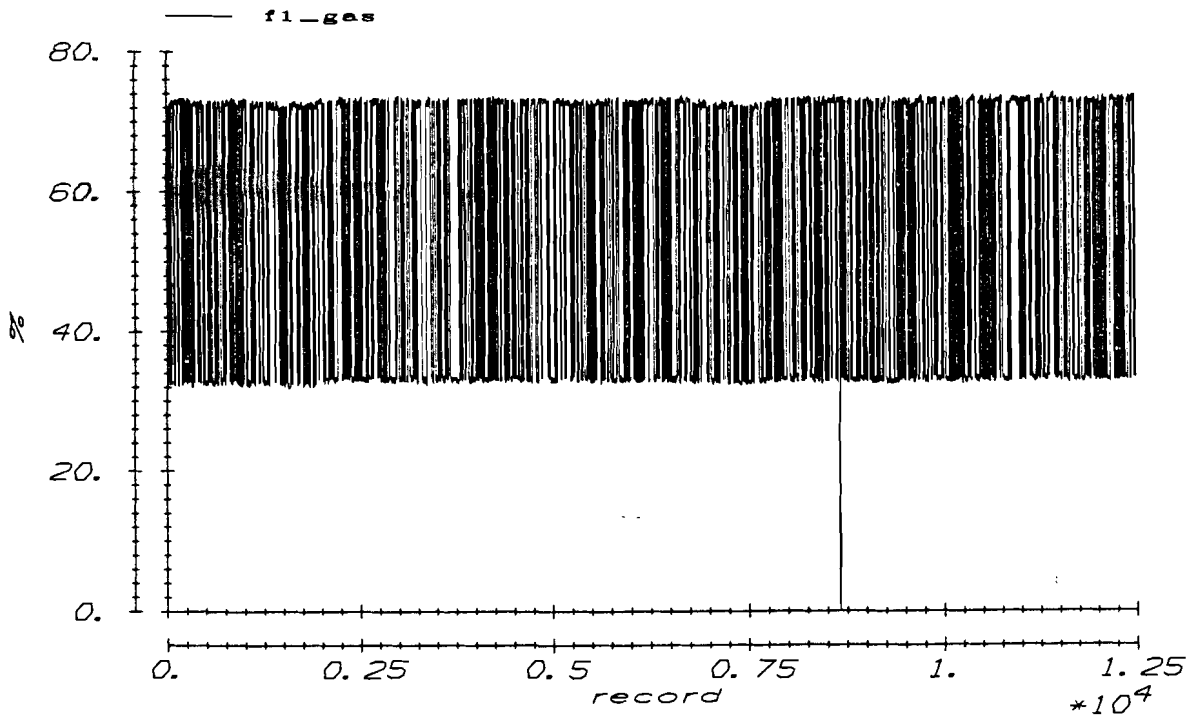

Input signal gas 1

Fig. 4-4 a Signal f1 gas as it is measured in the experiment PRBNS2.

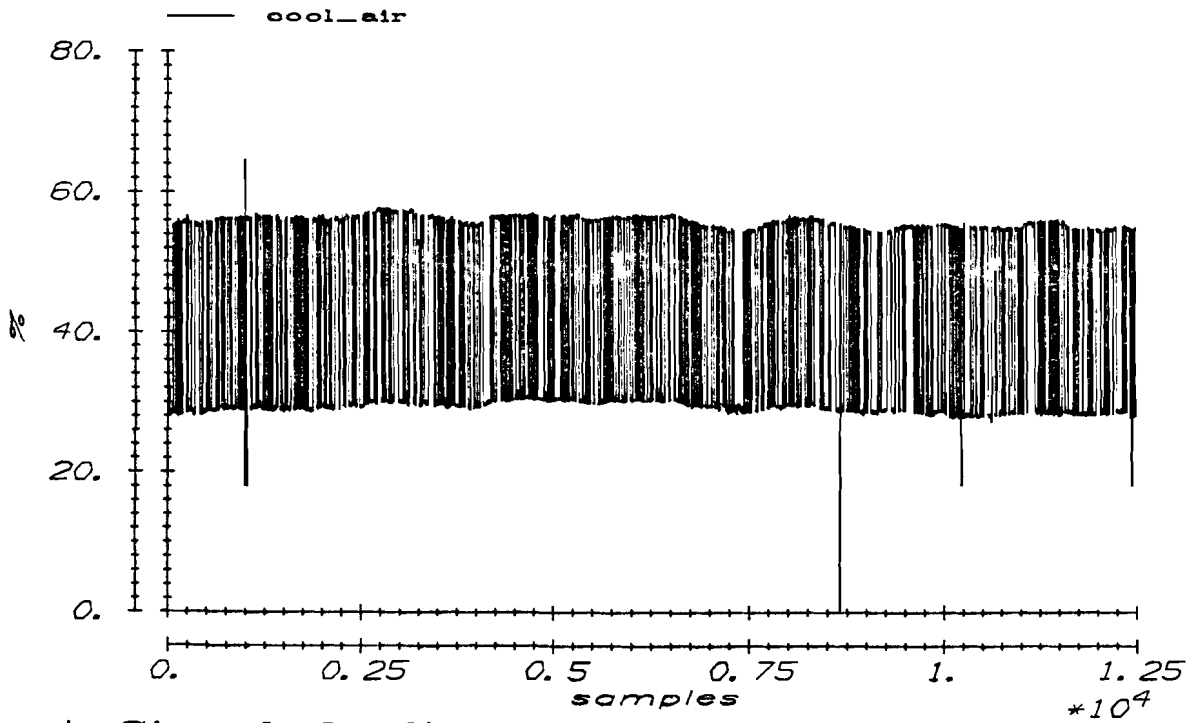

Input Signal Cooling air

Fig. 4-4 b Signal cool air as it is measured in the experiment PRBNS2.

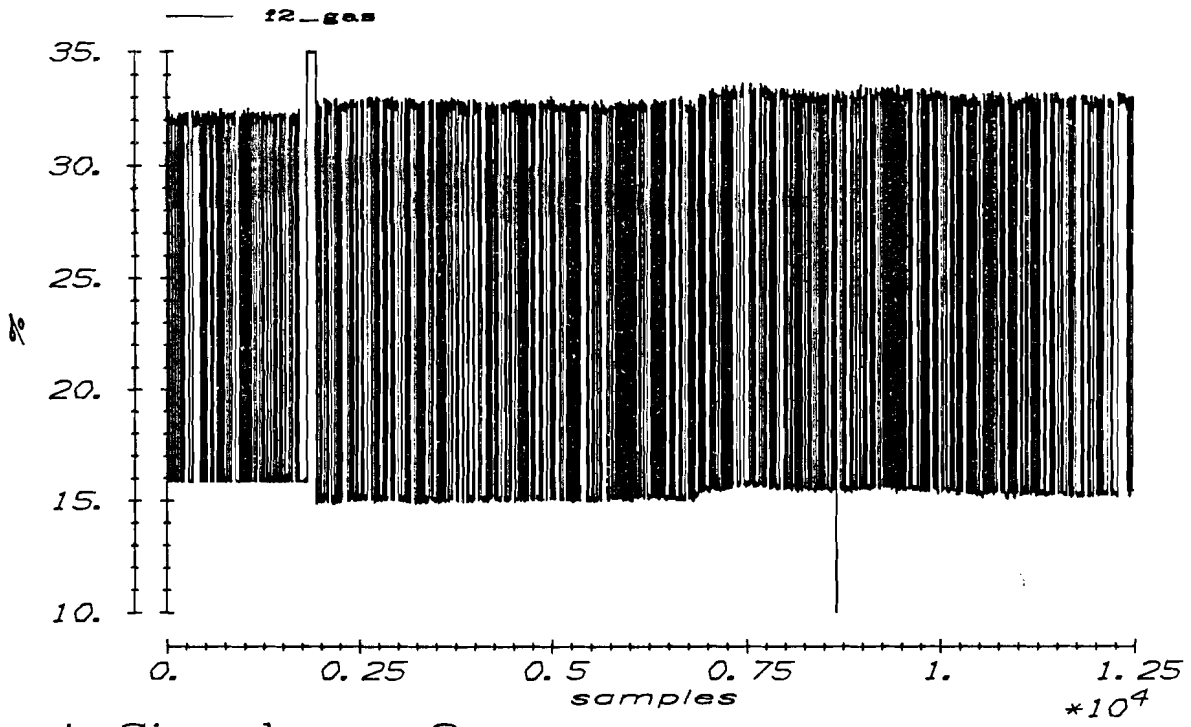

Fig. 4-4 c Signal f2 gas as it is measured in the experiment PRBNS2.

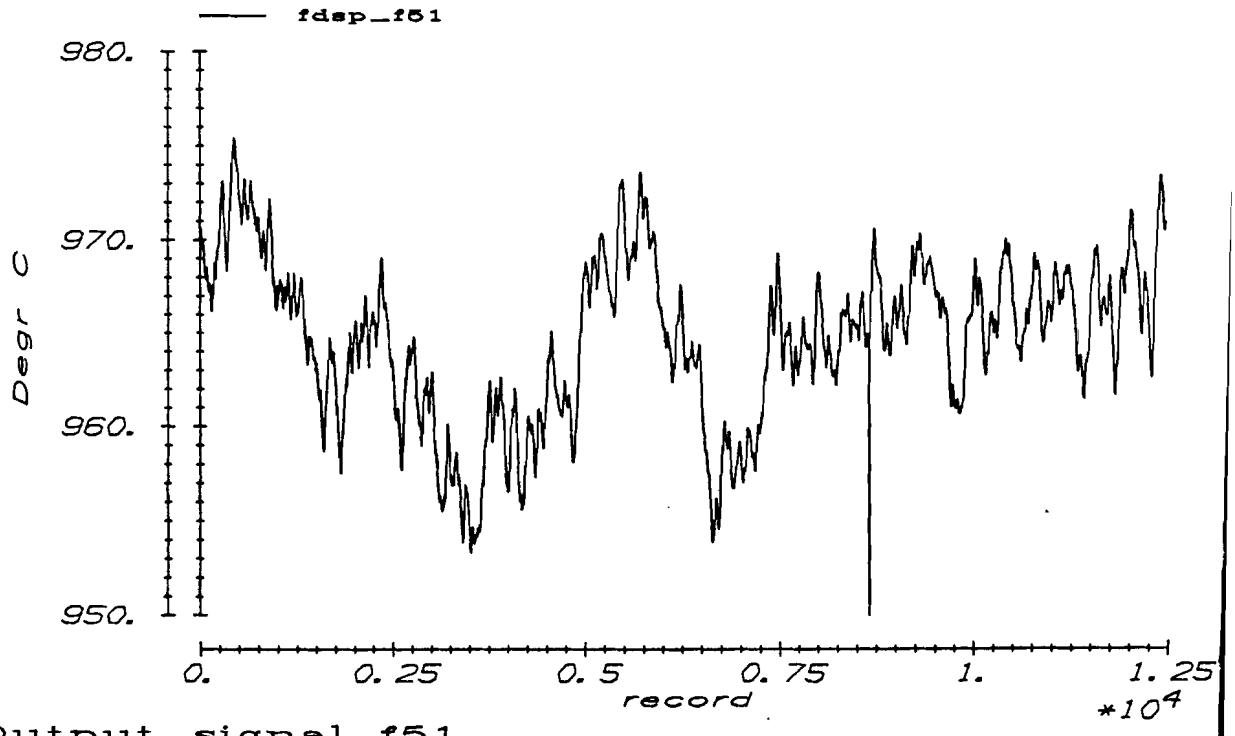

Fig. 4-4 d Signal fdsp_f51 as it is measured in the experiment PRBNS2.

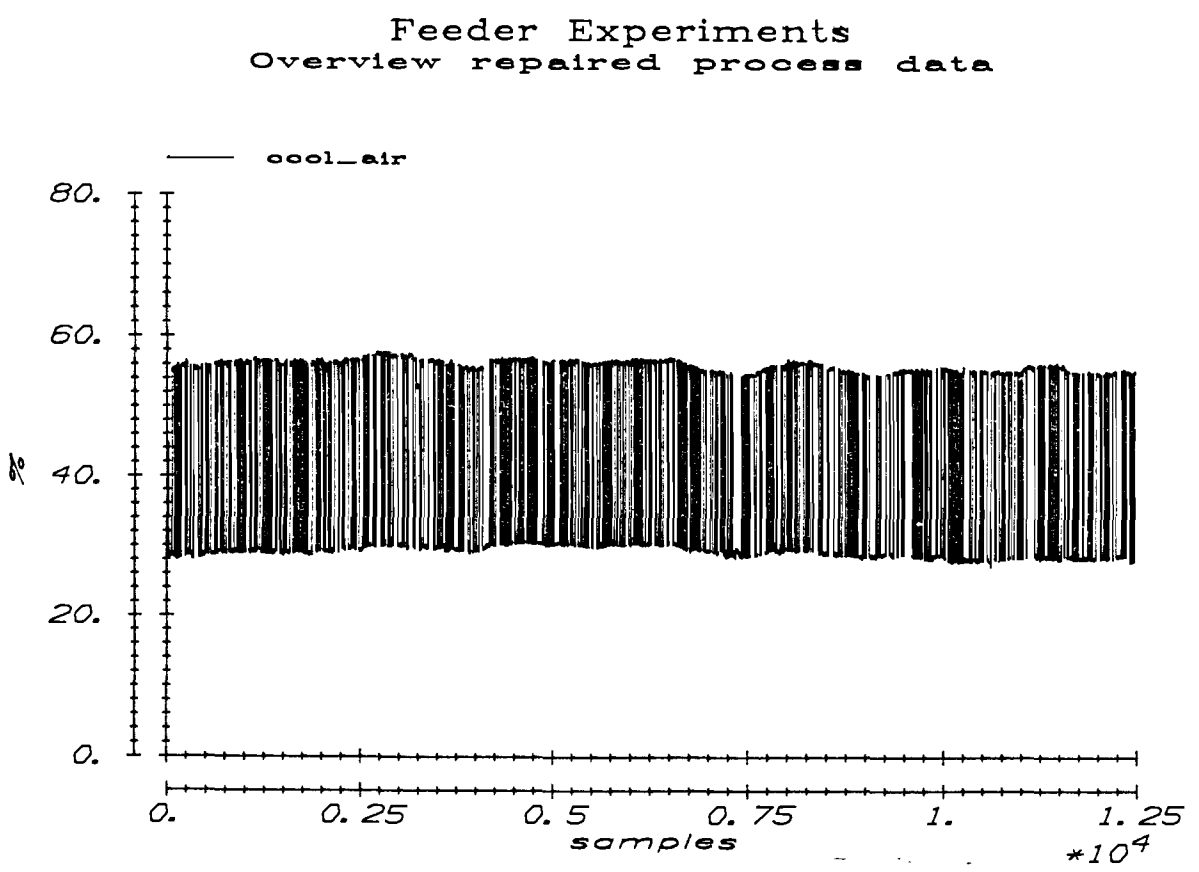

Fig. 4-5 a Repaired signal cool air of experiment PRBNS2.

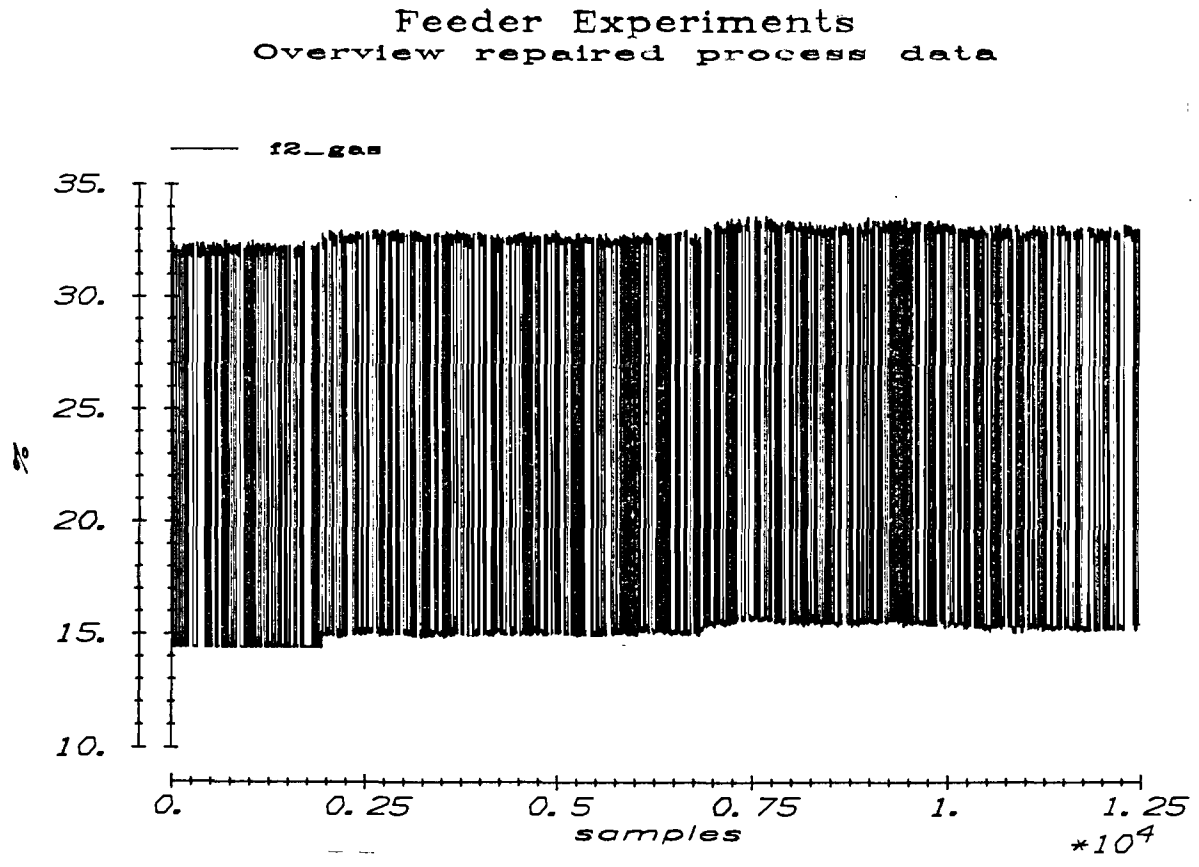

Fig. 4-5 b Repaired signal of f2 gas of experiment PRBNS2.

small number of peaks, the peak-shaving algorithm is not applied on the signals. Two examples of the repaired signals are shown in the figures 4-5.

Note that the PRBN-sequence is known to have the values +1 and -1 only. It must be certain however, that the disturbances are measuring disturbances and no failure of the actuator. This is checked by comparing the values with the plots on the control panel at the feeder plant. For instance the dip in the cool air at sample 3250 was an actuator failure. It has not been repaired.

4.2.2 Bandwidth analyses

A second way of inspection of the data is to check their frequency spectra. With this inspection three aims are served:

- Examination of harmonic disturbances at special frequencies.
  See figures 4-6a and b of f1 gas and fdsp_f51; cool air and f2 gas are omitted because they are the same as f1 gas. In the input spectrum we find indeed the clock frequency at 1/500 Hz. No special disturbances are seen in any of the signals.
- Checking whether the estimation experiment satisfied indeed the input constraints (right experiment design).
  In fig. 4-7 the input and output spectra are laid on top of each other. It is seen that the input is indeed equally excites all frequencies of the process. At the -3dB point of the input, the amplitude of the output is reduced to ~10%. It is interesting to check whether the experiment design in section 3.2 was done correctly. It was calculated that a clock period of 20 min would be optimal, i.e. at that corresponding bandwidth the output amplitude should be damped to 10%. Indeed we find here that at the frequency of $10/(2\pi.\tau_m)$Hz (=0.4/20 min with τ_m the approximated 'fastest' time constant of 1.5 hours), the output amplitude is reduced to (less than) 10%.
- Obtain preliminary insight in the frequency behaviour of the process.
  Consider fig. 4-6b. Of course the process has a low-pass behaviour. The very low frequencies (with a corresponding time period of more than 10 hours) have large energy. This is expected because during the experiments large drifts occurred. In the step responses very large time constants have been observed, so these drifts may also be process dynamics. Unfortunately these frequencies are not determined very accurately with the Fast Fourrier Transformation algorithm, because

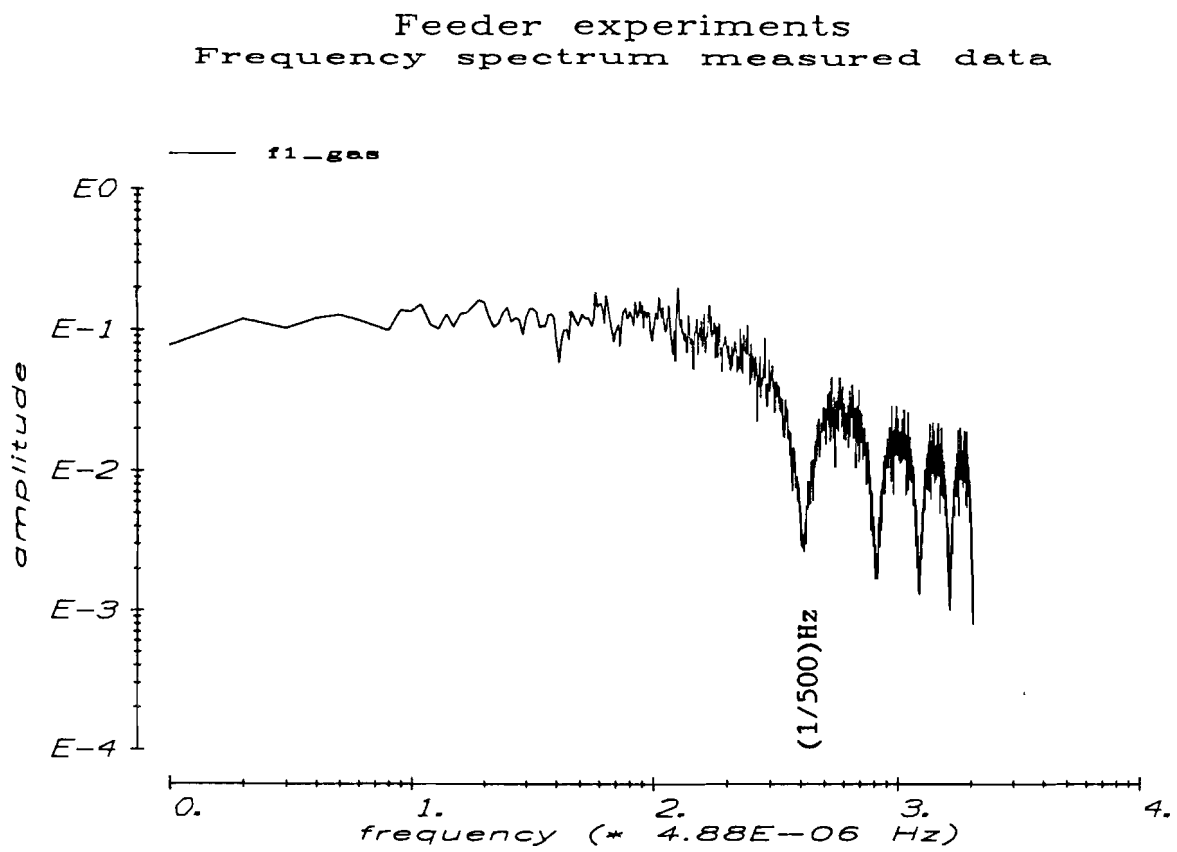

Fig. 4-6 a Spectrum of input f1 gas in experiment PRBNS2.

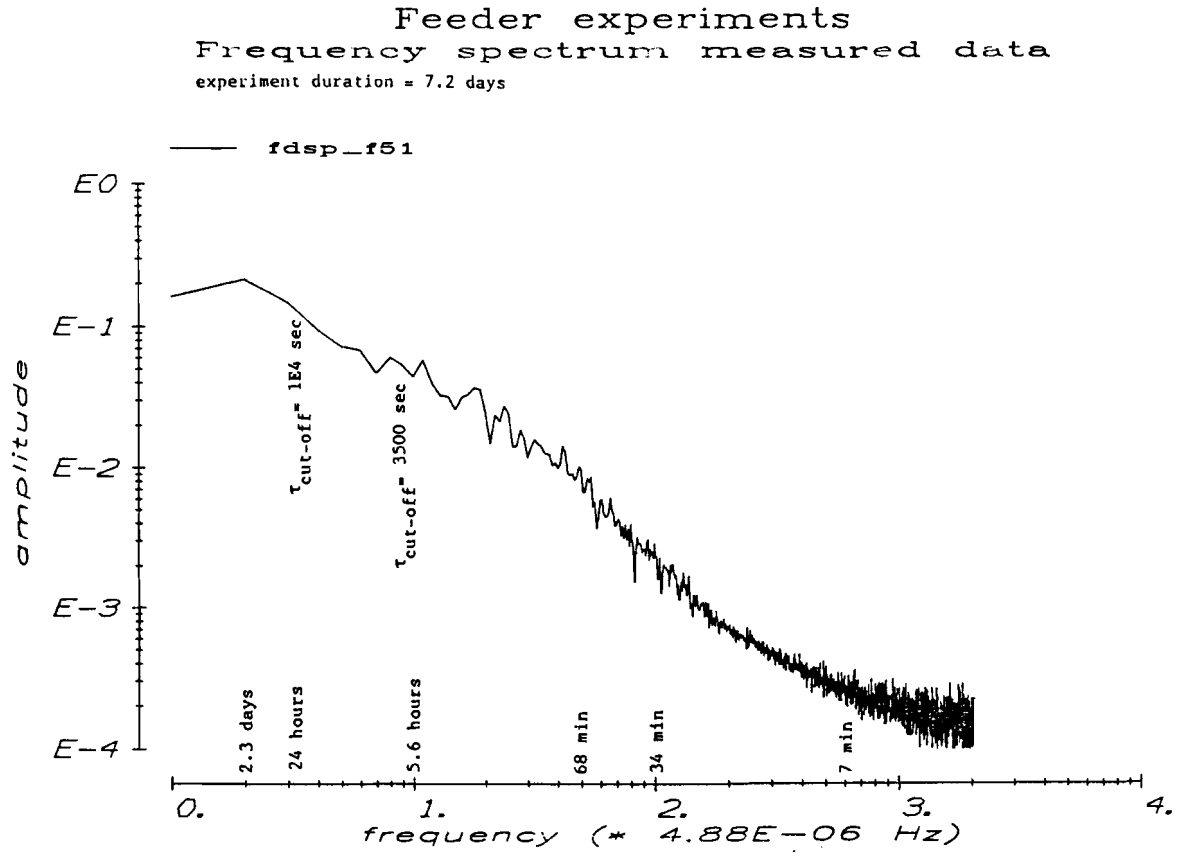

Fig. 4-6 b Spectrum of output f51 in experiment PRBNS2.

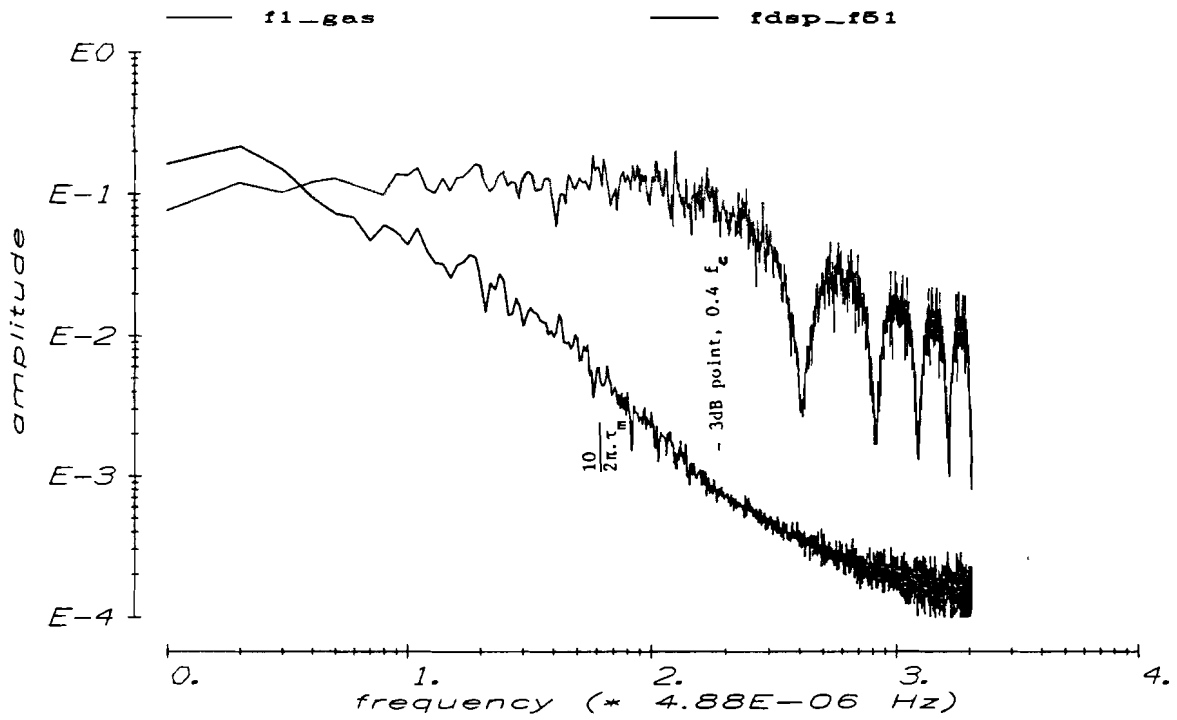

Fig. 4-7 Spectra of in- and output of experiment PRBNS2.
τ_m is the approximated 'fast' time constant of 1.5 hours.

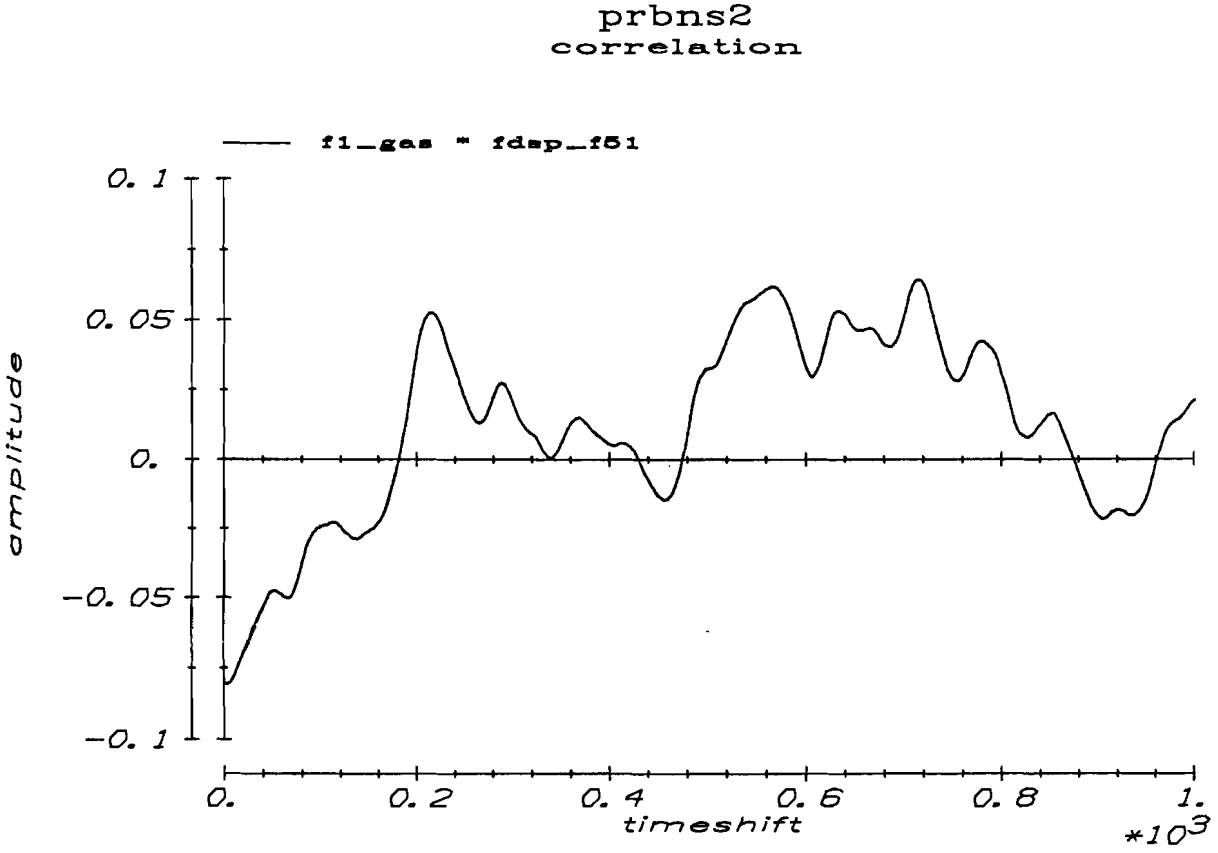

Fig. 4-8 a Cross-correlation of input f1 gas and output f51.

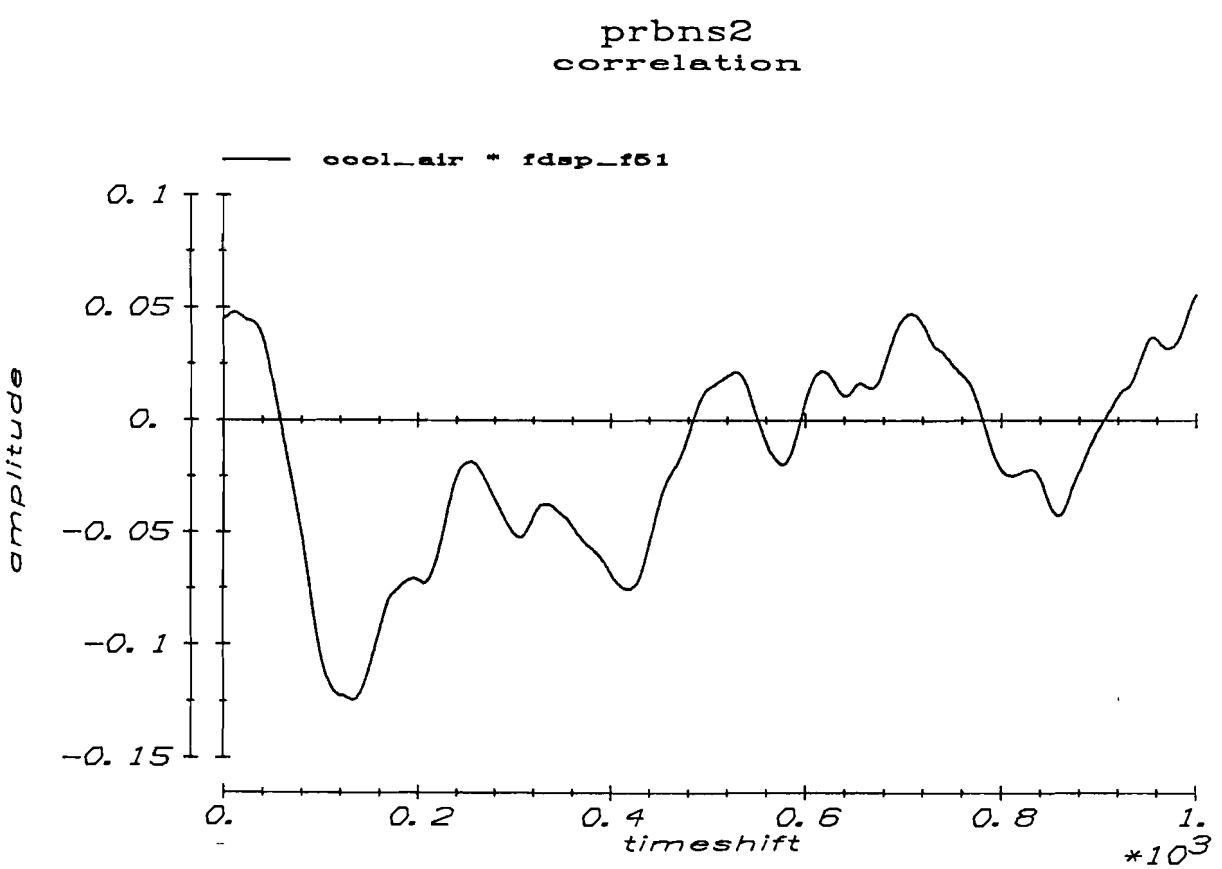

Fig. 4-8 b Cross-correlation of input cool air and output f51.

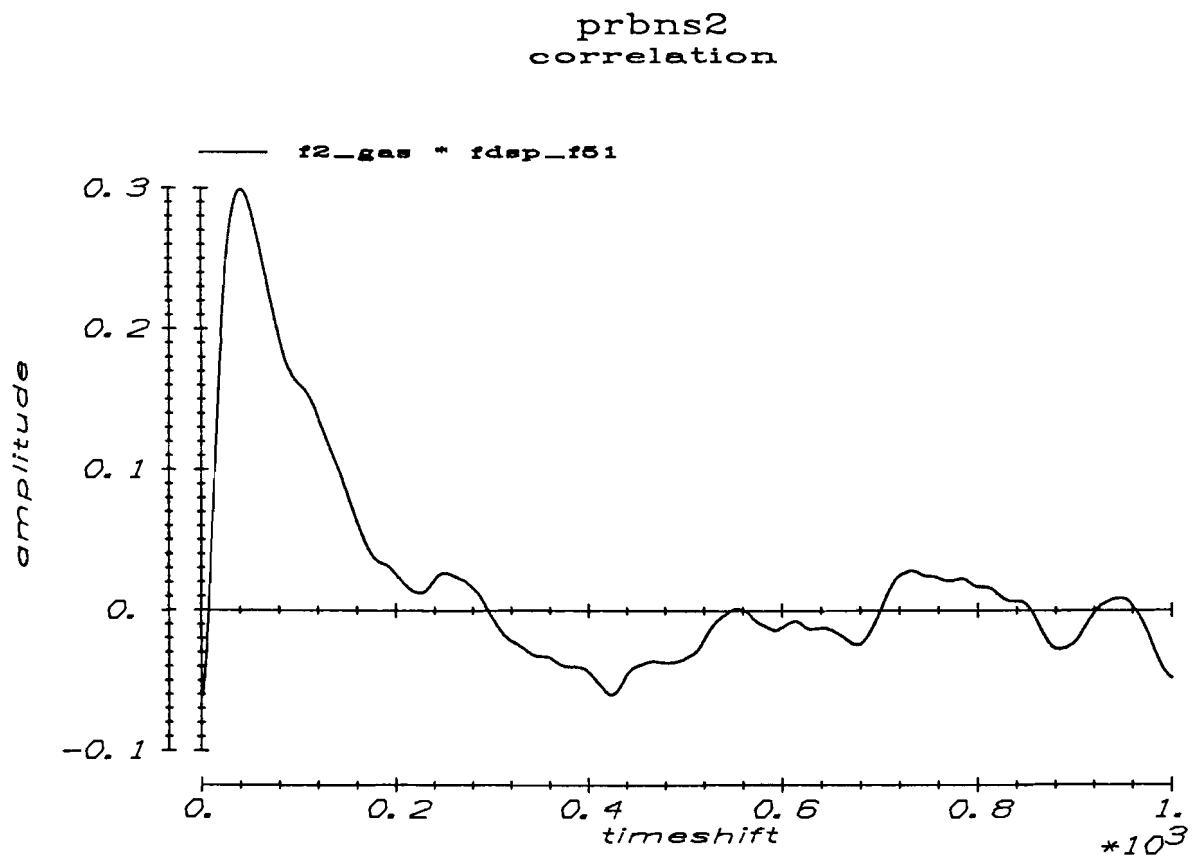

Fig. 4-8 c Cross-correlation of input f2 gas and output f51.

the experiment duration was short, related to this frequencies. Also is seen that frequencies with periods shorter than about 7 min are damped strongly by the process.

4.2.3 Cross-correlations

The three inputs are cross-correlated with the output (cf. figs 4-8a to c). Only the correlation of f2 gas and f51 shows a considerable correlation peak. In the figures 4-8a and b no correlation can be observed between the inputs at section 1 and the output at section 2. Apparently the cross-correlation result is disturbed by noise, as in the undisturbed case the correlation should contain a weighted impulse response of the particular transfer function. As a consequence no time-delay estimation can be done from these correlation analyses. In section 4.2.5 we will discuss another way to trace the delay-times, the presence of which we are sure from the global modelling.

4.2.4 Trend-correction

On the one hand it is known that the drift-phenomena or trends in the process outputs are not all process dynamics. They are not a response of the excitation at the input but may be originated by other causes. The DC-component of the output can be considered as the working point and is not taken into account when modelling the process dynamics (the PRBN-sequence has also zero mean).

On the other hand the estimation algorithm that will be used, only gives unbiased results if the input can be considered as white. Although the PRBN-sequence has a white spectrum, the signal can only be considered white if it is observed over a long period. For very low frequency parts this will not be the case. Consequently the estimation algorithm cannot model these frequencies properly.

For these two reasons, the data used for estimation may not contain trends. Trends would cause large estimation errors because their energy is large compared to the higher frequencies, as was seen in the spectrum of fig. 4-6b. Trends must be removed by high-pass filtering.

For the trend-correction a low-pass second order filter with real poles is used. The trend found by this filtering is subtracted from the data. The right cut-off frequency of this filter is derived with 'trial and error'. Two major arguments determine our choice. First, the number of periods corresponding to the low frequency parts that fit in the

experiment interval. Up to 5 periods in an experiment (here 7.2 days, so the periods of 1.5 days), may always be removed because a it is not possible to properly estimate process frequencies of which only 5 periods are measured.

The second argument is that the cut-off frequency depends on the intended use of the model. Our model will be applied in a model reference type of controller system. Use of the model in this controller requires that frequencies above $1/2\tau_d$, with τ_d the delay-time of the process transfer, are modelled properly. Lower frequencies do not necessarily have to be taken into account. Because this explanation only deals with the principle of the controller, it will be given in section 4.5, in which the use of the model is discussed. Here it suffices to know that the trend-correction applied in the following, will satisfy the controller constraints.

For detrending the outputsignal f51 is considered, because the inputs hardly contain trends. To avoid distortion from non constant time-lags that are caused by the frequency phase-shifts of the filter, non-causal filtering is used. The non-causal filtering that is applied has a zero phase shift and therefore, no phase-distortion occurs. First the signal is filtered forward, then backward (forward filtering on the reverse dataset) and finally the trend is formed by the mean of these two.

Filtering is applied with a cut-off frequency of $1/2\pi.\tau_c$ with $\tau_c=1.10^4$s, corresponding to a period of 17.5 hours (cf. fig. 4-6b). Later on at the estimation phase, a profile model was estimated on these data in which the impulse responses showed a strong 24 hours period. Because these periods were undesired regarding the intended use, a 'stronger' detrending is applied with a τ_c=3500 s (period of 6 hours). The trend of fdsp_f51 found with this filter is shown in fig. 4-9. The peaks at the beginning and end of the dataset are the transient responses of resp. forward and backward filtering.
The result of the detrending can be observed in figure 4-12. The input signals are detrended with the same filter.

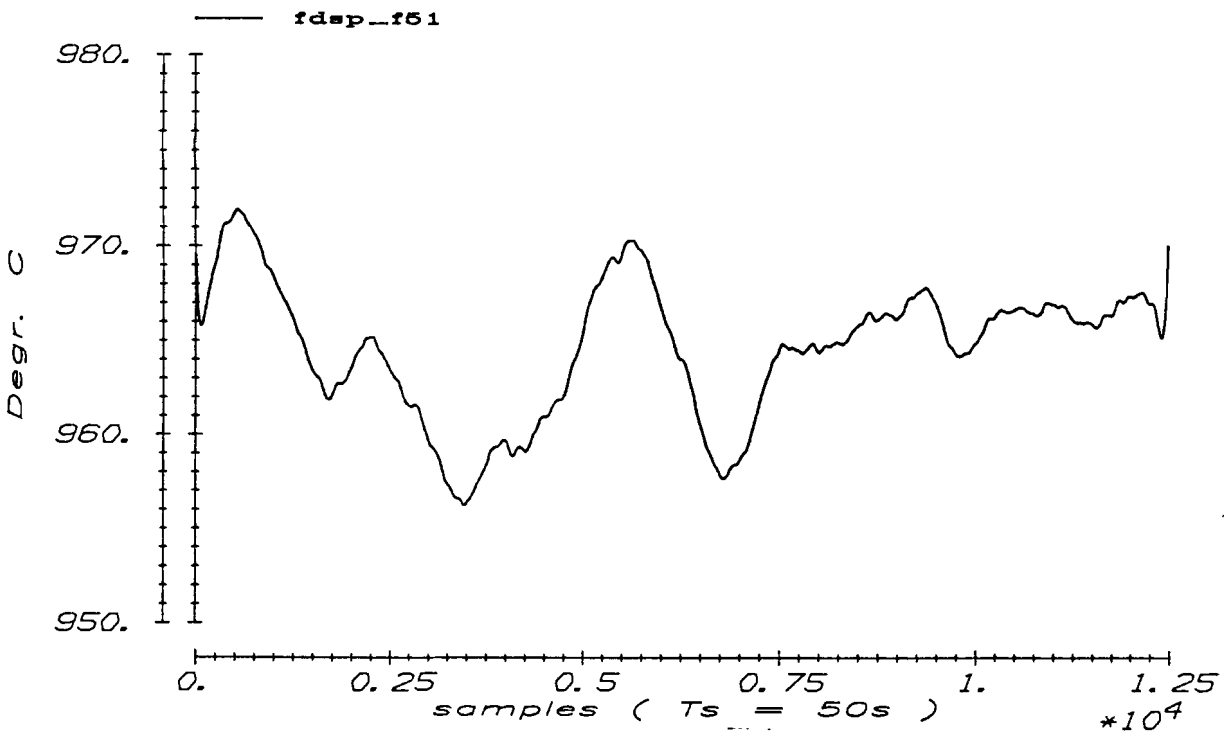

Fig. 4-9 Trend of signal f51 of PRBNS2 obtained by filtering with τ_c=3500 s.

4.2.5 Data reduction and scaling

The measuring experiment is done with a sampling time of 1/10 times the clock period of the PRBN-sequence. Data reduction is used to remove the samples of which the information has been used for detrending and repairing. It is essential that after sample reduction the spectrum of the input of the experiment that will be used for estimation, will be white. This is made plausible by the following.

If the estimation of the Finite Impulse Response (FIR) is executed, Markov parameters are searched for so that

$$\begin{pmatrix} \underline{y}_k & \underline{y}_{k+1} \cdot \cdot \underline{y}_{k+1} \end{pmatrix} = \begin{pmatrix} \hat{M}_1 & \ldots & \hat{M}_m \end{pmatrix} \begin{pmatrix} \underline{u}_{k-1} \cdot & \cdot & \cdot & \underline{u}_{k+1} \\ \vdots & \cdot & \cdot & \vdots \\ \underline{u}_{k-m-1} & \cdot & \cdot & \underline{u}_{k-m+1} \end{pmatrix} \quad (4.1)$$

with $\underline{y}_k$ the measured outputs,

$\hat{M}_i$ the i_{th} Markov parameter of the FIR-model, i= 1..m

$\underline{u}_k$ the measured inputs, k > m+1, l the number of samples of the sequence.

Denote the matrices with outputs, Markov parameters and inputs resp. as Y, $\hat{M}$, and Ω_m. The algorithm obtains the parameters $\hat{M}$ of equation (4.1) by calculating a matrix expression that is quite similar to

$$\hat{M} = Y\ \Omega_m^T(\ \Omega_m \Omega_m^T\ )^{-1}\ . \qquad (4.2)$$

In (4.2) the pseudo inverse of the input matrix Ω_m is calculated. This puts constraints on Ω_m. If the input bandwidth is too small, i.e. too small for the sampling rate that is used, the condition number of the matrix Ω_m will increase. As a result, problems will arise during inversion due the bad conditioning for high frequencies, and the Markov parameters of the FIR-model are badly estimated.

To assure that the input spectrum becomes white after data-reduction, we sample the data with a factor 10 (so 1 sample per clock period) . For a smaller reduction factor (i.e. a higher sampling frequency) the input bandwidth would become to small. With this oversampling rate all information of the outputs is still obtained without distortion. Remember that the filtering frequency in case of one sample per period becomes equal to the clock frequency f_c of the PRBNS, and f_c was far beyond the bandwidth of the process. With this sampling frequency it is sure that the output is measured without aliasing occurring.

The last step of the signal preparation phase is scaling. The various transfers have different amplitude because the in- and outputs have different units and different working points. To model each in/output transfer with equal weight in the estimation phase, the in- and output signals must be represented with equal power. The weight of the transfers is equaled by scaling the signals, so that the square roots of their variances become one. Because the average is subtracted first, the power of all signals becomes one too.

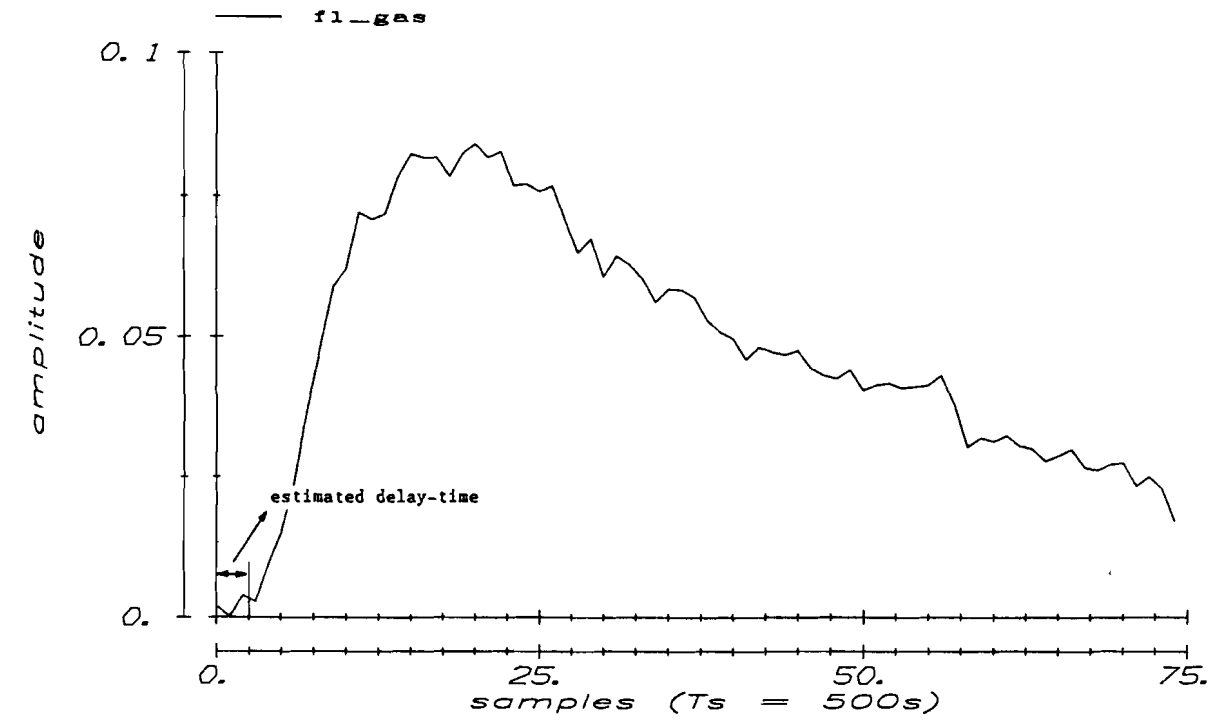

Fig. 4-10a Impulse response of f1 gas -> f51, obtained with the FIR-model estimation on data that was not corrected for delay times.

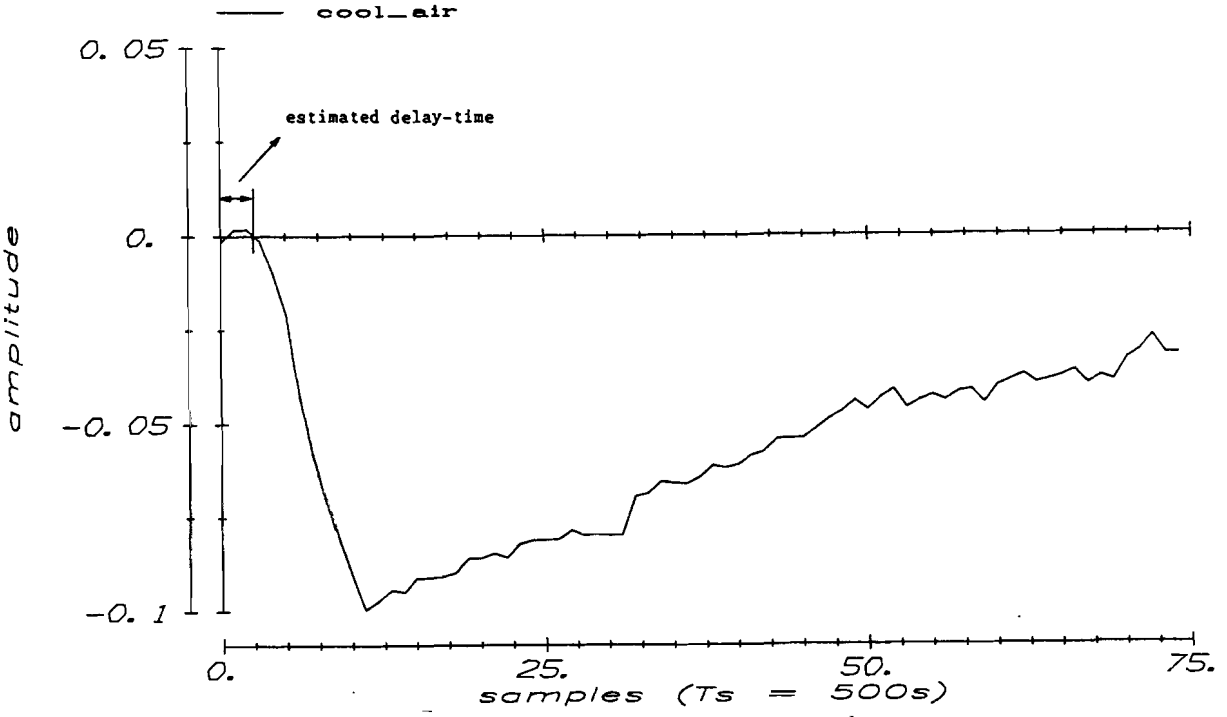

Fig. 4-11b Impulse response of cool air -> f51, obtained with the FIR-model estimation on data that was not corrected for delay times.

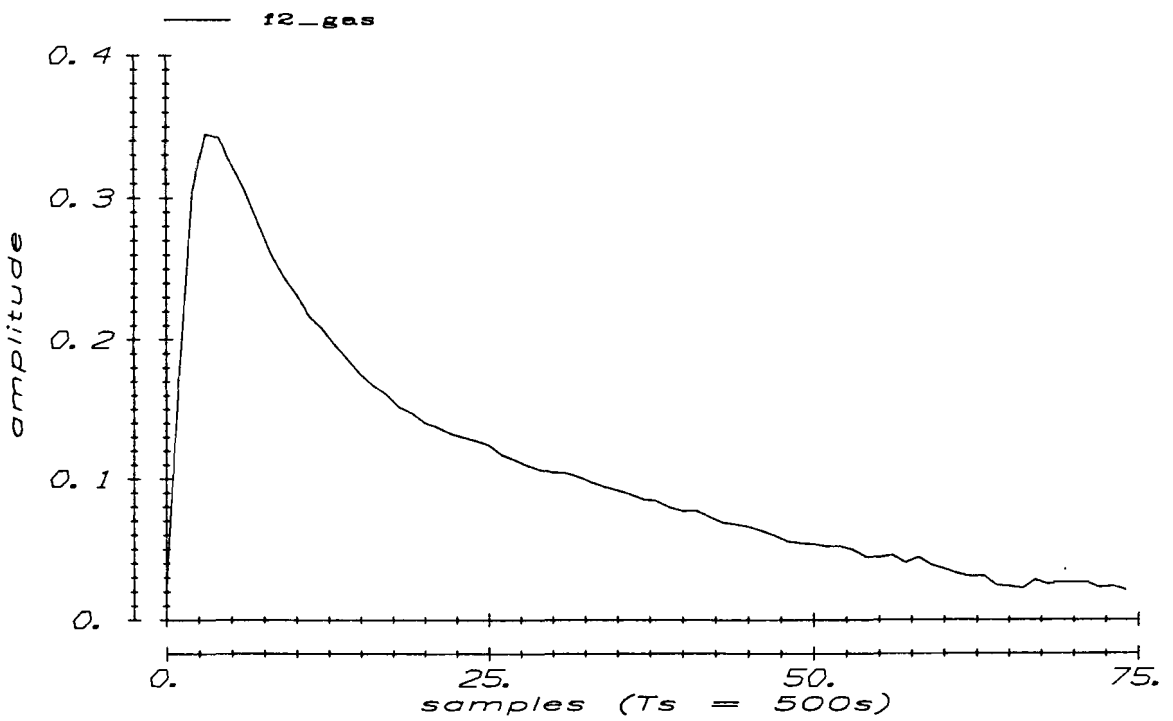

Fig. 4-11c Impulse response of f2 gas -> f51, obtained with the FIR-model estimation on data that was not corrected for delay times.

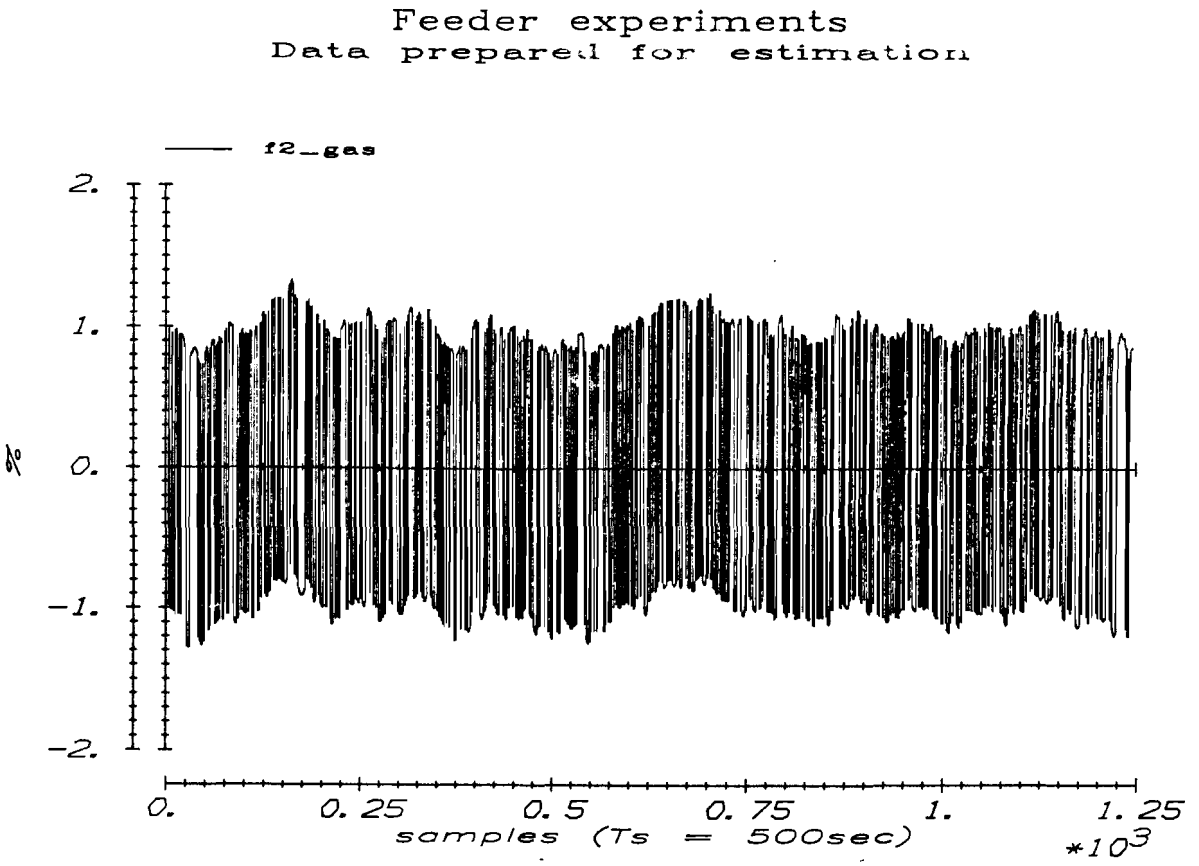

Fig. 4-12a Signal f2 gas of PRBNS2 prepared for estimation.

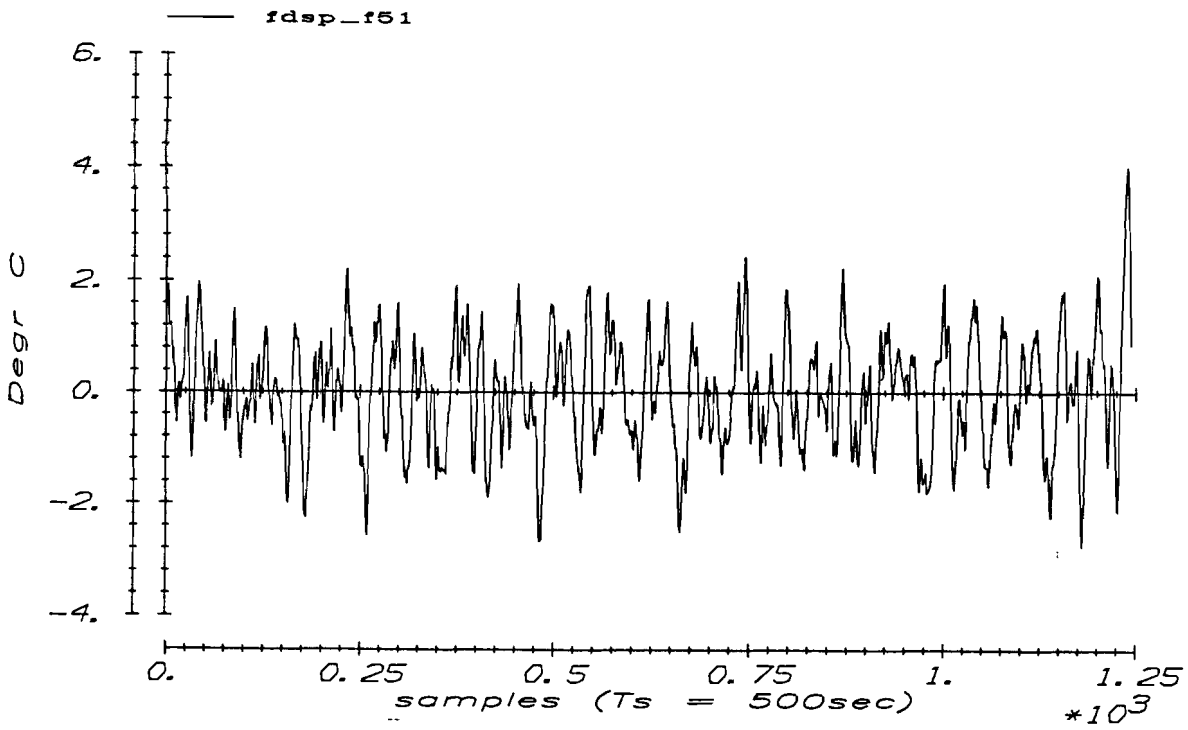

Fig. 4-12b Signal fdsp_f51 of PRBNS2, prepared for estimation.

Delay-time estimation

In this phase also a delay-time correction is applied. Because with cross-correlation the delay-time estimation failed, results of the first Finite Impulse Response models are used (cf. figs 4-11a and b). From these impulse responses a delay-time is derived as depicted in the figures. The time interval in which the impulse responses still were zero were taken as delay-time; 25 samples of 50 s (in total 20.8 min) for the transfers of section one to the spout temperature f51. The transfer of f2 gas had no delay-time. The delay-time estimation is used to correct the data for delay-time by shifting the whole dataset back in time for the particular signals.

Finally the following values are used in the this phase:

Signal	scaling factor	delay-time correction (sample=50 s)
f1 gas	0.05	0
coolair	0.0718	0
f2 gas	0.503	25
f51	1.99	25

The data are now prepared for estimation. View the examples of f2 gas and fdsp_f51 in fig. 4-12.

4.3 ESTIMATION

In section 1.3 it has been outlined what steps are distinguished in the estimation procedure. These steps will be discussed sequentially.

4.3.1 FIR-model

The FIR-model represents the process with impulse responses of finite length. A impulse response length of 75 samples is chosen, corresponding to 10.4 hours. The FIR model now becomes (cf. J. Vaessen, 1983):

$$\underline{y}(k) = \sum_{i=1}^{75} M_k \underline{u}(k-i) + \underline{e}(k) \qquad (4.3)$$

with $M_i, i=1..75$ the estimated Markov parameters

$\underline{e}(k)$ the estimated noise with 2 autoregressive parameters:

$\underline{e}(k) = A_1\underline{e}(k-1) + A_2\underline{e}(k-2) + \underline{\xi}(k)$,

$\underline{\xi}(k)$ white noise samples.

The impulse responses that result from this estimation are depicted in the figures 4-16a to c. The calculation of the noise parameters is used to obtain insight in the appearing noise. The noise parameters will not be used in the next steps anymore.

Remark that with the FIR-model of (4.3) the modelset is already limited:

- The model is a lumped parameter system.
- The model is linear.
- Markov parameters are independent of time; the model is stationary.
- The model has finite impulse responses; their tails are assumed to be neglectable.

4.3.2 MPSSM GERTH approach

For a finite dimensional system the following recurrent relation for the Markov parameters can be derived (cf. R. Oudbier, 1986):

$$M_{r+j} = \sum_{i=1}^{r} a_i M_{r+j-i} \qquad j \geq 1 \qquad (4.4)$$

in which a_i, i=1..r are called the minimal polynomial coefficients.

This means that the system can be described completely with a set of parameters $\{a_i, M_i \mid i \varepsilon I, 1 \leq i \leq r\}$. $M_1..M_r$ are called the start sequence Markov parameters. Before estimating the MPSSM-model first the degree r of the polynomial has to be known.

Order estimation

Derivation of the order would be easy if equation (4.4) had a deterministic solution. However, the process is usually outside the modelset and the Markov parameters are corrupted with noise, so only can be searched for the most obvious mutual dependences of the Markov parameters.

To this end a block Hankel matrix is observed filled with Markov parameters. The dependences of the Markov parameters will determine the rank of this Hankel matrix. Because we are only interested in the dependences of complete Markov parameters (cf. 4.4), the Markov parameters are written as vectors:

$$M = \begin{pmatrix} M_{11} & \cdot & \cdot & M_{1p} \\ \cdot & & \cdot & \cdot \\ M_{q1} & \cdot & \cdot & M_{qp} \end{pmatrix},$$

$$\mathrm{vec}(M) = (M_{11}..M_{q1}, M_{12}..M_{q2}, \ldots, M_{1p}..M_{qp})^T \qquad (4.5)$$

with p the number of inputs,
q the number of outputs.

Writing the Markov parameters as vectors, the dependences of the columns of the parameters itself are not taken into account. The matrix now becomes:

$$H_k = \begin{pmatrix} \mathrm{vec}(M_1) & \mathrm{vec}(M_2) & \ldots & \mathrm{vec}(M_n) \\ \mathrm{vec}(M_2) & \mathrm{vec}(M_3) & \ldots & \cdot \\ \cdot & \cdot & \ldots & \cdot \\ \mathrm{vec}(M_n) & \cdot & \ldots & \mathrm{vec}(M_{2n-1}) \end{pmatrix}. \qquad (4.6)$$

With a singular value decomposition of this Hankel matrix its rank is observed. The decomposition transforms the matrix to two matrices with

orthonormal vectors, and assigns to each direction a corresponding amplification factor. These factors are called the singular values. Because the Hankel matrix is a transfer of the post inputs to the future outputs of the system (cf. Glover,1984), the singular values determine the amplification of the decomposed transfers of the Hankel matrix. Large singular values correspond to important modes of the transfer. The singular values are ordened in size. Because the last singular values only indicate independences of the parameters due to (white) noise, they are small and equal to each other. The singular values of H_k of the FIR-model parameters are shown in figure 4-13. The first two singular values are taken anyway because they describe a significant part of the transfer. How many singular values are taken next is observed from the ratios of the singular values. If the ratios σ_{i+1}/σ_i of the singular values are observed in figure 4-14, these ratios indeed tend to go to 1 because the attribution of the (white) noise is equal for all directions. The rank of the Hankel matrix is now taken as that number i of the singular value (σ_i), of which the next (σ_{i+1}) is significantly smaller (cf. T. Backx, 1987). This can be deduced from a small ratio in figure 4-14. Of this singular value it is known that it yields a high contribution to the transfer, compared to its subsequent singular value. In figure 4-14 a degree 4 is found.

Now the minimal polynomials of degree 4 are fitted in least square sense to the FIR-model impulse responses. This is called the GERTH-approach. The results are depicted in figure 4-16. It is no coincidence that the first 4 parameters (start sequence) fit badly on the FIR-model. The GERTH-algorithm first estimates the polynomial coefficients $a_1..a_r$, and in a next step the start sequence is calculated such that the polynomial fits best (cf. H. van der Weijden, 1984). This means that the fit of the start sequence does not count very much in the criterion.

Remark that with the GERTH model the modelset is adjusted:
- The model is of reduced order.
- The impulse responses are not of finite length anymore.

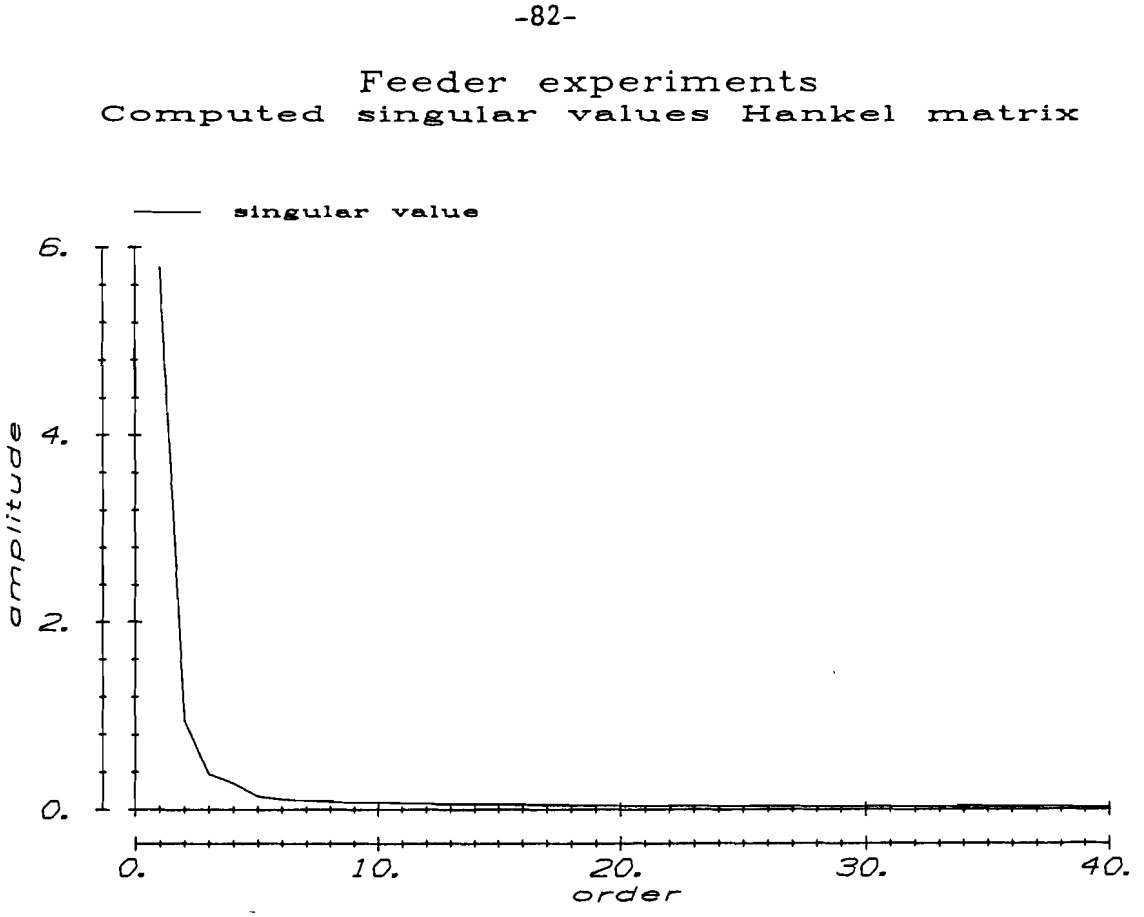

Fig. 4-13 Hankel singular values of Hankel matrix composed with Markov parameters from the FIR-model

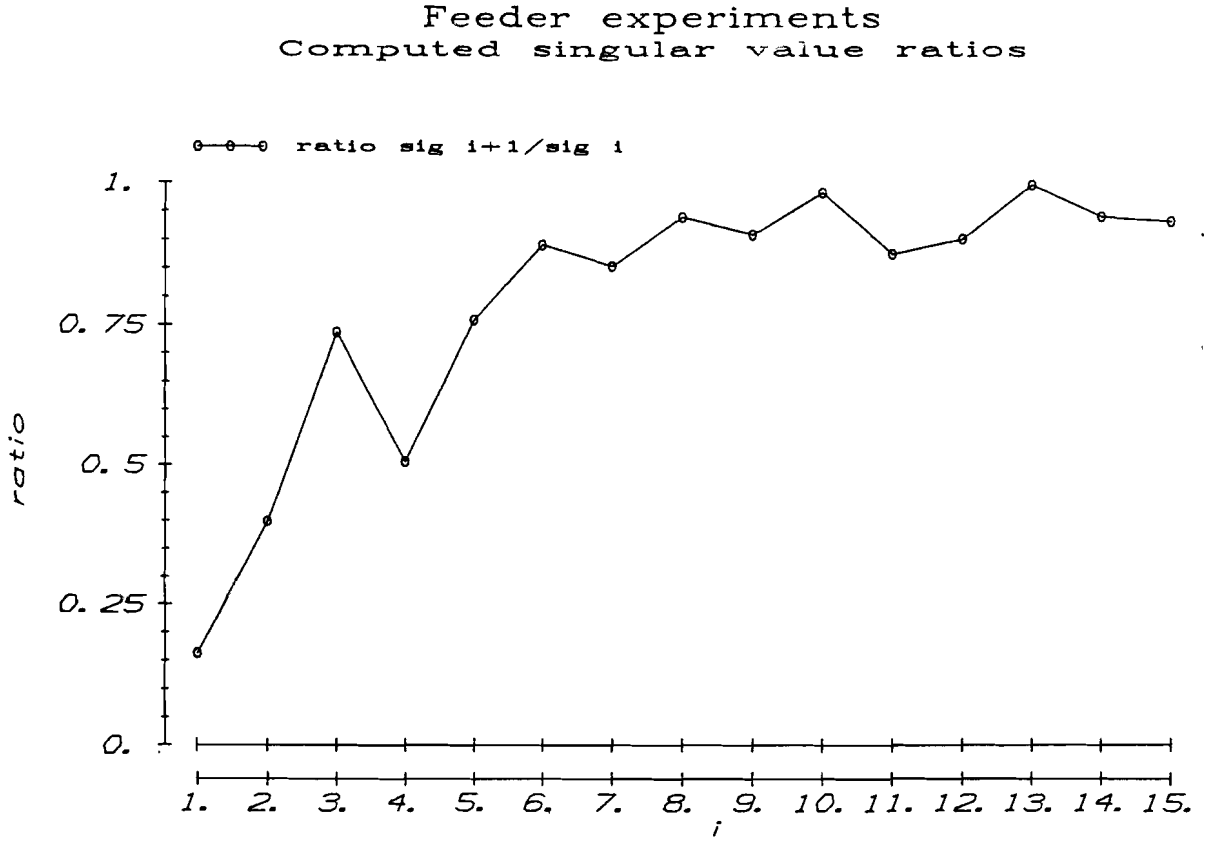

Fig. 4-14 Singular value ratios (σ_{i+1}/σ_i).

4.3.3 MPSSM DIRECT approach

The GERTH algorithm got all information to estimate the MPSSM model from the FIR-model. However, the FIR-model is a limited representation of the process for its impulse responses are of finite length. That is why the DIRECT method estimates the MPSSM parameters directly from the measured in- and outputs. It estimates the parameters $\{a_i, M_i \mid i\varepsilon I, 1\leq i\leq r\}$ so that the loss function

$$V_{a_i,M_i} = \text{tr}\,[(Y-\hat{Y})^T(Y-\hat{Y})] \qquad (4.7)$$

with $\hat{Y}$ the sum of the estimated outputs obtained from the MPSSM,

becomes minimal (cf. H. van der Weijden(1984) and R. Oudbier(1986)). The loss function V is not square in the parameters a_i, so hill climbing techniques must be used to find the minimum of the loss function. The parameters of the GERTH-model are taken as a start value for this algorithm.

In section 4.2.4 it has been remarked that with the estimation of the MPSSM model on the data detrended with $\tau_c=1.10^4$s, a period of 24 hours was found in the impulse responses of the profile model. Of course these periods could not be seen in the FIR- and GERTH-model, for the impulse responses of the FIR model were too short. Also the impulse response of the spout model showed a periodicity, although with a much greater period and a greater damping than the profile model. The impulse responses over a period of 1000 samples (5.8 days) are shown in figure 4-15. The exact cause of this phenomenon has not been recovered, but it is possible that the 24 hour disturbances in the estimation data that caused the periods in the profile model, also caused the periods in the impulse responses of the spout model. Later on the the estimation data are detrended with τ_c=3500s to remove these periods.

The results of the DIRECT estimation on the experiment PRBNS2 are also presented in figure 4-16.

The figure shows that the DIRECT estimated impulse responses fit close to the FIR responses in the first part. A difference is observed in the tail of the impulse responses of the FIR and the DIRECT method. The FIR impulse response decrease faster than the DIRECT impulse responses. In section 4.4.2 an explanation is given for this phenomenon.

As expected the impulse responses present a slow behaviour. Even after 14 hours the responses have not been died out. Conspicuous however, is how fast the impulse responses rise, especially to an excitation of f2 gas.

The 4 poles obtained from the MPSSM DIRECT model (i.e. the zeros of the characteristic equation $1 + a_1 z^{-1} + a_2 z^{-2} + a_3 z^{-3} + a_4 z^{-4} = 0$, with $a_1..a_r$ the minimal polynomial coefficients) are:

Poles of MPSSM spout model	z-domain	s-domain
	0.9819	1/7.6 hour
	0.9128	1/5.8 hour
	0.6329 + i0.125	1/(15.87 + i7.06)min
	0.6329 - i0.125	1/(15.87 - i7.06)min

What could be seen from the impulse responses is affirmed here: there is a large pole that causes the low frequency behaviour but also a small pole pair that makes the output to react fast.

The results of the profile model are also presented in the figures 4-34, that show the impulse responses obtained from the MPSSM model DIRECT estimation. Also a 4-th degree polynomial approximation has been used. The delay-times have been compensated by shifting input and outputs of section 2 with 15 samples of 50 seconds. We see that the impulse responses in general are faster than those of the spout model. The couples respond even almost immediately to the input f2 gas. In this impulse responses the discrepancy of the 'fast' and the 'slow' pole is more clear than in the spout model. Notice the difference between the response to the cool air of the spout model and that of the profile couples. The very clear bend in the profile response does not exist in the spout response. This is affirmed by the pole position of the profile model:

Poles of MPSSM profile model:	z-domain	s-domain
	0.9796	1/6.7 hour
	0.8410 +i0.0976	1/(33.8 + i23.4)min
	0.8410 +i0.0976	1/(33.8 - i23.4)min
	0.3024	1/7min

We see that the 'in between' pole of 1/5.8 hour does not exist in the profile model.

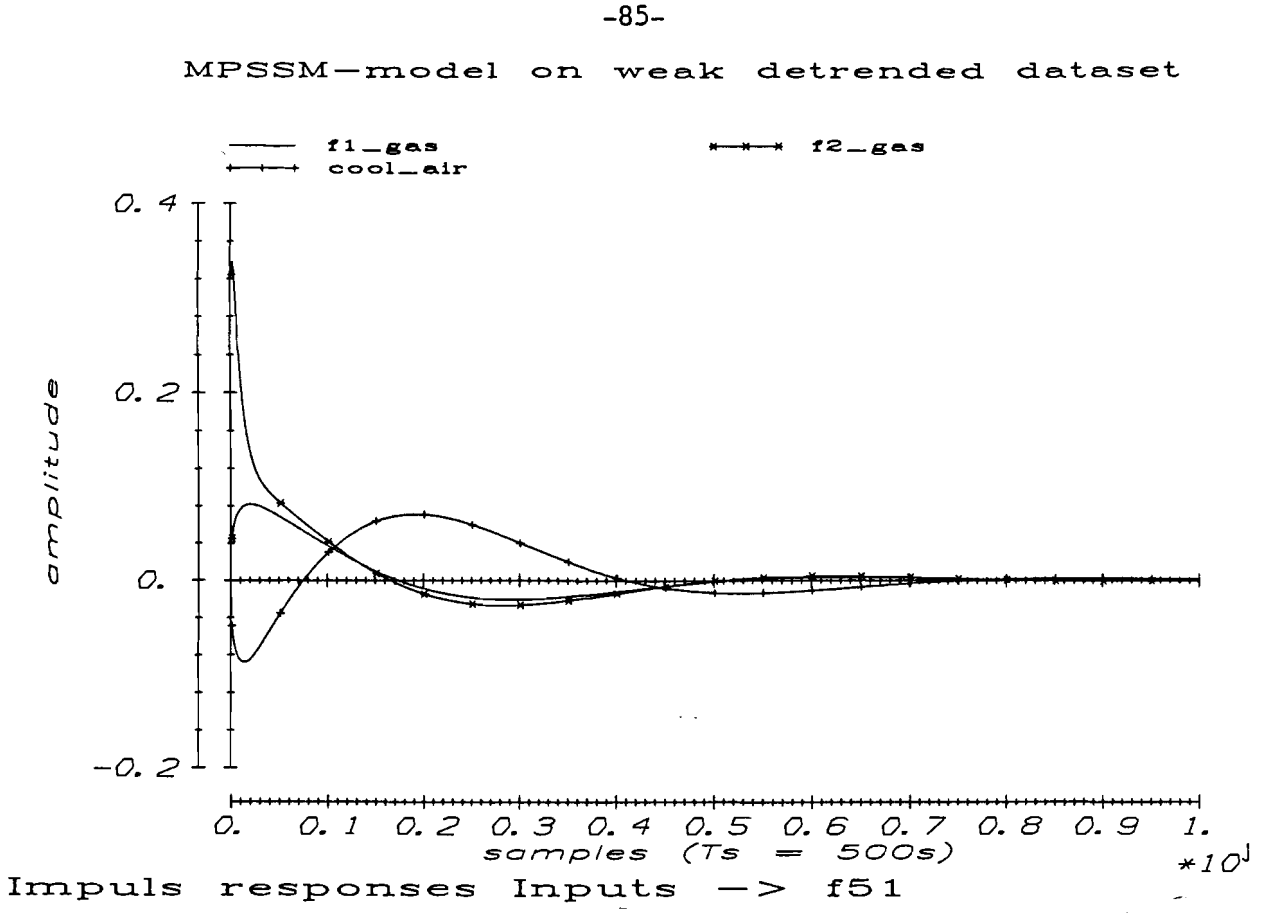

Fig. 4-15 Long impulse responses obtained from Direct estimation on PRBNS2, detrended with τ_c=1E04.

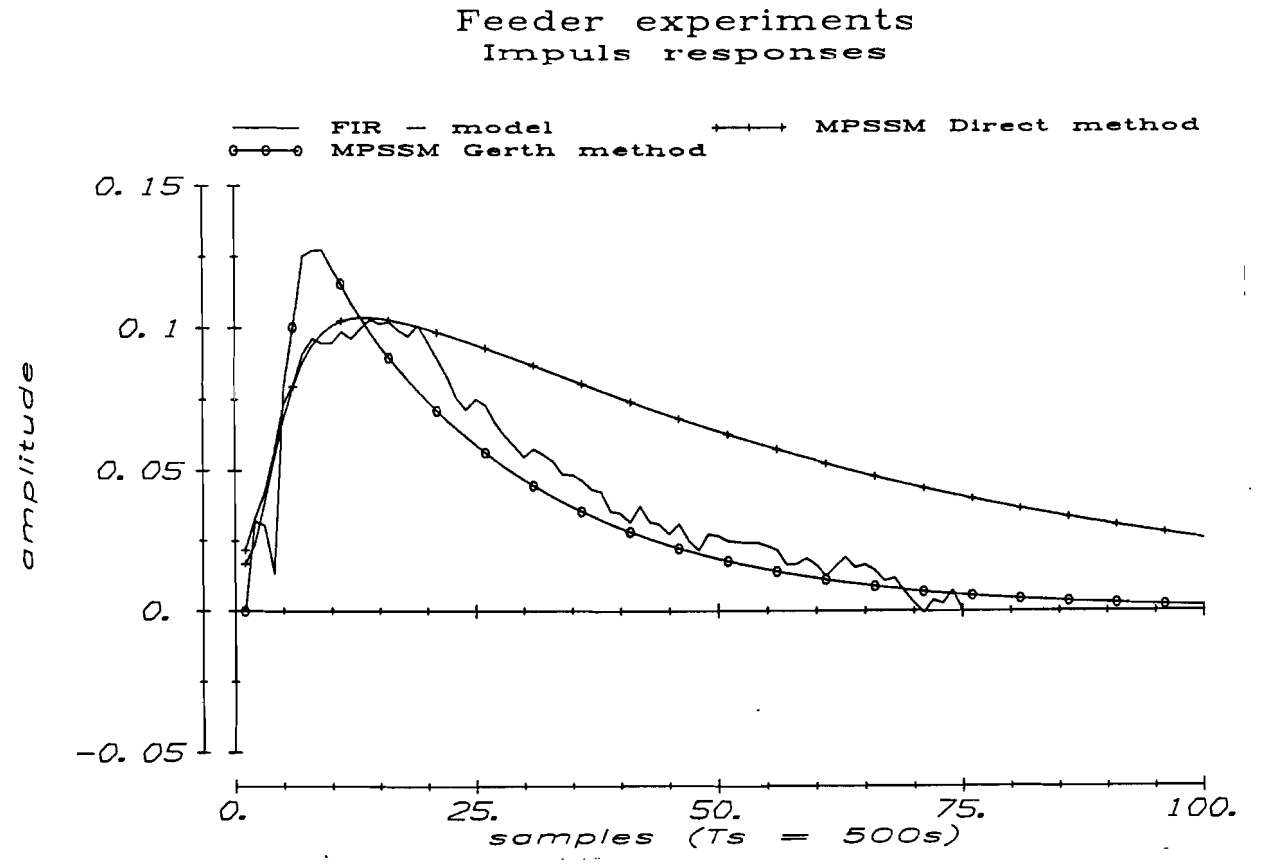

Fig. 4-16a Impulse responses of f1 gas -> f51, obtained from parameter estimation on PRBNS2, detrended with τ_c=3500s.

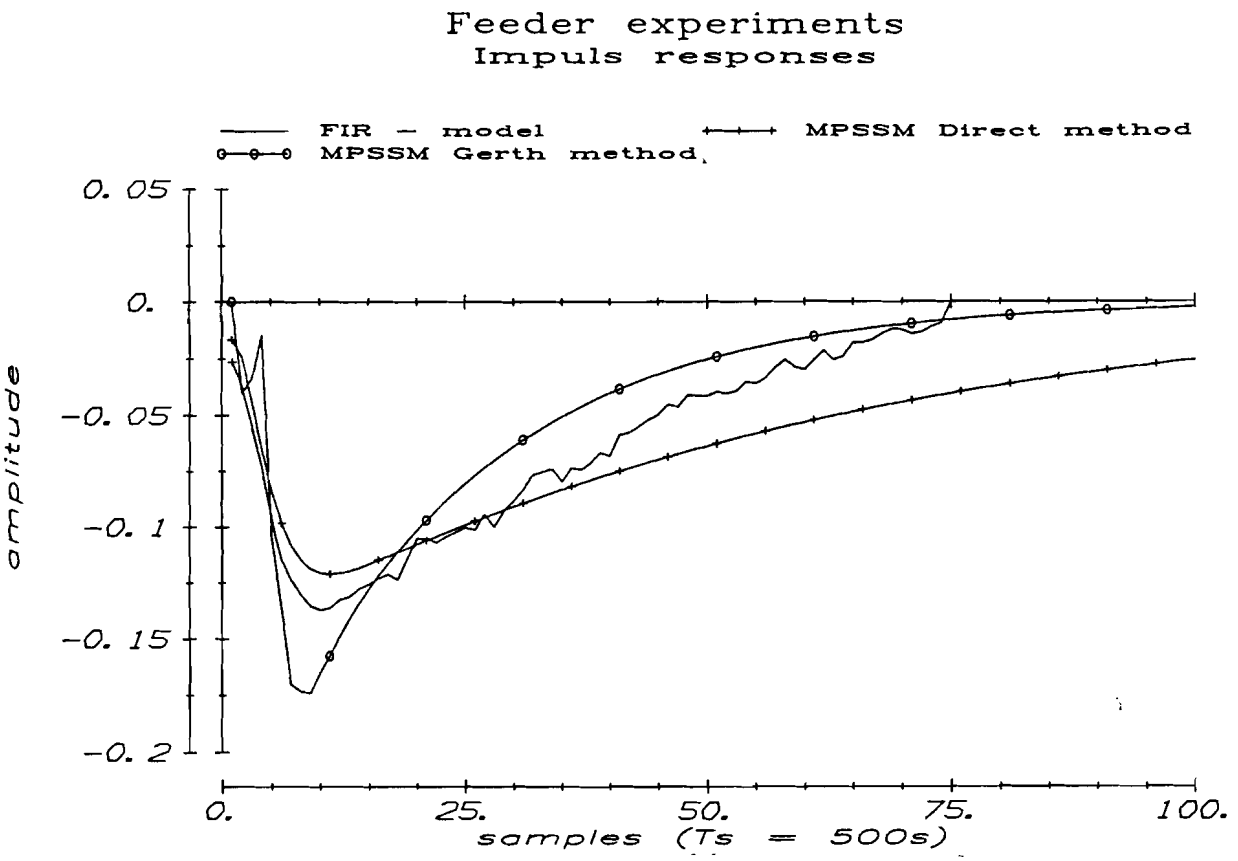

Fig. 4-16b Impulse responses of cool air -> f51, obtained from parameter estimation on PRBNS2, detrended with τ_c=3500s.

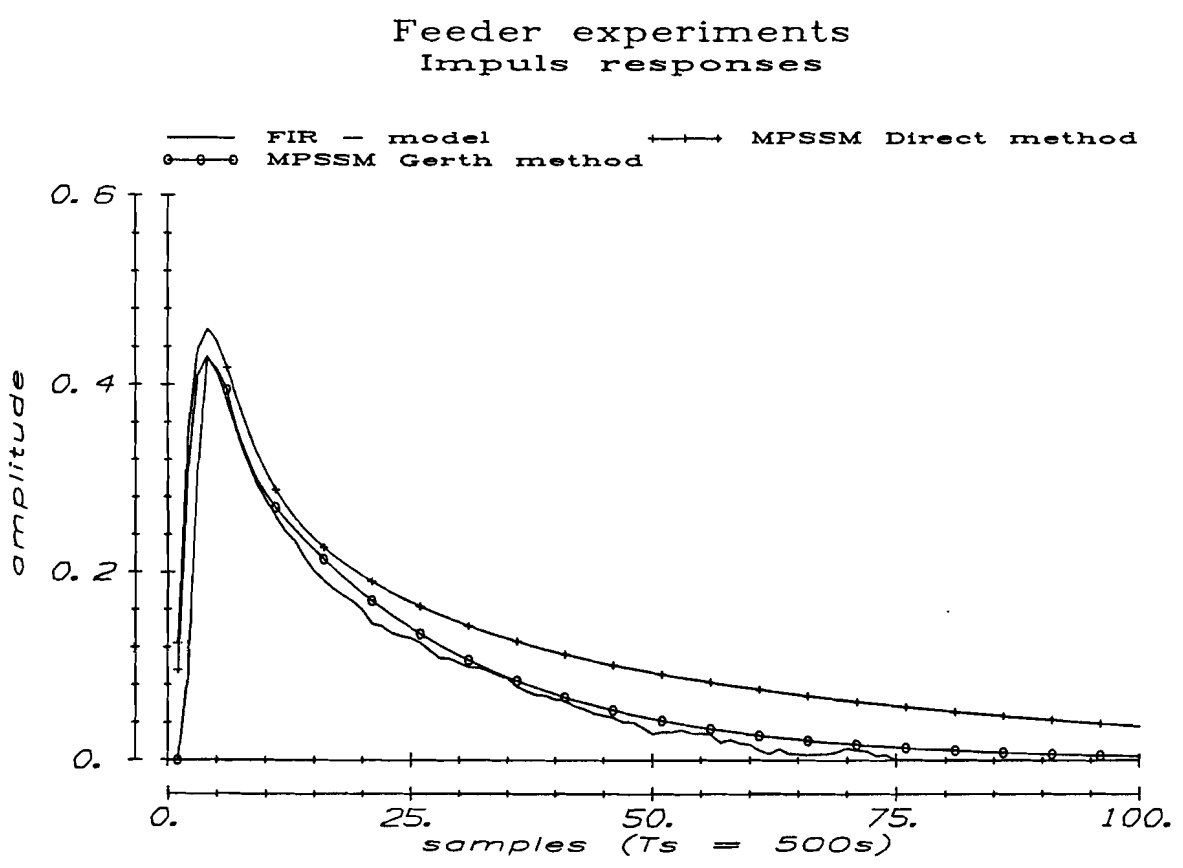

Fig. 4-16c Impulse responses of f2 gas -> f51, obtained from parameter estimation on PRBNS2, detrended with τ_c=3500s.

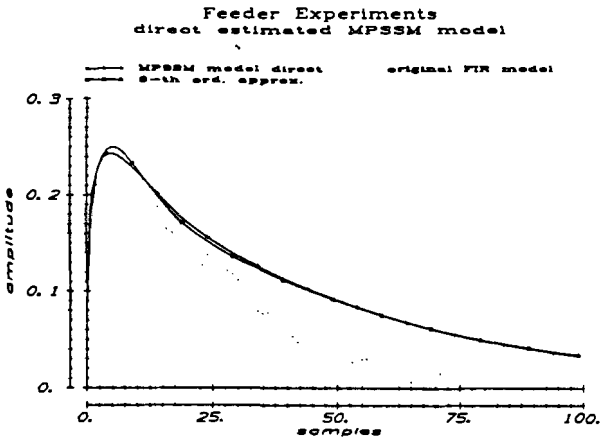

Fig. 4-17a Impulse response of f1_gas -> fm1 of the MPSSM model, and of its 6-th order approximate realization.

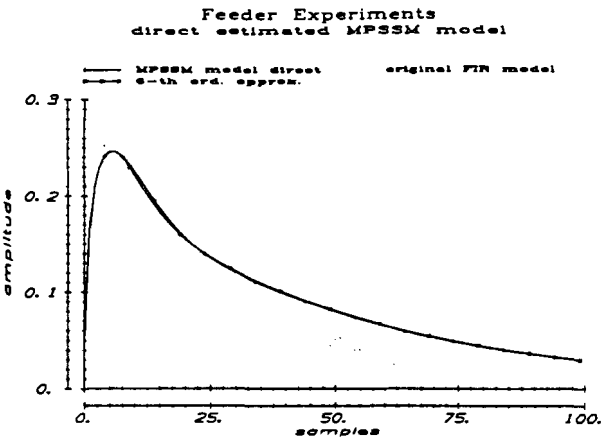

Fig. 4-17b Impulse response of f1_gas -> fm4 of the MPSSM model, and of its 6-th order approximate realization.

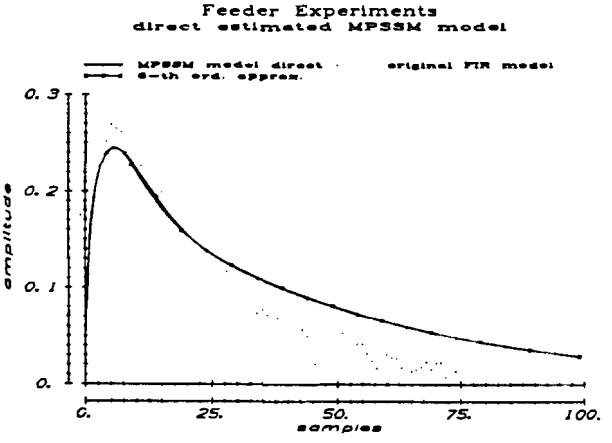

Fig. 4-17c Impulse response of f1_gas -> fm5 of the MPSSM model, and of its 6-th order approximate realization.

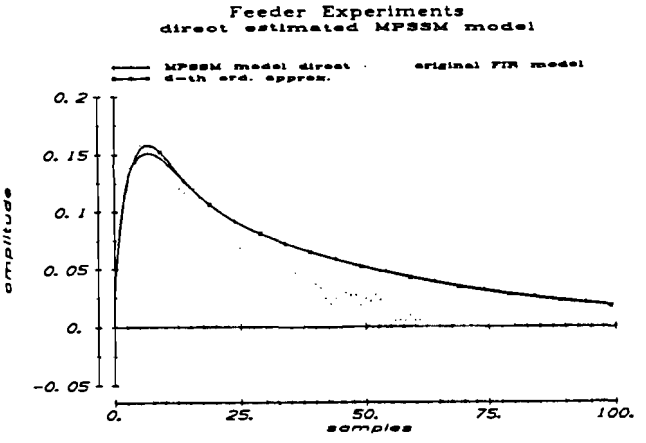

Fig. 4-17d Impulse response of f1_gas -> fl1 of the MPSSM model, and of its 6-th order approximate realization.

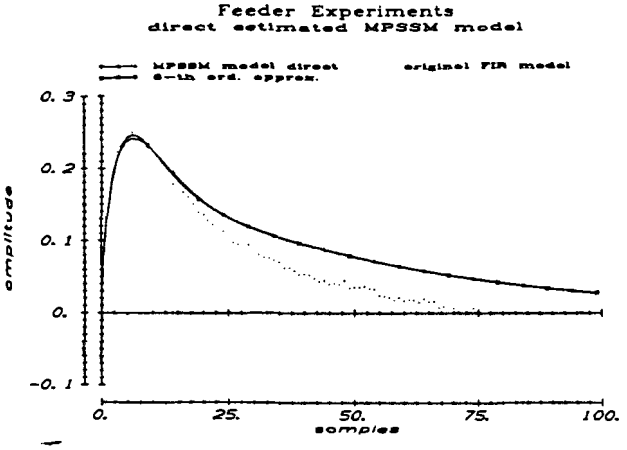

Fig. 4-17e Impulse response of f1_gas -> fl2 of the MPSSM model, and of its 6-th order approximate realization.

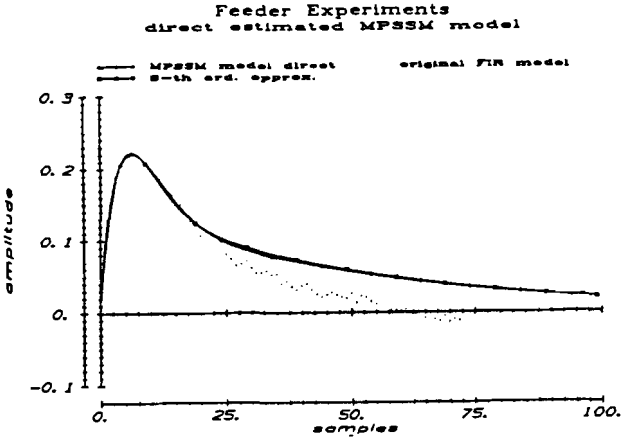

Fig. 4-17f Impulse response of f1_gas -> fr2 of the MPSSM model, and of its 6-th order approximate realization.

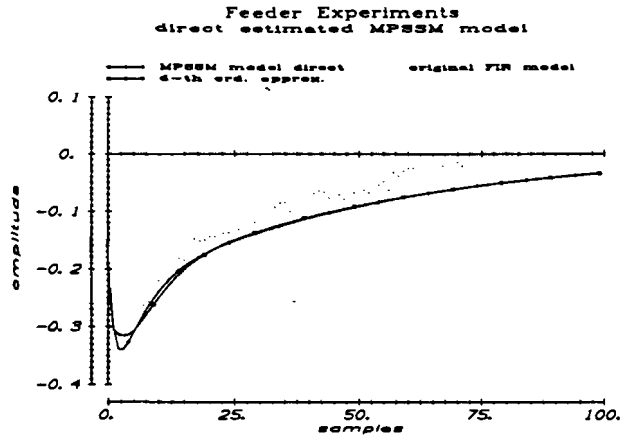

Fig. 4-17g Impulse response of cool_air -> fm1 of the MPSSM model, and of its 6-th order approximate realization.

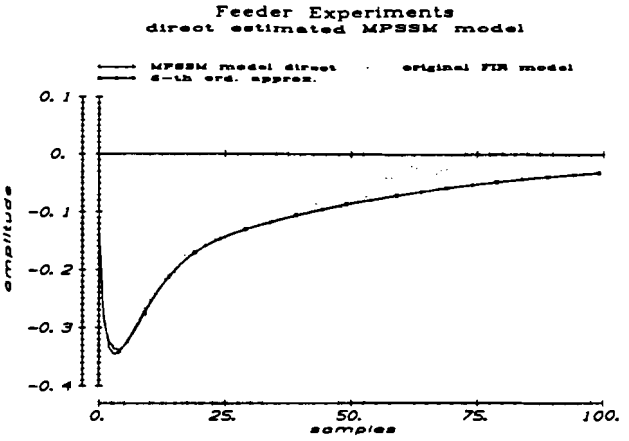

Fig. 4-17h Impulse response of cool_air -> fm4 of the MPSSM model, and of its 6-th order approximate realization.

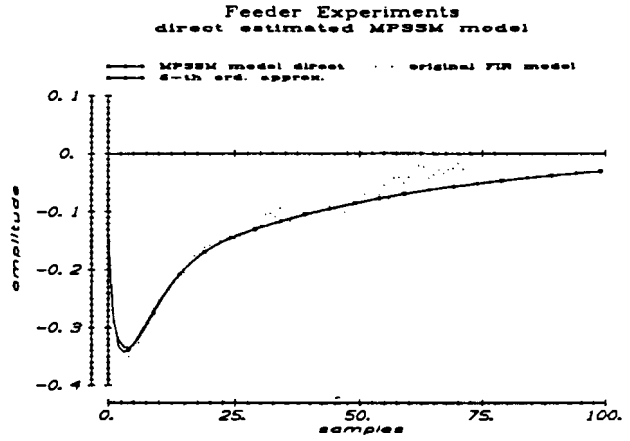

Fig. 4-17i Impulse response of cool_air -> fm5 of the MPSSM model, and of its 6-th order approximate realization.

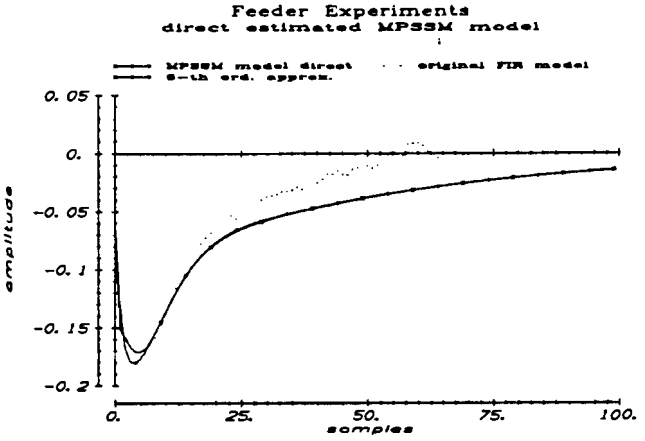

Fig. 4-17j Impulse response of cool_air -> fl1 of the MPSSM model, and of its 6-th order approximate realization.

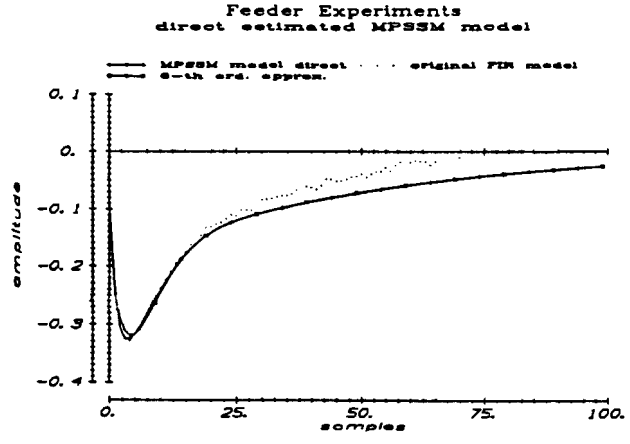

Fig. 4-17k Impulse response of cool_air -> fl2 of the MPSSM model, and of its 6-th order approximate realization.

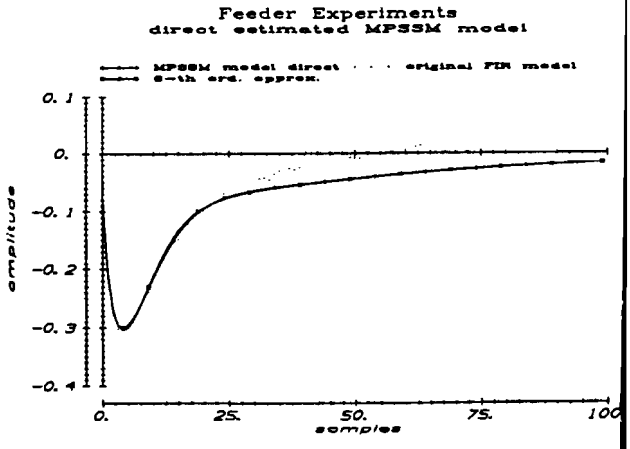

Fig. 4-17l Impulse response of cool_air -> fr2 of the MPSSM model, and of its 6-th order approximate realization.

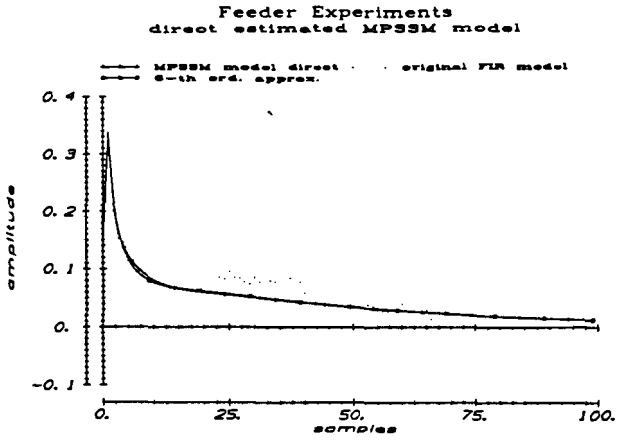

Fig. 4-17m Impulse response of f2_gas -> fm1 of the MPSSM model, and of its 6-th order approximate realization.

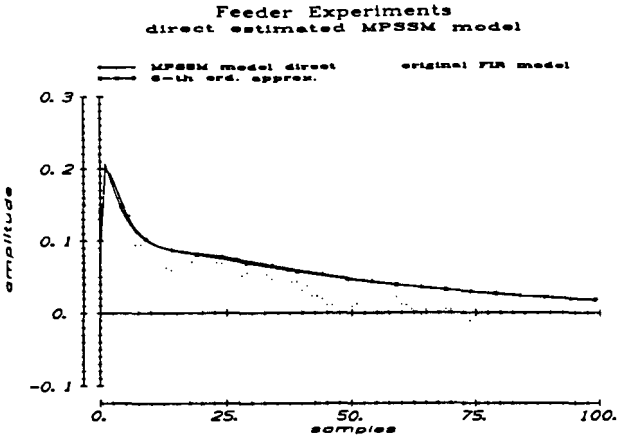

Fig. 4-17n Impulse response of f2_gas -> fm4 of the MPSSM model, and of its 6-th order approximate realization.

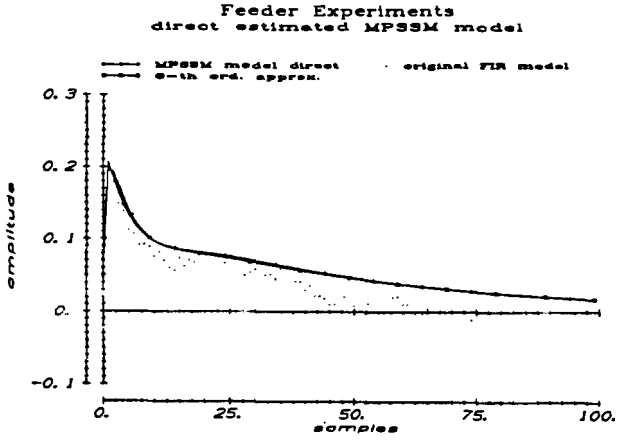

Fig. 4-17o Impulse response of f2_gas -> fm5 of the MPSSM model, and of its 6-th order approximate realization.

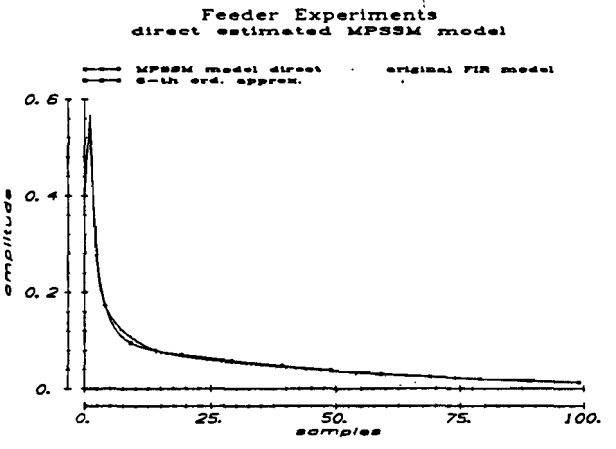

Fig. 4-17p Impulse response of f2_gas -> fl1 of the MPSSM model, and of its 6-th order approximate realization.

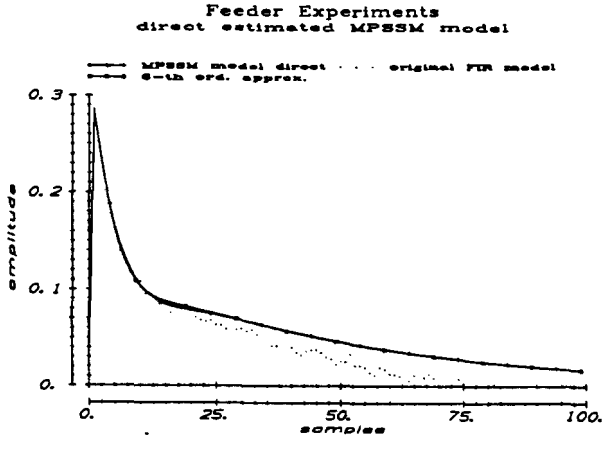

Fig. 4-17q Impulse response of f2_gas -> fl2 of the MPSSM model, and of its 6-th order approximate realization.

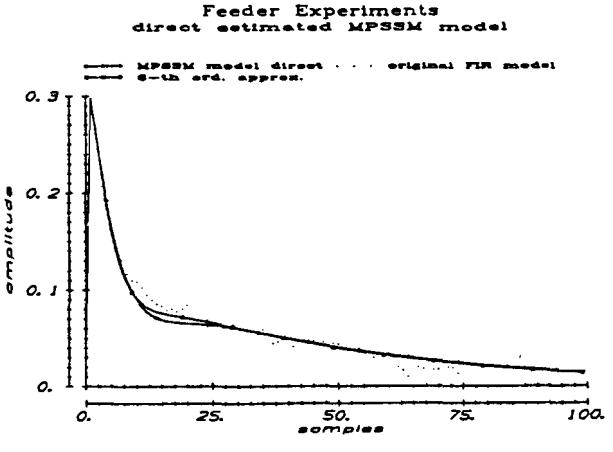

Fig. 4-17r Impulse response of f2_gas -> fr2 of the MPSSM model, and of its 6-th order approximate realization.

For the present, a first interpretation can be made of these models. It is striking how fast the outputs react to input variations. Even temperatures at the bottom and also the spout temperature reach their highest amplitude of the impulse response within half an hour. It is expected that the mechanism of radiation is the origin of this fast behaviour. The very slow dynamics must be caused by the refractory material of the feeder. Because of the heat-capacity of this material, it takes a long time to lose its heat. The 'in between' pole of the spout model can be explained by the fact that the glass is blended strongly in the spout, before it reaches the outlet. More comments on the interpretation of the resulted models is given in section 4.6.

4.3.4 State space realization

For control purposes a state space description of the MPSSM model is desired:

$$\underline{x}_{k+1} = F\,\underline{x}_k + G\,\underline{u}_k \qquad (4.8)$$
$$\underline{y}_k = H\,\underline{x}_k + D\,\underline{u}_k$$

with $\underline{x}_k$ the state of the process at the moment k.

This state vector is essential in the controller principle outlined in section 4.5.

In general the order n of state space model (i.e. dimension of matrix F) exceeds the degree r of the minimal polynomial. It can be shown (cf. R. Oudbier, 1986) that

$$n \leq r.\min(p,q) \qquad (4.9)$$

with p the number of inputs,
q the number of outputs of the model.

This implies that the spout model has an equivalent state space realization of order 4. This state space model is used for the final validation in section 4.4.

The profile model however, has only an equivalent state space model of order 12. This order is reduced again on the basis of the Hankel

singular values of the system. The Hankel singular values are calculated by solving the Lyaponov equations of the balanced realization of the system. By retaining the best observable, best controllable part of the system a low order approximation is obtained (cf. Pernebo and Silverman, 1982). We restrict ourselves to mentioning the result of this step. A 6-th order state space realization is obtained from this order reduction. The impulse responses of this model are depicted in the figures 4-34.

4.4 VALIDATION

To validate the obtained modelling results several activities have been performed.

First the model has been compared with the a priori knowledge of the feeders behaviour. In the former section a possible interpretation of the model has been proposed. Also the delay times found, 20 min of section 1 to the spout temperature, correspond with the flow time calculations done at the feeder (cf. P. Schout, 1987). Consequently, the model is not falsified by the a priori knowledge of the feeder behaviour.

Second, simulations have been done with the models on measured data sets. Section 4.4.1 deals with these validation experiments.

Third, the noise behaviour of the non-exited process has been observed and the results are compared with the results of the validation experiments of the former section. This is discussed in section 4.4.2.

4.4.1 Validation experiments

To obtain insight in the validity and performance of the spout model, outputs of the model have been computed from the measured input data. These simulated outputs have been compared with the measured outputs according to figure 4-18.

First, the output error of the simulated outputs with the spout model on the estimation experiment PRBNS2 is calculated. The results are depicted in figure 4-19. The output error is quantified by computing a ratio of the average power of the output error divided by the average power of the measured output signal:

$$E = \frac{\sum_{i=1}^{l} (y_i - \hat{y}_i)^2}{\sum_{i=1}^{l} y_i^2} = \frac{\sum_{i=1}^{l} \hat{e}_i}{\sum_{i=1}^{l} y_i^2} \qquad (4.10)$$

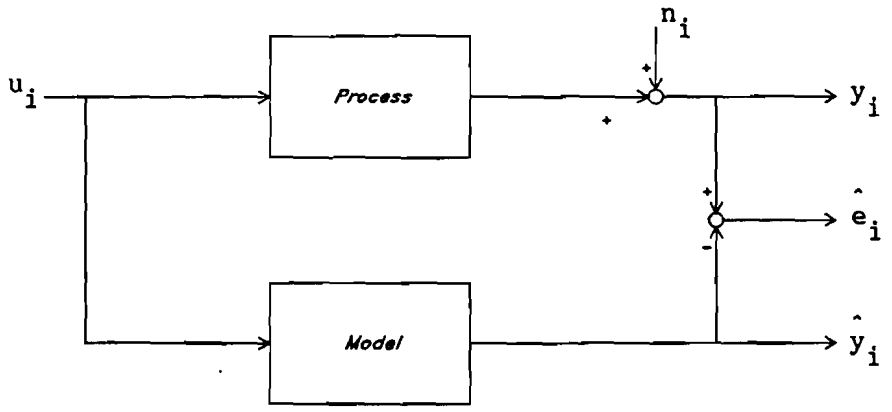

Fig. 4-18 Outline of the derivation of the output error $\hat{e}_i$.

This E has been computed from simulations obtained with the four different models. To avoid considering also the errors due to the transient responses of the filtering applied with detrending, the first and last 100 samples are not taken into account. So E has been obtained from an interval of 100..1150 samples.

PRBNS2	FIR	GERTH	DIRECT	State space
E of output f51	0.0216	0.0670	0.0455	0.0146

On the relative error of the MPSSM method has to be remarked that it has been simulated with only 75 Markov parameters. The entire MPSSM DIRECT model has the same performance as the state space model because this realization is exact. As a consequence the 3% difference with the state space model represents the effect of the tail parameters.

Of course the relative error of the FIR model is smaller compared to the MPSSM DIRECT model, because it has more degrees of freedom. The fact that it is 0.5% worse than the state space model may be caused by the Fir estimation algorithm EXACTMARK. EXACTMARK only performs one iteration of the minimization of the high order function of the Markov parameters and the AR-noise parameters (cf. J. Vaessen, 1983).

The MPSSM GERTH simulation (also simulated with 75 Markov parameters) results in the largest relative error.

A next validation has been done on experiment PRBNS4. The sampling time of this experiment was 30 seconds, while the clock period of the PRBNS was 15 min. The amplitudes of the inputs were different from PRBNS2 and also the working point differed slightly. The data have been prepared similar to data of PRBNS2. The state space model first has been transformed to the right sampling time. In figure 4-20 the simulated output is depicted, together with the output error. The relative output error has been computed as

PRBNS4	State space
E output f51	0.109

From figure 4-20 it can be seen that the high frequencies are modelled better than the low frequencies. High peaks show that a part of the errors is caused by linearity errors; the simulated output here always has a smaller amplitude.

Also the frequency spectrum has been observed. In figure 4-21a and b the spectra of the output error of the simulation on PRBNS2 with the FIR and the DIRECT model is shown. At the very low frequencies the output error decreases. This is expected because these frequencies are removed in the signal preparation phase by detrending. We also see that the power of low frequency errors is about the same for both simulations. From these facts the difference of the tail of the impulse responses of the FIR and DIRECT estimation can be explained.

After detrending the input estimation data cannot be considered white anymore for low frequencies. This means that in the FIR estimation the last Markov parameters, the parameters of the tail, cannot be estimated accurately. In addition, because of the small energy of the low frequencies in the estimation data, not much weight is put on errors caused by a badly estimated tail. Hence not too much value can be attached to the last Markov parameters.

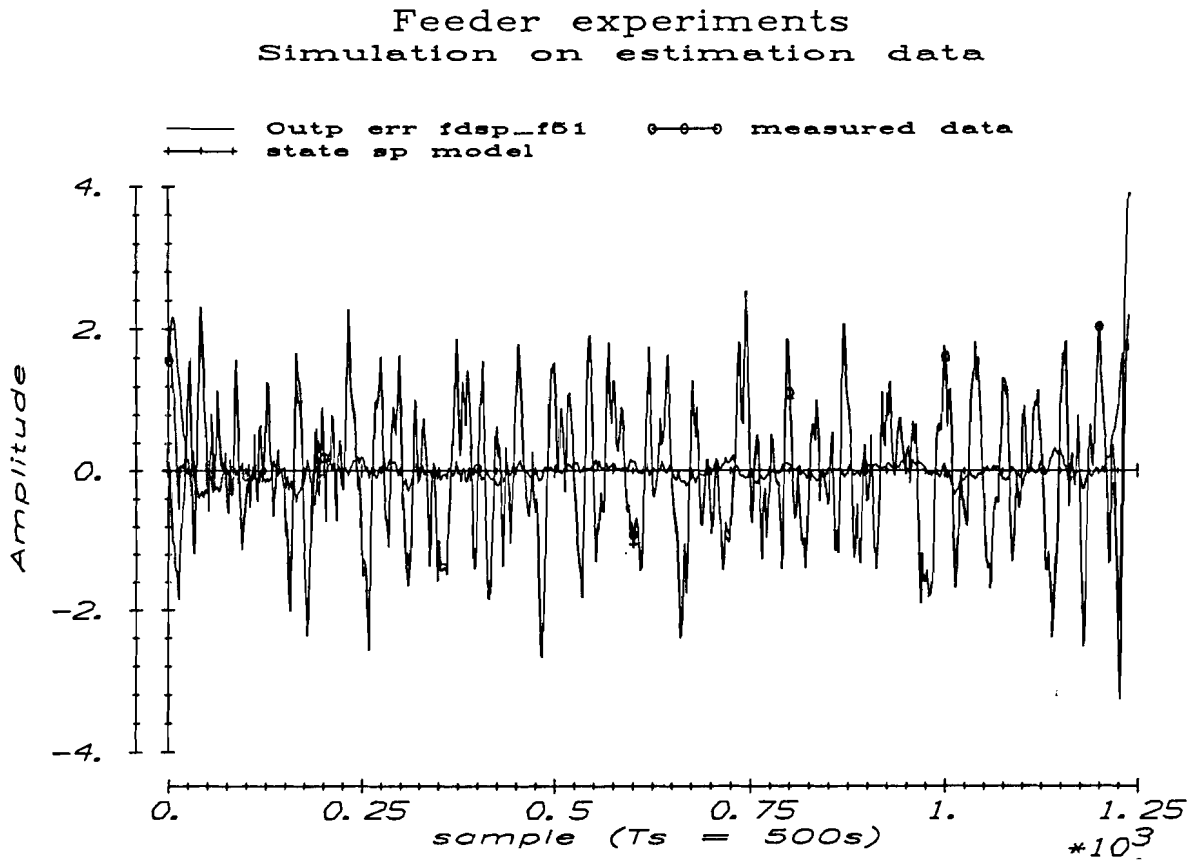

Fig. 4-19 Simulation and output error of spout model on the same data as used for estimation.

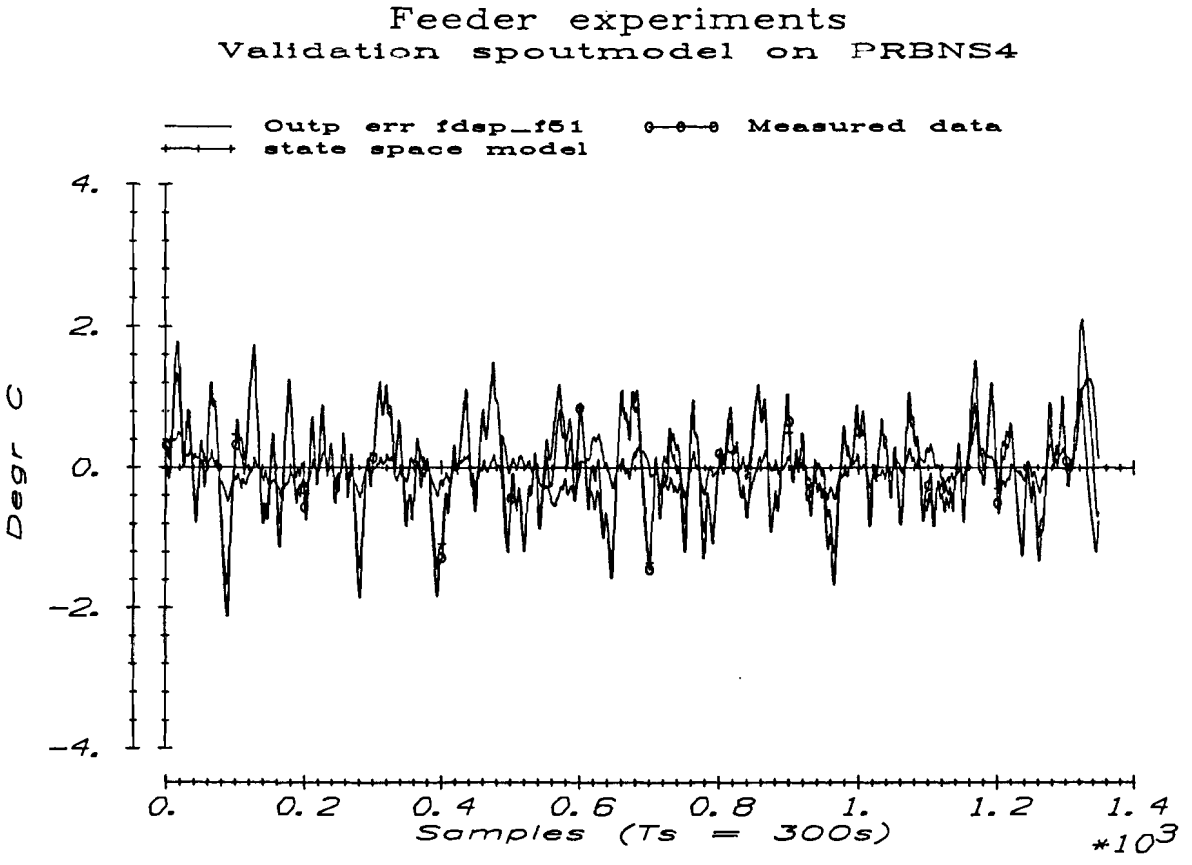

Fig. 4-20 Simulation and output error of the spout model on the data of experiment PRBNS4.

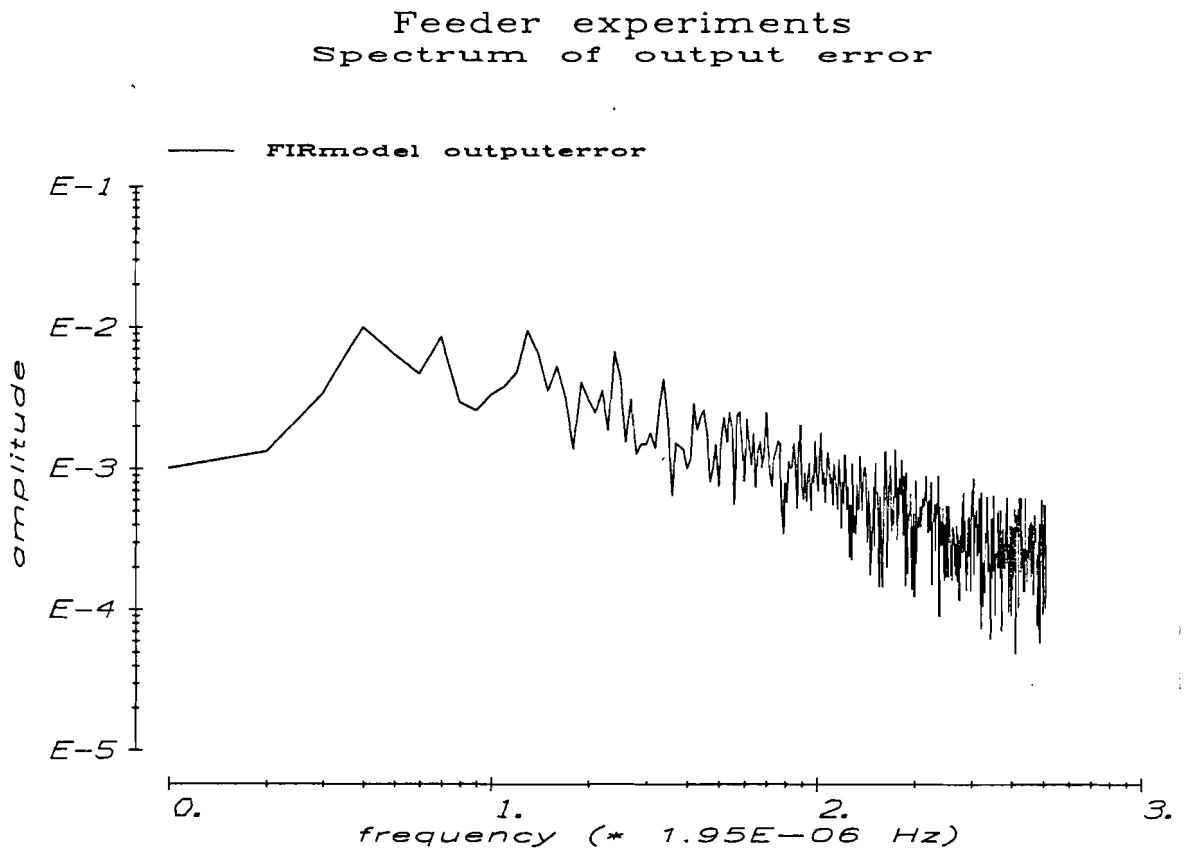

Fig. 4-21a Frequency spectrum of output error of simulation with the FIR model on PRBNS2.

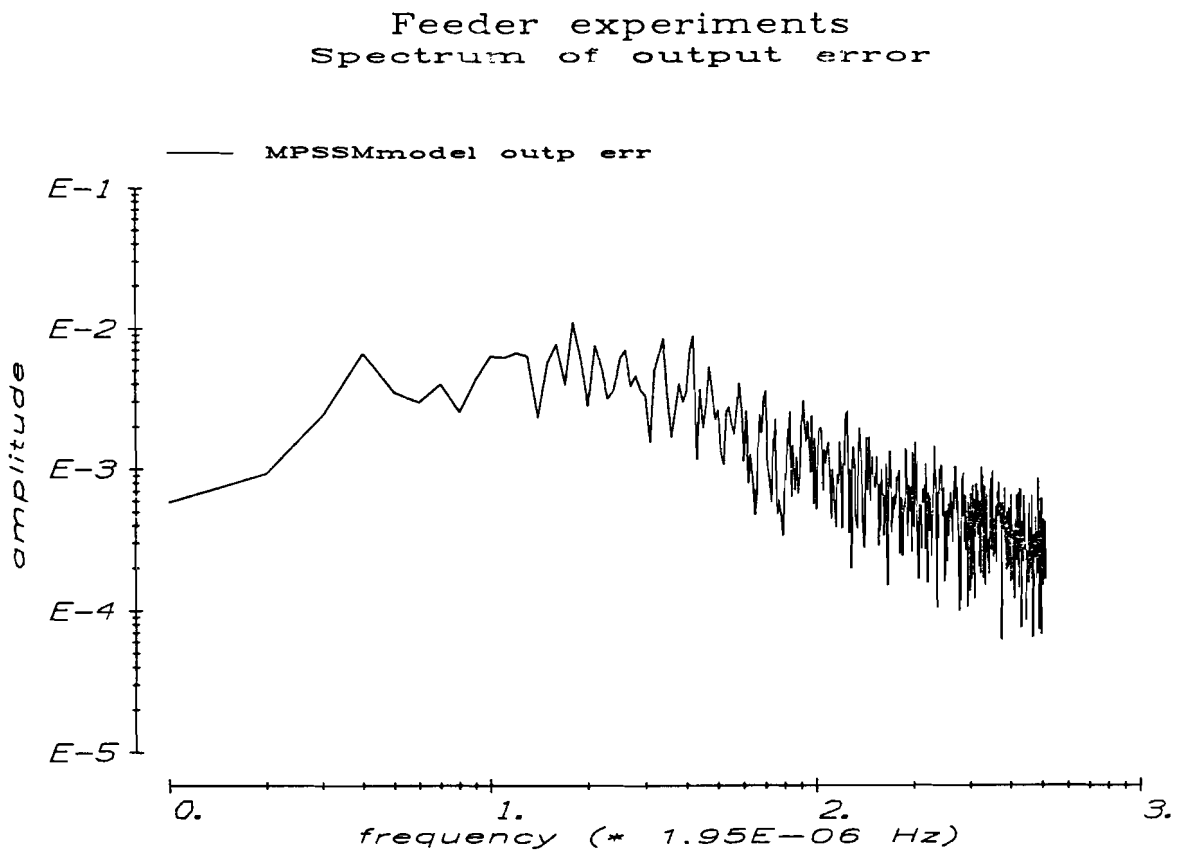

Fig. 4-21b Frequency spectrum of output error of simulation with the MPSSM DIRECT model on PRBNS2.

The same holds for the impulse responses of the DIRECT estimation. However, the DIRECT estimation does not have the degrees of freedom that the FIR estimation has. In the FIR estimation each Markov parameter is estimated separately, so that the loss function becomes minimal. The DIRECT method is forced to use its freedom where it yields the smallest loss function, i.e. where an error is punished least. Because the estimation data contain small energy for the low frequencies, the DIRECT estimation puts all its effort in the first part of the impulse response. This implies that not much freedom is left for the last part and that the loss function allows the DIRECT method to estimate the tail the way it is done now.

4.4.2 Noise considerations

The results obtained from the output error computations can only be judged properly in relation to the signal to noise ratios that are valid for the measurements.

To get an impression of the noise that was of influence at the feeder experiments, the experiment SIM130 has been done. During 3 days the outputs of the feeder have been measured while no excitation were injected at the inputs. From this experiment an indication of the noise power has been obtained by just computing the power of the outputs. Thus the noise that is inherent for the process plus the measuring noise is measured. The data have been prepared similarly to the former experiments, for the noise power is compared to the signal power of the these experiments.

Under the assumption that the noise behaviour is stationary, the average power of the signal output y_k of the experiments with excited inputs, is

$$\overline{y_k^2} = \overline{y_k^{*2}} - 2\,\overline{y_k^* n_{sk}} + \overline{n_{sk}^2} \qquad (4.11)$$

with y_k the real process output of the excited process without disturbances,

y_k^* measured output of excited experiment,

n_{sk} process + measuring noise from experiment SIM130.

If y_k and n_{sk} are considered independent and n_{sk} is considered to be white, we resolve

$$S/N = \frac{\overline{y_k^2}}{\overline{n_{sk}^2}} = \frac{\overline{y_k^{*2}}}{\overline{n_{sk}^2}} + 1 \qquad (4.12)$$

With this formula the following values have been computed:

		fdsp f51	
SIM130	$\overline{y_k^{*2}}$	0.0046	
PRBNS2	$\overline{y_k^{*2}}$	0.986	
	S/N	217	N/S = 0.5%
PRBNS4	$\overline{y_k^{*2}}$	0.449	
	S/N	98	N/S = 1%

Notice that the values are only valid for this particular signal preparation and can only be compared with estimation errors from simulations for which a similar preparation is used. A different detrending would cause a completely different result of S/N calculations, for the spectrum of the noise is certainly coloured.

To get an idea of the variance of the calculation of the S/N ratios the S/N ratio has been computed from 5 different intervals of the experiment. The variances appeared to be up to 50% of the values depicted in the former table. This implies that these values are only a rough indication. Nevertheless, it gives insight in what part of the output error may be caused by noise influences. Comparing the noise percentage of .5% of PRBNS2 with the 1% relative error of the simulation, the 1% output error is very good. This can be explained by the fact that this model was estimated on PRBNS2 and therefore was especially suited for prediction of the output of this.

Compared to the noise ratio of 1% of PRBNS4, the 10% output error is less good if related to the error of the estimation experiment, as can be expected. The errors must be caused by modelling errors; improper

modelling because of an improper modelset i.e. using a model that is linear, stationary, of too low order and with lumped parameters. With PRBNS4 a representative validation is done for the input amplitude, and even the working point, differed from the estimation experiment. As a result, it is expected that in practice with this model the output of the feeder can be predicted with an accuracy of about 10%.

Finally it has to be remarked that no attention is paid to the variances of the estimated parameters.

4.5 USE OF THE MODEL

The purpose of the models obtained by estimation is the use in a controller that controls the temperature distribution of the feeder (MIMO control). With the spout and profile model either the spout temperature f51 or the profile temperatures can be controlled, because the models use the same inputs. Because with the three inputs not all outputs of the profile model can be controlled, it is better to define 3 outputs as a function of the profile temperatures, that fix the temperature distribution. For example with the following definition of three outputs:

1. vertical temperature gradient (fm4-fl2)
2. horizontal temperature gradient (fm1-fm5)
3. absolute temperature (fm4)

the main properties of the temperature profile can be controlled. In future a new model can be estimated that beneath the profile temperatures, also takes the spout temperature into account. Always a choice must be made what can be controlled best with the three degrees of freedom that are available. Moreover, the controllability of the newly defined outputs must be studied. For example, from the impulse responses of fig. 4-16 it can be seen that the sensibility of the centre- and side couples to cooling air and gas do not differ very much. Therefore it may be a problem to control horizontal temperature gradients. In future this will be subject of study, whereas until now only a few simulations have been done with the controller based on spout and profile model. The principle of the controller will be explained in order to clarify the use of the models and their validity for this application.

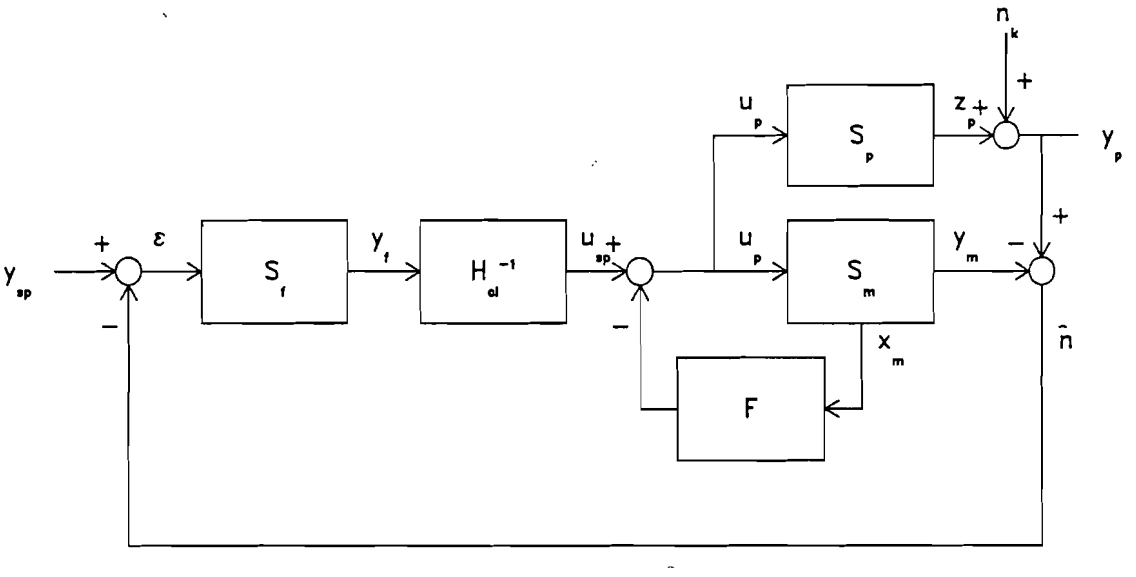

Fig. 4-22 Outline of the MIMO model reference controller.

A model reference type of control system is applied. Fig. 4-22 shows an outline of the model reference controller. Inputs of the controller are the setpoints y_{sp} that usually will be step functions to another temperature and/or temperature gradient. The outputs are the real temperatures of the process that are forced by the controller to follow the setpoints.

In the controller the real outputs y_p of process plus noise are compared with the simulated outputs y_m. S_m and S_p denote resp. the the model (state space model), and the real process. The model S_m predicts the process behaviour on the basis of the same inputs u_p as the process is excited with. The control input u_p is partly determined by the state feedback matrix F, that has the states of the model as input. Matrix F provides a modification of the dynamical behaviour of the system with transfer u_{sp}-> y_m (model with feedback) by means of pole placement and other controller design methods, so that the system becomes, for example, a first order system with poles at z=0.75. Because the process S_p resembles the model S_m, y_p reacts to u_{sp}like this first order system. As the control input u_p interacts before the output responses of the

process appear, this controller part is called the feedforward controller.

The model output y_m is compared with the process output plus disturbances, so $\hat{n}$ represents the model errors plus the process and measuring noise that appear. This output noise $\hat{n}$ is fed back in an outer loop and compared with the setpoints y_{sp}. From error ε is calculated what input u_{sp} is needed to yield this ε as output of the process. This is done with H_{cl}^{-1}, the inverse of the transfer $u_{sp} \rightarrow y_m$, the transfer of the model with state feedback. So the outer loop is a normal feedback loop that controls u_{sp} until y_p equals y_{sp}.

It is important to know that the feedback controller part cannot control high frequency disturbances, because time delays may occur in the process (and model) transfer. The feedforward controller does not reduce disturbances at all. Only disturbances with frequencies less than $1/2\tau_d$, with τ_d the time delay of the process, can be reduced by the outer loop. Therefore the low-pass filter S_f is designed so that only those frequencies are controlled by feedback.

At this stage it can be verified whether the model bandwidth is sufficient, i.e. if the detrending is applied correctly. In figure 4-22 is outlined which frequencies are controlled by feedforward and feedback parts. The spout model has a time delay of ≈20 min. The filter S_f can be designed so that only frequencies below $\sim 4.10^{-4}$Hz (periods larger than 40 min.) are passed. The lowest frequencies captured by the model are those of 10^{-5}Hz (periods smaller than 6 hours). This implies that indeed the feedforward controller can easily control frequencies below the maximum frequencies that can be controlled by the feedback part.

Simulations showed that with the model reference controller nice control of the spout and profile temperatures is possible. Figure 4-24 shows a simulation of the response to a step on the setpoint of the spout temperature f51 when the controller is applied. In the controller a state feedback matrix F is used so that the model with state feedback becomes a first order system with a pole on 0.75. 1.5 Hour after the setpoint is adjusted with a step, the output temperature reached the

setpoint value within 10%. Only input excitations during a period of an half hour are therefore required (cf. fig 4-15b). This must be compared with the period of about one day that was needed to switch the feeder to another setpoint with use of the PID-controllers (cf. section 1.2).

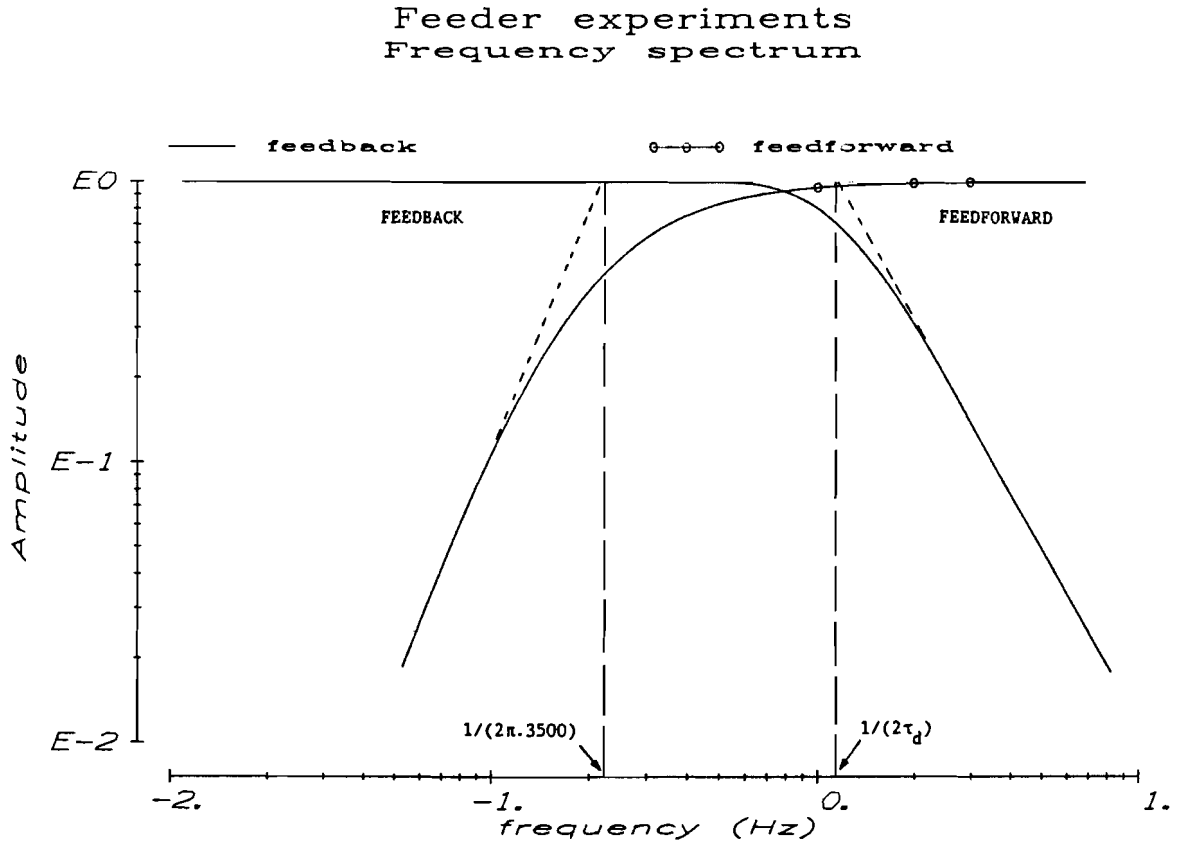

Fig. 4-23 Frequencies controlled by the feedforward and the feedback part of the controller.

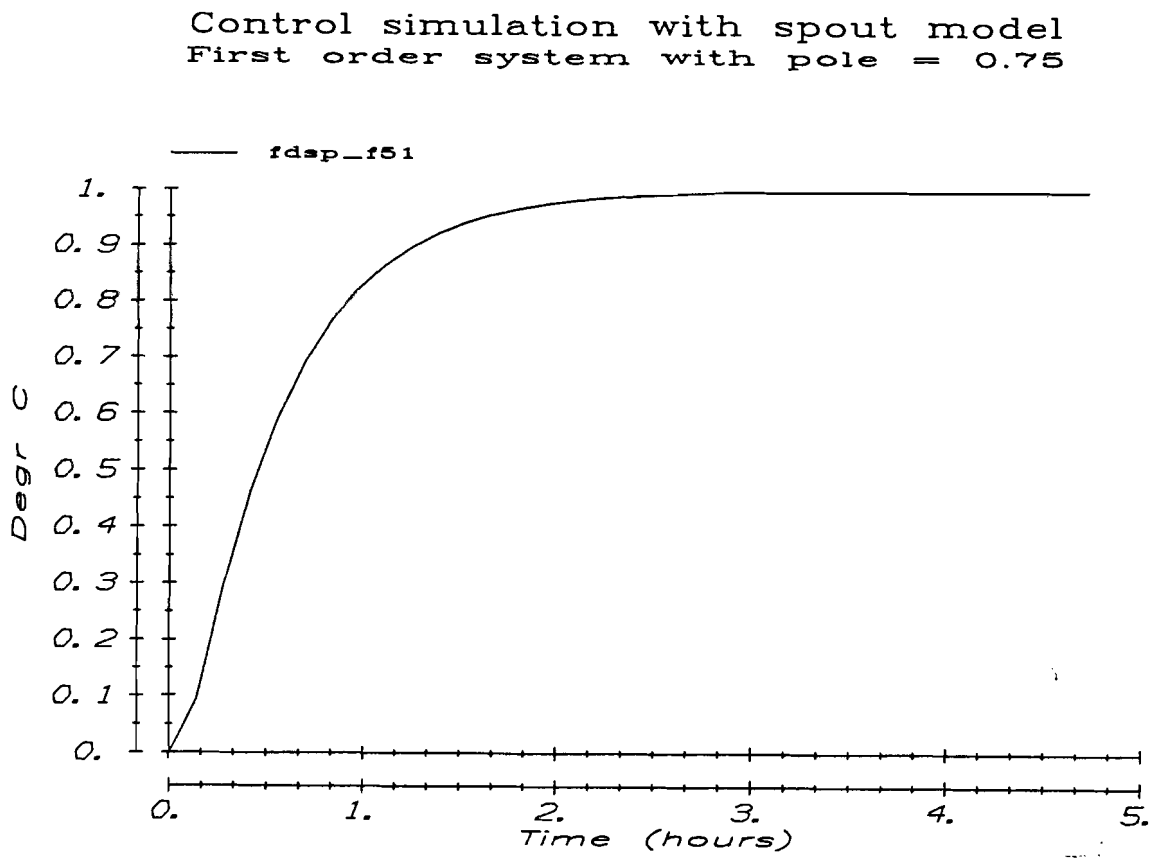

Fig. 4-24a Simulation of the step response of f51 to a setpoint adjustment of 1.0, when the process is controlled with a model reference controller using the spout model.

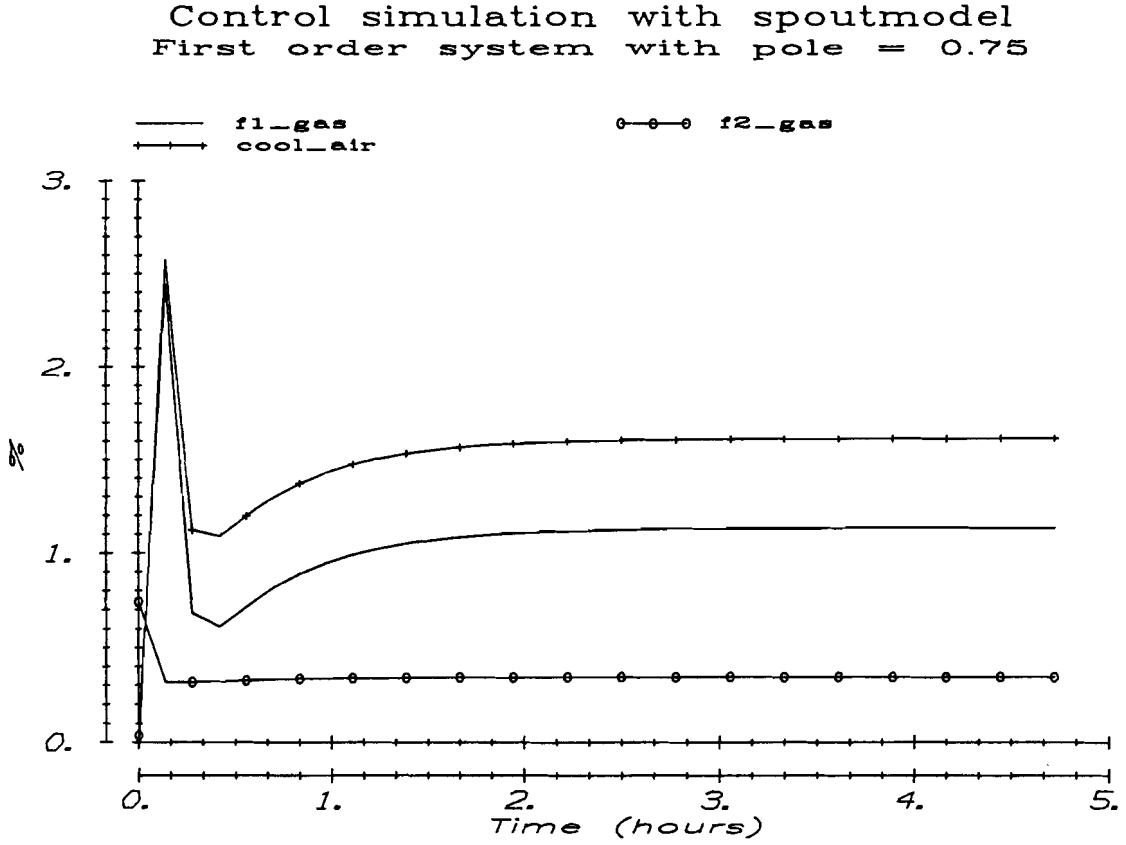

Fig. 4-24b Inputs generated by the model reference controller used to generate a setpoint step of 1.0 of the output f51.

4.6 CONCLUDING REMARKS

In this section identification of the feeder process has been discussed. It has been shown how signal preparation has been done to prepare the data for estimation. A state space realization of a spout model and a profile model has been derived.

Modelling

Despite the fact that the process is outside the modelset, the estimation resulted in valuable models. It appeared that modelling of a process with such difficult characteristics as a feeder still was possible with the method under study. The spout model describes the behaviour of the spout temperature with an accuracy of 10%. Consideration of the noise behaviour of the process and the measuring system, showed that of this error a small part can be explained by noise disturbances.

Not much attention is paid to linearity. Validation showed that linearity is not a big problem. The linear model can describe the process appropriately in its working point unless large input amplitudes have been applied. Quantative linearity analyses would still be useful in order to gain more insight in this subject.

Process mechanisms

From the models, insight has been obtained about some underlying mechanisms of the feeder behaviour. However, one has to be careful just ascribing effects to the most obvious cause. Conversation with glass specialists showed that for interpretation of the models, thorough knowledge and a lot of experience about the physics of a feeder is required. Still, some considerations are presented here:

- The fast part of the impulse response can be explained by addicting the heat transport of atmosphere into glass to transmission. The transmission speed is known to be faster than that of convection or conduction. The optical density of the glass however, plays an important role. When the glass has a large optical density the upper glass will absorb much heat, but the bottom glass will be nearly heated by radiation. With a small optical density all radiation passes through the glass to the bottom where it is absorbed by the refractory material. The material gets heated and will radiate this heat back

into the glass. With a very small optical density it is even possible that the couples are heated by radiation while the glass is not. In this case the measured temperature does not represent a glass temperature!

- In the models the temperatures showed a greater sensitivity to the cool air than to the gas. From thermic considerations this is also expected because the temperature difference of cool air and glass is much larger than that of combustion air and glass.

  The fast mode of the impulse response of the cool air was about equal to the fast mode of the gas. This may be explained to the fact that the cool air in the first place cools the roof and combustion air above the glass, so the inverse effect of gas-heating.
- The slow response may be explained by the large heat-capacity of the refractory material. It would be better to have a material with good isolation properties combined with a small heat-capacity. The present mass and type of material are designed for the situation that the feeder is not controlled with good controllers; each disturbance has then to be suppressed by the feeder dynamics, i.e. by the slow response of the feeder itself. This hinders, however, a good controllability of the temperatures of the feeder.

It is clear that the estimated black box models do not give a definite answer to the heat-transport problem in the feeder. Most important is that the results obtained in this study are fixed in indisputable models with concrete values. This appeared to be of use for a process at which a lot of facts are known from research with non-quantative results.

Experiment validation

Now the estimation has been done, a conclusion can be drawn about the validity of the experiments described in chapter 3.

For estimation and validation the experiments have been designed appropriately. Apparently the test signal parameters have been chosen properly.

It would have been better if at the estimation experiments the process was exited with more low frequency power. Because of a lag of time this was not possible. It should be considered if a smaller clock frequency of the PRBN-sequence with the same experiment duration, so with a relatively shorter experiment, would have yielded better results.

Control

Control simulation resulted in the conclusion that the derived state space models are suitable for use in a model reference controller. Simulations of control of the spout temperature f51 on the basis of the spout model showed that within one or two hours, dependent on the input amplitudes allowed, this temperature can be set to another value.

5 GENERAL CONCLUSIONS

In this report the identification of a feeder process has been discussed.

- A measuring system has been developed that has been used to do the measuring experiments. On a Micro-VAX a VAXELN task has been written that was suited for this purpose. The software package PRIMAL has been used fruitfully for 'on-line' analysis of the measuring signals. During one month the necessary experiments have been done at a BH-F feeder.

- To get insight in the dynamic behaviour of the feeder around a working point, identification of the input/output behaviour of the feeder is done. After preparation of the data, impulse response models have been estimated. Finally, from a 4-th order minimal polynomial impulse response model, a state space model is derived.
  Two models have been estimated:
  . A spout model has been obtained that has the gas flows at two sections and the cooling air flow as inputs. It describes the temperature at the exit of the feeder around a working point corresponding to a glass pull rate of 130 kg/hour. It is a 4-th order state space model.
  . A profile model has been obtained with the same inputs as the spout model and 6 temperatures at a cross section of the spout section as outputs.
  The process and measuring noise consisted primarily of low frequency disturbances. Many temperature drifts were observed at the feeder. These low frequencies have not been taken into account for modelling. The models describe the temperature behaviour above a frequency of 4.5 10^{-5}Hz (corresponding to periods of 6 hours). For the spout model a delay time of 20 minutes has been estimated from inputs to the spout temperature.

- Validation with the spout model showed that the spout temperature could be predicted with an accuracy of 10%. Two different modes dominated the transfer; a very slow mode, of which the transients were not even died out after 12 hours, and a fast mode, that let the

estimated impulse responses reach their top within one hour. This fast mode provides the possibility of good control of the feeder.

The feeder is a non-linear, non-stationary process and a system with distributed parameters. Nevertheless, the lumped models obtained with the method under study could describe the dynamic behaviour of the feeder appropriately in one of its working points.

- The models are suitable for use in a model reference controller. In this controller a feedforward control is applied on the basis of the model. The low frequencies that are not described accurately by the model, are controlled by feedback. Control simulation with the spout model showed that it is possible to bring the spout temperature to another setpoint within one or two hours, dependent on the input amplitudes that are allowed. From this result it is expected that in future the feeder temperatures can be controlled relatively fast compared to the present situation, in which a switch to another setpoint took about 1 day. It may be expected that in future faster and more accurate control and increasing flexibility can be realized. Futher research will be done on the design of the controller and its application in practice.

- Finally, the most important conclusion is that the newly developed identification- and control procedures of the PICOS group appeared a valuable tool for modelling of a difficult industrial process like a feeder.

ACKNOWLEDGEMENTS

The practical character of this study implies that there has been collaborated with many persons.
Without the effort and patient work of Ruud van Leersum and Herman Vos the PICOS measuring system would not have been operational in this short time period.
The assistance of all people involved at the Universal furnace plant formed an essential contribution to the succes of the measurements at the feeder.
I should like to thank Anton Koenraads for the pleasant work we did together on the feeder project.
I am thankful to Owen Burgh for our good co-operation. Our team-work also enlightened the sometimes dull work behind the terminal.
In general I like to express my thanks to all the members of the PICOS group for their assist and advice.
Furthermore, the comments of Prof. P. Eykhoff and Dr. A. van den Boom from the Eindhoven University of Technology were a valuable contribution to this report.
Finally, I am grateful to my coach Ton Backx. Not only his capability, but also his remarkable dedication to the work will be of influence to my future functioning as an engineer.

REFERENCES

Backx, T. (1987) Identification of an Industrial process: A Markov parameter approach
PhD Thesis, Philips, 1987.

Van den Boom, A., e.a. (1985)
Stochastic System theorie
Course notes, TUE 1985, ch. 2.

Burg, O. and G. van Vucht (1987)
Registration Feeder experiments Universal furnace, spring '87
Internal report, PICOS-R-082, Philips PICOS Glass, in Dutch.

Glover, K. (1984) All optimal Hankel approximations of linear multivariable systems and their L^{∞}-error bounds.
Int.J. Control 1984, vol. 39, no.6, 1984.

NBS (1974) Thermocouple Reference Tables Based on the IPTS-68
U.S. department of commerce, National Bureau of standerds 1974, p. 17.

Oudbier, R. (1986) A different approach to the minimal polynomial and start seqence of Markov-parameter estimation problem
Internal report, PICOS-R-070, Philips PICOS Glass

Pernebo, L. and L.M. Silverman (1982)
Model reduction via balanced state space realization
IEEE Trans A.C., Vol AC-27, no.2, 1982, p. 382-387

Schout, P. (1987) Calculations at the U.O.-Vello-installation
Philips internal report, 1987.

Vaessen, J. (1983) Least squares and maximum likelihood estimation of Markov parameters
Internal report, PICOS-R-011, Philips PICOS Glass

van Vucht, G. (1987) PICOS Measuring System User Manual
Internal report, PICOS-R-084, Philips PICOS Glass

van der Weijden, H. (1984)
The estimation of polynomial coefficients and a start sequence of Markov parameters
Internal report, PICOS-R-026, Philips PICOS Glass

Wilming, H. (1979) Mathematisches Modell der Glasströmung in eimen Speiserkanal als Grundlage fur eine Prozeß-steuerung,
Dissertation Fakultät für Hüttenwesen der Rheinisch-Westfälischen Technischen Hochschule Aachen, 1979.

IDENTIFICATIE VAN EEN GLAS-FEEDER PROCES

SAMENVATTING

In de PICOS groep (Process Identification and Control Systems) van Philips HTG Glas is gewerkt aan het modelleren van het dynamisch gedrag van een glas-feeder proces. Een feeder is het laatste deel van een glas-oven waarin de glastemperaturen geconditioneerd worden.
Het betreffende proces is bestudeerd en er is met name gekeken naar de moeilijkheden die onstaan als het proces wordt geregeld met standaard feedback regelingen.
Op een Micro-VAX is een meetsysteem ontwikkeld dat speciaal gechikt is voor identificatie. Aan de meet-computer is een 'host'-computer verbonden, zodat met het interactieve programmapakket PRIMAL eerste 'on-line' analyse van de meetgegevens gedaan kon worden.
De metingen zijn uitgevoerd op de feeder van de 'Universeel oven' in Eindhoven.
De identificatie van het input/output gedrag van de feeder in een van zijn werkpunten is uitgevoerd in verschillende stappen. Na uitgebreide voorbewerking van de signalen, zijn met gebruik making van deze data impulsresponsie modellen geschat. In een laatste stap wordt uit een minimaal-polynoom impulsresponsie model een toestandsmodel afgeleid.
Het model beschrijft de uitgangstemperatuur van de feeder op 10% nauwkeurig. Met behulp van het model is meer inzicht verkregen in de mechanismen die aan het feeder proces ten grondslag liggen.
Het toestandsmodel is geschikt om een procesregelaar met toestandsterug-koppeling te ontwerpen. Simulaties hebben laten zien dat met deze regelaar de temperatuur aan de uitgang van de feeder binnen 2 uur op een andere waarde gebracht kan worden. Met de vroegere feedback regelaar was hiervoor een dag nodig.
Hoewel de feeder een niet-lineair, niet-stationair systeem is met gedis-tribueerde parameters, is gebleken dat de methode als beschreven in het verslag, zeer geschikt is voor de identificatie van dit industriële proces.